

**INVESTIGATION AND PREPARATION OF 3D POROUS SCAFFOLDS  
BASED ON SILK SERICIN AND HYDROXYL CONTAINING POLYMER  
FOR DERMAL RECONSTRUCTION SCAFFOLD**



**A Thesis Submitted to the Graduate School of Naresuan University  
in Partial Fulfillment of the Requirements  
for the Master of Science Degree in Industrial Chemistry**

**May 2017**

**Copyright 2016 by Naresuan University**

Thesis entitled "Investigation and preparation of 3D porous scaffolds based on silk sericin and hydroxyl containing polymer for dermal reconstruction scaffold" by Miss Maytinee Yooyod has been approved by the Graduate School as partial fulfillment of the requirements for the Master of Science Degree in Industrial Chemistry of Naresuan University

**Oral Defense Committee**

.....*Sirisart Ouajai*..... Chair  
(Assistant Professor Sirisart Ouajai, Ph.D.)

.....*[Signature]*..... Advisor  
(Assistant Professor Sukunya Ross, Ph.D.)

.....*Sararat Mahasaranon*..... Co – Advisor  
(Sararat Mahasaranon, Ph.D.)

.....*Nungruthai Suphrom*..... Co – Advisor  
(Nungruthai Suphrom, Ph.D.)

.....*[Signature]*..... Internal Examiner  
(Associate Professor Jarupa Viyoch, Ph.D.)

Approved

.....*[Signature]*.....

(Panu Putthawong, Ph.D.)

Associate Dean for Administration  
and Planning for Dean of the Graduate School

15 MAY 2017

## ACKNOWLEDGEMENT

First of all, I would like to gratefully and sincerely thank my advisor, Assistant Professor Sukunya Ross for her guidance, understanding, patience, and most importantly, her friendship during my graduate studies. For everything you have done for me, I thank you. And I would like to thank my co-advisors, Dr. Sararat Mahasaranon, Dr. Nungruthai Suphrom for her teaching and advice. I would not have achieved this far and this thesis would not have been completed without all the support that I have always received from them. In addition, I am very grateful Dr. Gareth Ross for his kind and patience for his great advice during my study as well as checking in english grammar of my thesis. Additionally, I am very grateful for the friendship of all of the members of our Biopolymer group, my lovely sisters and brothers especially M.Sc.'s friends for all their help.

I would like to thank the Department of Chemistry, Faculty of Science and Naresuan University (Phitsanulok, Thailand), for their financial support for the duration of my work.

Last but not the least, I would like to thank my family for giving birth to me at the first place and supporting me spiritually throughout my life.

Maytinee Yooyod

**Title** INVESTIGATION AND PREPARATION OF  
3D POROUS SCAFFOLDS BASED ON SILK SERICIN  
AND HYDROXYL CONTAINING POLYMER FOR  
DERMAL RECONSTRUCTION SCAFFOLD

**Author** MaytineeYooyod

**Advisor** Assistant Professor Sukunya Ross, Ph.D.

**Co - Advisor** SararatMahasaranon, Ph.D.  
NungruthaiSuphrom, Ph.D.

**Academic Paper** Thesis M.S. in Science in Industrial Chemistry, Naresuan  
University, 2016

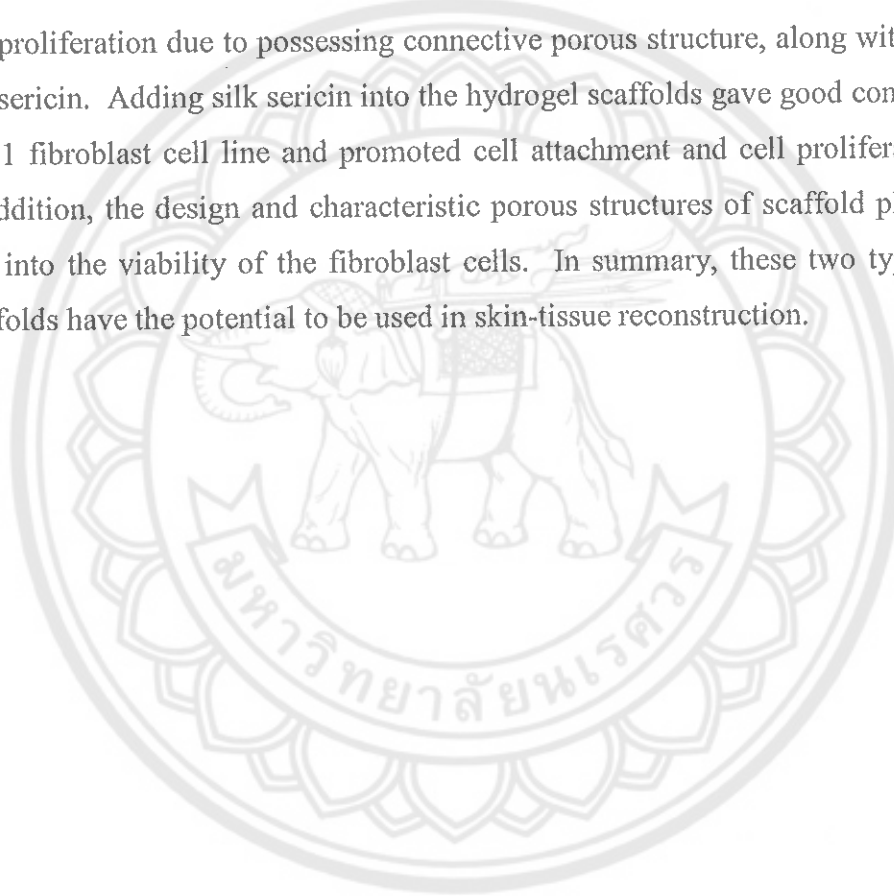
**Keywords** Silk sericin, scaffold, poly(vinyl alcohol), hydrogel  
poly(hydroxyethyl acrylamide), semi-interpenetrating  
polymer networks

### ABSTRACT

In this work, two different types of novel three-dimensional (3D) porous scaffolds based on silk sericin (SS) and hydroxyl containing polymers were successfully fabricated *via* different synthetic reactions and cross-linking systems. The porous structures of the scaffolds were promoted using a lyophilization technique. The first type of scaffold was a 3D porous scaffold of poly(vinyl alcohol) (PVA) and silk sericin, prepared by cross-linking with a classical condensation reaction in the presence of dimethylolurea (DMU). The fully cross-linking networks of PVA and SS were generated from not only the chemical cross-linked bond but also possessed physical cross-links. The effect of concentration of DMU onto the morphology (surface and cross-section) and cell culture tests (cell proliferation and adhesion of human feline fibroblasts cell line (HFF-1) were observed. The results showed that the PVA/SS scaffold at 10% DMU with porous diameters of 10-30  $\mu\text{m}$  showed the best efficiency for skin cell proliferation and adhesion. This work was also suggested that the scaffolds at low %DMU having low structure arrangement, good interconnecting



structure, various size distributions and high porous density that promoted better cell proliferation than scaffolds with high %DMU. The second type of scaffold was fabricated using *N*-hydroxyethyl acrylamide (HEA) and silk sericin *via* conventional free-radical polymerization, to form a semi-interpenetrating network (semi-IPN). The effect of cross-linker and silk sericin contents onto the properties of scaffold such as; morphology, swelling ratio, release of silk sericin, in vitro degradation and cell culture test, were studied. The results showed that the 3D porous semi-IPN hydrogel scaffold of PHEA/SS-1.25 was the most suitable for HFF-1 cells to migrate and then promote cell proliferation due to possessing connective porous structure, along with containing silk sericin. Adding silk sericin into the hydrogel scaffolds gave good compatibility of HFF1 fibroblast cell line and promoted cell attachment and cell proliferation ability. In addition, the design and characteristic porous structures of scaffold play a critical role into the viability of the fibroblast cells. In summary, these two types of novel scaffolds have the potential to be used in skin-tissue reconstruction.

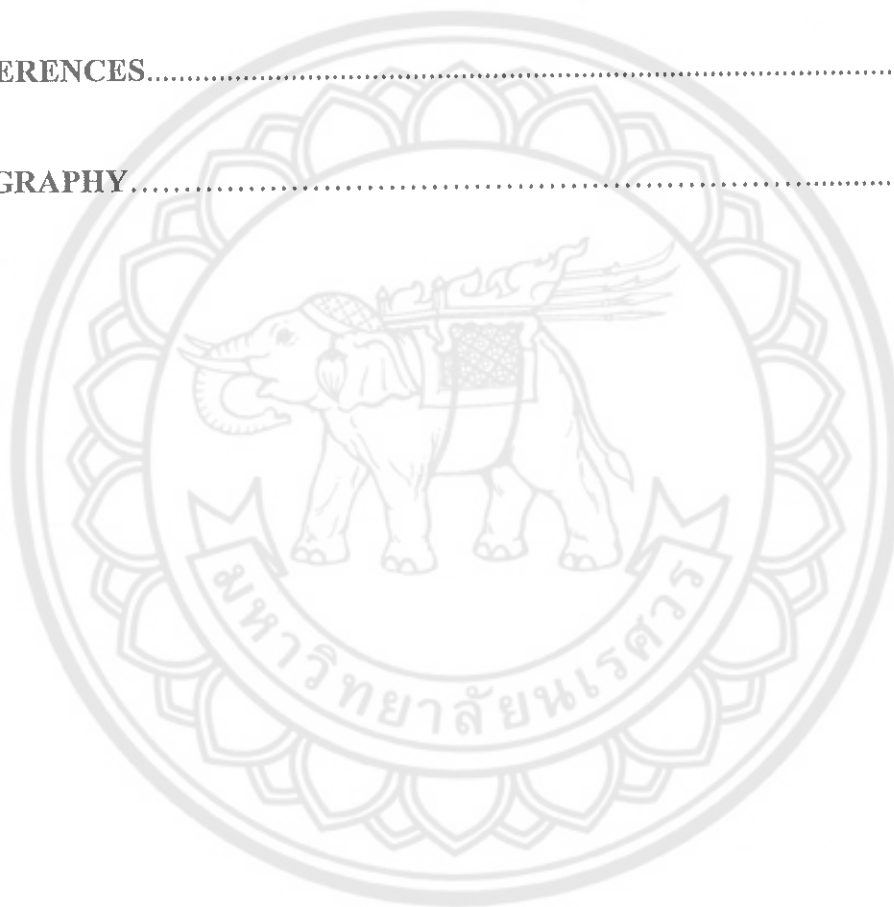


# LIST OF CONTENT

| Chapter  | Page      |
|--|-----------|
| <b>I INTRODUCTION.....</b>   | <b>1</b>  |
| Introduction.....  | 1         |
| Objectives .....   | 25        |
| Overview of the research.....  | 25        |
| <b>II LITERATURE REVIEWS.....</b>  | <b>27</b> |
| Information and applications of silk sericin in biomaterials.....  | 27        |
| Poly(vinyl alcohol) based biodegradable and biocompatible materials..  | 30        |
| Design and requirement to fabrication silk into scaffold for<br>tissue engineering.....  | 32        |
| <b>III RESEARCH METHODOLOGY.....</b>   | <b>37</b> |
| Materials.....   | 37        |
| Instruments.....   | 39        |
| Preparation of silk sericin powder.....  | 40        |
| 3D porous scaffold of poly(vinyl alcohol) (PVA) and silk sericin<br>(SS).....  | 40        |
| Three dimensional (3D) porous semi-IPN hydrogel scaffolds of<br>poly(hydroxyethyl acrylamide) (PHEA)/silk sericin (SS).....      | 48        |
| <b>IV RESULTS AND DISCUSSION.....</b>  | <b>56</b> |
| Part 1: Preparation of silk sericin (SS).....  | 56        |
| Part 2. Approach I: 3D porous scaffolds of PVA/SS.....   | 58        |
| Summary of approach I.....   | 76        |
| Part 3 : Approach II: 3D porous semi-IPN hydrogel scaffolds of<br>poly(hydroxyethyl acrylamide) (PHEA)/silk sericin<br>(SS)..... | 76        |
| Summary of approach II.....  | 96        |

## LIST OF CONTENT (CONT.)

| Chapter                   | Page       |
|---------------------------|------------|
| <b>V CONCLUSIONS.....</b> | <b>97</b>  |
| Conclusion.....           | 97         |
| Recommendation.....       | 101        |
| <b>REFERENCES.....</b>    | <b>102</b> |
| <b>BIOGRAPHY.....</b>     | <b>110</b> |



## LIST OF TABLES

| Table |   | Page |
|-------|---|------|
| 1     | The used forbiomaterials .....  | 2    |
| 2     | Biomaterial in organ.....   | 3    |
| 3     | Biomaterials for use in the body.....   | 4    |
| 4     | The compositions of fibroin and silk sericin.....   | 7    |
| 5     | Structure of silk from <i>Bombyxmorisilk</i> worm.....  | 9    |
| 6     | Silk protein composition, percentage of amino acids found.....  | 10   |
| 7     | Functions of extracellular matrix (ECM) in native tissues and of<br>scaffolds in engineered tissues.....  | 17   |
| 8     | The information of materials used in this work.....   | 37   |
| 9     | The formulation of the fabrication of 3D porous scaffolds of PVA/SS<br>with different concentrations of DMU.....  | 43   |
| 10    | The formulation of the fabrication of 3D porous semi-IPN hydrogel<br>scaffolds of PHEA/SS with different cross-linker and silk sericin<br>contents.....                                   | 49   |
| 11    | The physical appearance of 3D porous scaffolds of PVA/SS.....   | 59   |
| 12    | The physical appearances and gelation times of 3D porous semi-IPN<br>hydrogel scaffolds of PHEA/SS by using different loadings of<br>cross-linker (N'-N-methylene bisacrylamide, XL)..... | 78   |
| 13    | The physical appearances of 3D porous semi-IPN hydrogel scaffolds<br>of PHEA/SS by using different silksericin contents.....  | 79   |

## LIST OF FIGURES

| Figures |   | Page |
|---------|---|------|
| 1       | <i>Bombyxmori</i> silkworm spinning a cocoon of silk threads around itself (left) for made silk cocoon (right).....   | 5    |
| 2       | Life cycle of silkworm from <i>Bombyxmorisilkworm</i> .....   | 6    |
| 3       | <i>Bombyxmori</i> silkworm silk fibers showing fibroin and silk sericin.....  | 7    |
| 4       | The molecular chains stack together to form the three-dimensional, beta pleated sheet crystal.....  | 8    |
| 5       | Chemical structure of amino acids of silk sericin.....  | 10   |
| 6       | Chemical structure of poly(vinyl alcohol, PVA).....   | 11   |
| 7       | Structure of skin (anatomy of skin).....  | 12   |
| 8       | The phase of wound healing is continuous; (a) inflammatory phase, (2) proliferation phase and (3) Maturation phase.....   | 14   |
| 9       | Phases of wound healing with times.....   | 15   |
| 10      | Classification of IPN in different base on.....   | 22   |
| 11      | (Upper) Simultaneous IPN, prepared by polymerization and cross-linking of a mixture of two monomers or two linear pre polymers, with phase separation suppressed due to the rapidly increasing viscosity; (lower) sequential IPN, in which a network is swollen in monomers, the subsequent polymerization and cross-linking of which yields an IPN; phase separation is usually greater for sequential IPNs..... | 24   |
| 12      | Mechanical stability of the equilibrium swelled sericin/polyacrylamide cylindrical hydrogels of 10 mm thick and 13 mm in diameter as a function of various sericin composition: (a) Compressive strength (n=3, mean $\pm$ SD, *p < 0.05).....   | 29   |

## LIST OF FIGURES (CONT.)

| Figures |  | Page |
|---------|--|------|
| 13      | Confocal microscopic images of fibroblast cells grown on (a) polystyrene plates, cross linked PVA films with different wt% sericin concentrations of (b) 0% (S0), (c) 0.5% (S0.5), (d) 1% (S1), (e) 2% (S2) and (f) 5% (S5).....   | 31   |
| 14      | Scanning electron microscopy images of silk protein sericin/gelatin matrices. (A) 2-D films with sericin/gelatin wt.% ratios of (a) 0.5:5, (b) 1:5, (c) 2.5:5, (d) 5:5, (e) 7.5:5. (B) 3-D scaffolds with sericin/gelatin wt.% ratios of (a) 2:2, (b) 2:5, (c) 5:2, (d) 5:5, (e) 5 wt.% pure gelatin scaffold. For all films in(A) the magnification bar represents 50 um, while for the scaffolds in (B) the magnification bar represents 100 um..... | 34   |
| 15      | Initial modulus of SF, SF/poloxamer blend, and SF/poloxamer SIPNs.....   | 35   |
| 16      | Schematic picture of preparation of silk sericin powders.....  | 40   |
| 17      | Schematic diagram of preparation of three-dimensional (3D) porous scaffolds of PVA/SS with different concentrations of DMU via classical condensation reaction and followed by lyophilization technique.....   | 42   |
| 18      | schematic picture of Leo Model 1455VP scanning electron microscope (SEM).....  | 44   |
| 19      | Electronic photograph of human feline fibroblast cell line (HFF1, $1 \times 10^6$ cells) (left: picture from optical microscope) seeded into 3D porous scaffolds of PVA/SS (right: scaffolds were in sterilized 96-well plate).....  | 45   |
| 20      | The active mitochondrial of the viable cells reduce the yellow colored solution of MTT.....  | 46   |

## LIST OF FIGURES (CONT.)

| Figures |   | Page |
|---------|---|------|
| 21      | The color of samples after adding MTT solution into three-dimensional (3D) porous scaffolds of PVA/SS.....  | 47   |
| 22      | The area scale (middle) of cell count for calculated number of cell by the hemocytometer.....   | 47   |
| 23      | Schematic picture of synthetic of 3D porous semi-IPN hydrogel scaffoldsPHEA/SS by conventional free-radical polymerization.....   | 50   |
| 24      | Electronic photograph of human feline fibroblast cell line (HFF1, $1 \times 10^6$ cells) (left below: picture from optical light microscope) seeded into dehydrated of 3D poroussemi-IPN hydrogelsscaffold of PVA/SS (right below: scaffolds were in sterilized 24-well plate)..... | 54   |
| 25      | Electronic photograph of 3D porous semi-IPN hydrogel scaffoldsof PHEA/SS before and after adding MTT solution.  | 55   |
| 26      | SEM images of silk fibers; (a) before and (b) after hot-water degumming process, at magnification of 5000x (a) and 1000x(b).....  | 57   |
| 27      | Electric photograph of silk sericin powder after dried in an oven   | 58   |
| 28      | The reaction of preparation of 3D porous scaffolds of PVA/SS; a. PVA-DMU-PVA, b. SS-DMU-SS and c. PVA-DMU-SS...   | 62   |
| 29      | SEM images of PVA/SS at low % DMU; a. 0 %DMU, b. 10 %DMU and c. 20 %DMU, the surface images (500x, left) and cross-sectioned images (100x, right).....  | 64   |
| 30      | SEM images of PVA/SS at moderate % DMU; a. 40 %DMU, b. 50 %DMU and c. 60 %DMU, the surface images (500x, left) and cross-sectioned images (100x, right).....  | 66   |

## LIST OF FIGURES (CONT.)

| Figures |  | Page |
|---------|--|------|
| 31      | SEM images of PVA/SS at high % DMU; a. 80 %DMU, b. 90 %DMU and c. 100 %DMU, the surface images (500x, left) and cross-sectioned images (100x, right).....                                  | 68   |
| 32      | Pore diameter, structure arrangement, interconnecting matriced, size disribution and porous density of 3D porous scaffolds of PVA/SS.....  | 70   |
| 33      | Cartoon structure of thecross-linking system of 3D porous scaffolds that differential of cross-linker content.....   | 71   |
| 34      | Electronic photograph of the result from cell culture test of 3D porous scaffolds of PVA/SS (10%DMU of PVA/SS) by MTT assay for 3 days of culture.....                                     | 72   |
| 35      | Optical density of cell scaffolds of PVA/SS at different concentrations of DMU at 3 and 6 days of culture using MTT assay together with their SEM images (500x).....                       | 73   |
| 36      | Percentage of adhered cells on 3D porous scaffolds of PVA/SS at different concentrations of DMU.....   | 75   |
| 37      | Examples of thephysical appearance of 0.25% XL PHEA/SS-5 (a.), 2.0%XL PHEA/SS-5 (b.) and 0.5% XL PHEA/SS-1.25 (c.), which were used to represent other scaffolds after lyophilization..... | 80   |
| 38      | The synthetic reaction of producing 3D porous semi-IPN hydrogel scaffolds of PHEA/SS by a conventional free radical polymerization.....  | 81   |
| 39      | Gelation times of 3D porous semi-IPN hydrogel scaffolds of HEA/SS with different loading ofcross-linker at room temperature (n = 3).....   | 84   |



## LIST OF FIGURES (CONT.)

| Figures |   | Page |
|---------|---|------|
| 40      | SEM images of 3D porous semi-IPN hydrogel scaffolds of PHEA/SS at different concentrations of crosslink: (a) 0%XL PHEA/SS-5 (b) 0.125%XL PHEA/SS-5 (c) 0.25%XL PHEA/SS-5 (d) 0.5%XL PHEA/SS-5 (e) 1.0%XL PHEA/SS-5 and (f) 2.0%XL PHEA/SS-5.....                              | 85   |
| 41      | Swelling ratio of 3D porous semi-IPN hydrogel scaffolds of PHEA/SS with different loading of cross-linker (n = 3).....  | 87   |
| 42      | Gelation times of 3D porous semi-IPN hydrogel scaffolds of PHEA/SS with different loadings of sericin.....  | 89   |
| 43      | SEM images of 3D porous semi-IPN hydrogel scaffolds of PHEA/SS at effect of silk sericin content: (a) PHEA/SS-0; (b) PHEA/SS-1.25; (c) PHEA/SS-2.5 and (d) PHEA/SS-5....  | 90   |
| 44      | Swelling ratio of 3D porous semi-IPN hydrogel scaffolds of PHEA/SS with different loadings of silk sericin.....   | 91   |
| 45      | The silk sericin released from 3D porous semi-IPN hydrogel scaffolds of PHEA/SS with different loadings of silk sericin...  | 92   |
| 46      | <i>In-vitro</i> degradation of 3D porous semi-IPN hydrogel scaffolds of PHEA/SS with different loadings of silk sericin at day 30..   | 93   |
| 47      | Cartoon drawing represented the formazan crystals of the active mitochondria of the viable cells on 3D porous semi-IPN hydrogel scaffolds of PHEA/SS with different loadings of silk sericin and positive control (polystyrene plates) after 3, 7 and 14 days of culture..... | 95   |
| 48      | Cell proliferation of HFF-1 on 3D porous semi-IPN hydrogel scaffolds of PHEA/SS with different loading of silk sericin content and positive control (polystyrene plates) after 3, 7 and 14 days of culture.....   | 95   |

## LIST OF FIGURES (CONT.)

| Figures |  | Page |
|---------|--|------|
| 49      | Cartoon structure of approach I, 3D porous polymer network of PVA/SS and crosslinking reaction scheme between PVA, SS and DMU..... | 98   |
| 50      | Cartoon structure of approach II, the synthetic of 3D porous semi-IPN hydrogel scaffolds of PHEA/SS .....                          | 100  |



# CHAPTER I

## INTRODUCTION

### Introduction

The importance of this research work was to study the fabrication of 3D porous scaffolds from silk sericin (from silk cocoon *Bombyx mori*) and biocompatible polymers for dermal reconstruction materials. The work was separated into two approaches. The first approach is the fabrication of poly(vinyl alcohol) (PVA) and silk sericin (SS) into the form of 3D porous scaffold *via* classical condensation reaction and following by lyophilization technique. The second approach is the fabrication of 3D porous hydrogels scaffold of silk sericin (SS) and hydroxyethyl acrylamide (HEA) *via* conventional free radical polymerization, in the form of a semi-interpenetrating network (semi-IPN). This chapter gives an introduction on biomaterials used in this work; silk sericin, poly(vinyl alcohol) and poly(hydroxyethyl acrylamide), as well as the information of skin and wound damage, background information of scaffolds and polymerization techniques, are introduced.

### Background information of biomaterials

The term "Biomaterials" is defined as a synthetic material used to make devices to replace part of a living system or to function in intimate contact with living tissue. Biomaterials can be used in the fields of science and engineering, biology and physiology and clinical sciences. They are used to make devices to replace a part or a function of the body in safe, reliably economically, and physiologically acceptable manner. A variety of devices and materials are used in the treatment of disease or injury. Commonplace examples include suture needles, plates, teeth fillings, etc. Table 1 shows the examples of applications for biomaterials.

**Table 1 The used for biomaterials**

| <b>Uses for biomaterials</b>             | <b>Example</b>                                |
|--|---|
| Replacement of diseased and damaged part | Artificial hip joint, kidney dialysis machine |
| Assist in healing                        | Sutures, bone plates and screws               |
| Improve function                         | Cardiac pacemaker, intra-ocular lens          |
| Correct functional abnormalities         | Cardiac pacemaker                             |
| Correct cosmetic problem                 | Mastectomy augmentation, chin augmentation    |
| Aid to diagnosis                         | Probes and catheters                          |
| Aid to treatment                         | Catheters, drains                             |

As the number of available materials increases, it becomes more and more important to be protected from unsuitable products or materials, which have not been thoroughly evaluated. The most common classes of materials used as biomedical materials are polymers, metals, and ceramics. For polymers there is a large number of polymeric materials that have been used as implants or part of implant systems. The polymeric systems include acrylics, polyamides, polyesters, polyethylene, polysiloxanes, polyurethane, and a number of reprocessed biological materials. As bioengineers search for designs of ever increasing capabilities to meet the needs of medical practice, polymeric materials alone and in combination with metals and ceramics are becoming increasingly incorporated into devices used in the body. The metallic systems most frequently used in the body are iron-base alloys of the 316L stainless steel, titanium and titanium-base alloys and cobalt base alloys. The most frequently used ceramic implant materials include aluminum oxides, calcium phosphates, and apatites and graphite. Glasses have also been developed for medical applications. The applications of ceramics are in some cases limited by their generally poor mechanical properties: (a) in tension; (b) load bearing, implant devices that are to be subjected to significant tensile stresses must be designed and manufactured with great care if ceramics are to be safely used.

Biomaterial should not be toxic and the designed is an important element of tissue engineering, incorporating physical, chemical and biological cues to guide cells into functional tissues via cell migration, adhesion and differentiation. Many biomaterials need to degrade at a rate commensurate with new tissue formation to allow cells to deposit new extracellular matrix (ECM) and regenerate functional tissue. In addition, biomaterials may need to include provisions for mechanical support appropriate to the level of functional tissue development. In general, biomaterials must be biocompatible and elicit little to no host immune response [1].

Another class of materials that is receiving increased attention is biodegradable materials. Generally, when a material degrades in the body its properties change from their original values leading to altered and less desirable performance. It is possible, however, to design into an implant's performance the controlled degradation of a material, such that natural tissue replaces the prosthesis and its function. Table 2 shows the example of biomaterials in organ.

**Table 2 Biomaterials in organ**

| Organ   | Example of biomaterials   |
|---------|---|
| Heart   | Cardiac pacemaker, artificial heart valve, Totally artificial heart |
| Lung    | Oxy-generator machine   |
| Eye     | Contact lens, intraocular lens                                      |
| Ear     | Artificial stapes, cochlea implant                                  |
| Bone    | Bone plate, intra-medullary rod                                     |
| Kidney  | Kidney dialysis machine   |
| Bladder | Catheter and stent  |

Most materials used in the body, device perform satisfactorily, improving the quality of life for the recipient or saving lives. Table 3 shows the example of biomaterials for use in the body.

**Table 3 Biomaterials for use in the body**

| <b>Materials</b>   | <b>Advantages</b>                                       | <b>Disadvantages</b>                           | <b>Examples</b>   |
|--|---|--|---|
| Polymers (nylon, silicon<br>Rubber, polyester, PTFE, etc)  | Resilient<br>Easy to Fabricate                          | Not strong<br>Deforms with time<br>May degrade | Blood vessels,<br>Sutures, ear, nose,<br>Soft tissues   |
| Metals (Ti and its alloys Co-Cr alloys, stainless Steels)  | Strong Tough<br>ductile                                 | May corrode,<br>dense,<br>Difficult to make    | Joint replacement,<br>Bone plates and<br>Screws, dental root<br>Implant, pacer, and<br>suture |
| Joint replacement,<br>Bone plates and<br>Screws, dental<br>root<br>Implant, pacer,<br>and suture | Very<br>biocompatible<br>Inert strong in<br>compression | Difficult to make<br>Brittle<br>Not resilient  | Dental coating<br>Orthopedic<br>implants<br>Femoral head of<br>hip                            |
| Composites<br>(Carbon-carbon,<br>wire<br>Or fiber reinforced<br>Bone cement)                     | Compression<br>strong                                   | Difficult to make                              | Joint implants<br>Heart valves  |

### Silk cocoon

The secret to silk production is the tiny creature known as the silkworm, which is the caterpillar of the silk moth *Bombyx mori*. It feeds solely on the leaves of mulberry trees. Only one other species of moth, the *Antheraea mylitta*, also produces silk fiber. This is a wild creature, and its silk filament is about three times heavier than that of the cultivated silkworm. The life cycle of the *Bombyx mori* begins with eggs laid by the adult moth. The larvae emerge from the eggs and feed on mulberry leaves. In the larval stage, the *Bombyx* is the caterpillar known as the silkworm. The silkworm spins a protective cocoon around itself so it can safely transform into a chrysalis. In nature, the chrysalis breaks through the cocoon and emerges as a moth. The moths mate and the female lays 300 to 400 eggs. A few days after emerging from the cocoon, the moths die and the life cycle continues. Figure 1 shows electronic photograph of *Bombyx mori* silkworm spinning a cocoon of silk threads around itself (left) for made silk cocoon (right) and figure 2 shows the life cycle of silkworm from *Bombyx mori* silkworm.

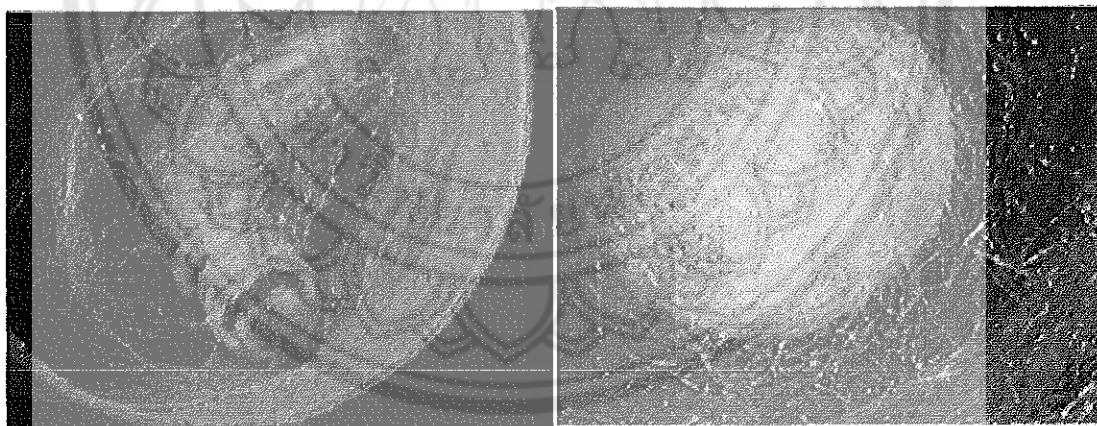


**Figure 1** *Bombyx mori* silkworm spinning a cocoon of silk threads around itself (left) for made silk cocoon (right)

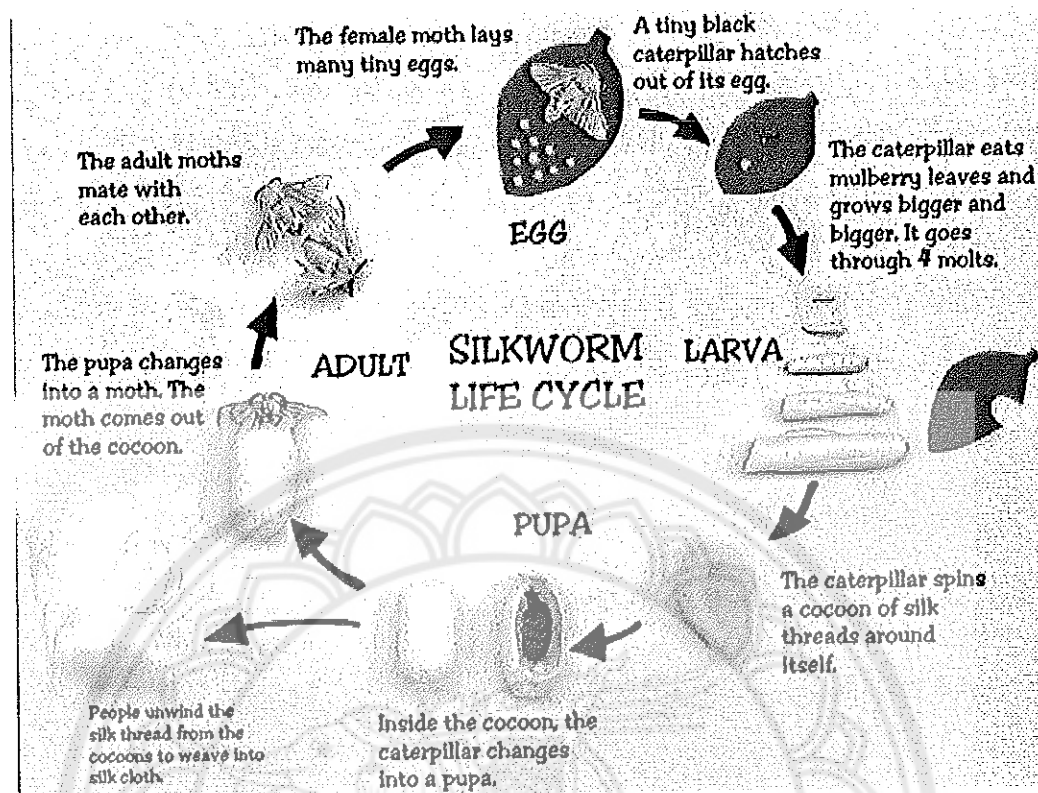


Figure 2 Life cycle of silkworm from *Bombyx mori* silkworm

The cultivation of silkworms for the purpose of producing silk is called sericulture. Over the centuries, sericulture has been developed and refined to a precise science. Sericulture involves raising healthy eggs through the chrysalis stage when the worm is encased in its silky cocoon. The chrysalis inside is destroyed before it can break out of the cocoon so that the precious silk filament remains intact. The healthiest moths are selected for breeding, and they are allowed to reach maturity, mate, and produce more eggs.

Generally, one silk cocoon produces between 1,000 and 2,000 feet of silk filament, made essentially of two elements. The fiber, called fibroin, makes up between 75 and 90%, and silk sericin, the gum secreted by the caterpillar to glue the fiber into a cocoon, comprises about 10-25% of silk. Other elements include fats, salts, and wax[2]. *Bombyx mori* silkworm is silk cocoon that are interested to use in this research work, it contains at least two major fibroin proteins, light and heavy chains, 25 and 325 kDa, respectively [3]. These are composed of two proteins fibroin and



sericin, as said earlier (figure 3). Both silk fibroin and silk sericin were used in biomedical applications particularly as sutures.

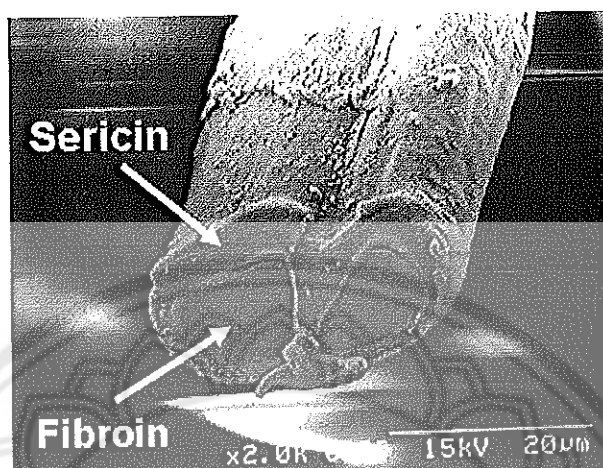


Figure 3 *Bombyx mori* silkworm silk fibers showing fibroin and silk sericin [4]

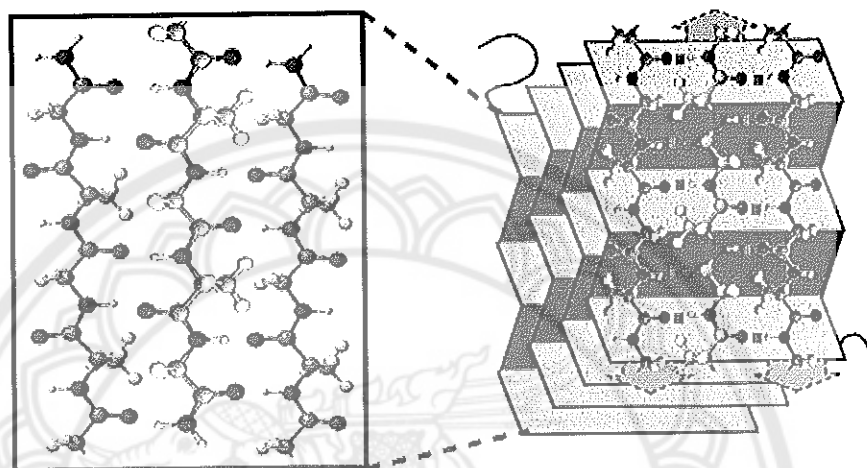
Both fibroin and silk sericin contain the same 18 amino acids such as glycine, alanine and serine in different amounts. The core fibroins are encased in a coat of silk sericin, a family of hydrophilic proteins which holds two fibroin fibers together [4] and the composition of C, H, N and O varies a little between fibroin and silk sericin as shown in Table 4 [5].

Table 4 The compositions of fibroin and silk sericin

| Element | Fibroin(%) | Silk sericin(%) |
|---------|------------|-----------------|
| C       | 47.6       | 46.5            |
| H       | 6.4        | 6.0             |
| O       | 18.3       | 16.5            |
| N       | 27.7       | 31.0            |

Fibroin is a giant molecule comprising a crystalline portion of about two-thirds and an amorphous region of about one-third. Fibroin is composed of glycine (40 %), alanine (25 %) and serine (13 %). They are regularly ordered with glycine in every

second position like  $-G-A-G-X-G-A-$  (G: glycine, A: alanine, X: other amino acid), forming an antiparallel  $\beta$ -sheet and leading to the stability and mechanical properties of the fiber [6]. Figure 4 shows three-dimensional, beta pleated sheet crystal of fibroin.



**Figure 4 The molecular chains stack together to form the three-dimensional, beta pleated sheet crystal [7]**

Fibroin is a glycoprotein composed of two equimolar protein subunits of 370 and 25 kDa covalently linked by disulphide bonds. Fibroin filament is made of both crystalline and amorphous domains. The amorphous domains are characterized by the presence of amino acids with bulkier side chains, whereas the crystalline domains are characterized by high percentage of alanine, glycine, and serine, which contains short side chains to permit the close packing densities for overlying sheets [8].

Generally, the main secondary structures of fibroin are of the random-coil and amorphous type and the antiparallel  $\beta$ -sheet type, which is formed through hydrogen bonds between adjacent peptide chains [9]. The silk fibroins are characterized as natural block copolymers comprising hydrophobic blocks with short side-chain amino acids such as glycine and alanine, and hydrophilic blocks with larger side chain amino acids, as well as charged amino acids [10]. The former blocks lead to  $\beta$ -sheets or crystals through hydrogen bonding [11]. The two main distinct structures in silk fibroin are silk I and silk II. The structure of silk I contains random-coil and

amorphous regions. The silk II structural form of the fibroins has been characterized as an antiparallel  $\beta$ -sheet structure. The former structure is a watersoluble structure while the latter excludes water and is insoluble in several solvents including mild acid and alkaline conditions [1] (Table 5).

**Table 5 Structure of silk from *Bombyx mori* silk worm**

| Silk fiber       | Silk fibroin (72-81%)   |         |                   | Silk sericin (19-58%)                       |
|------------------|---|---------|-------------------|---|
|                  | H chain   | L chain | P 25 glycoprotein | A glue-like protein                         |
| Molecular weight | 325 kDa   | 25 kDa  | 25 kDa            | 300 kDa                                     |
| Polarity         | Hydrophobic   |         |                   | Hydrophilic                                 |
| Structure        | Silk I (random-coil or unordered structure)<br>Silk II (crystalline structure)<br>Silk III (unstable structure) |         |                   | Non- crystalline structure                  |
| Function         | The structure protein of fibers filament core protein   |         |                   | Binds two fibroins together coating protein |

Silk sericin is a second type of silk protein, which contains 18 amino acids including essential amino acids and is characterized by the presence of 32 percent of serine. The total amount of hydroxyl amino acids in serine is 45.8 percent. There are 42.3 percent of polar amino acid and 12.2 percent of nonpolar amino acid residues. Sericin contributes about 20-30 percent of total cocoon weight. Table 6 shows the percentage of amino acids of silk protein composition, their main role is to envelop the fibroin. Figure 5 shows the chemical structure of amino acids of silk sericin. In presence of silk sericin the fibers are hard and tough and become soft and lustrous after its removal. Silk sericin occurs mainly in an amorphous random coil and to a lesser extent, in a  $\beta$ -sheet organized structure. The randomly coiled structure easily changes to  $\beta$ -sheet structure, as a consequence of repeated moisture absorption and mechanical stretching [8]. Silk sericin also contains various amino acids like fibroin.

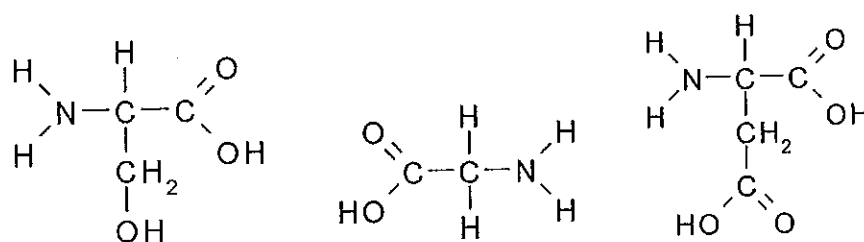


**Figure 5 Chemical structure of amino acids of silk sericin**

**Table 6 Silk protein composition, percentage of amino acids found**

| Symbol | Amino acid    | Fibroin | Silk sericin |
|--------|---------------|---------|--------------|
| G      | glycine       | 45      | 14           |
| A      | alanine       | 29      | 5            |
| S      | serine        | 12      | 33           |
| Y      | tyrosin       | 5       | 3            |
| V      | valine        | 2       | 3            |
| D      | Aspartic acid | 1       | 15           |
| R      | arginine      | 1       | 3            |
| E      | Glutamic acid | 1       | 8            |
| I      | isoleucine    | 1       | 1            |
| L      | leucine       | 1       | 1            |
| F      | phenylalanine | 1       | 1            |
| T      | threonine     | 1       | 8            |
| C      | cystine       | 0       | 0            |
| H      | histidine     | 0       | 1            |
| K      | lysine        | 0       | 4            |
| M      | methionine    | 0       | 0            |
| P      | proline       | 0       | 1            |
| W      | tryptophan    | 0       | 0            |

According to the US Pharmacopeia's definition, silk is classified as non-degradable. However, from the literature, it can be considered as a degradable

material. The reason may be connected to the fact that silk degradation behavior is usually mediated by a foreign body response [3]. Different from synthetic materials, the degradable behavior of silk fibroins doesn't lead to an immunogenic response. Biodegradation is the breakdown of polymer materials into smaller compounds. The processes vary greatly, and the mechanisms are complex. Normally, the encompass physical, chemistry and biological factors. Depending on the mode of degradation, silk fibroins can be classified as enzymatically degradable polymers [12, 13].

#### Poly(vinyl alcohol) (PVA)

PVA is a water soluble, biodegradable and biocompatible synthetic polymer. It is a dry solid, and is available in granule and powdered forms. PVA was prepared *via* the hydrolysis of poly(vinyl acetate) in ethanol with potassium hydroxide, the basic structure as show in figure 6. The most important properties, which affected to the majority of applications, are depending on the degree of polymerization and degree of hydrolysis. In the partially hydrolyzed grades, 86-89 mole% of acetate group is replaced by alcohol group. Likewise, in the fully hydrolyzed grade, 98.5-99.2 mole % of acetate group is replaced by alcohol group. Fully hydrolyzed grade PVA can be easily dissolved in over 90°C water, but it only swells in water at the room temperature. The glass transition temperature of PVA is approximately 85°C and the melting point is 230°C. Figure 6 shows the chemical structure of PVA.

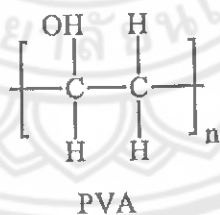
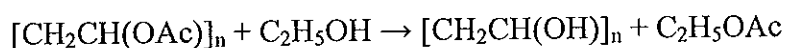


**Figure 6 Chemical structure of poly(vinyl alcohol, PVA)**

PVA is not prepared by polymerization of the corresponding monomer. The monomer, vinyl alcohol, is unstable with respect to acetaldehyde. PVA instead is prepared by first polymerizing vinyl acetate, and the resulting poly(vinylacetate) is converted to the PVA [14]. Other precursor polymers are sometimes used, with formate, chloroacetate groups instead of acetate. The conversion of the polyesters is usually conducted by base-catalysed transesterification with ethanol:



The properties of the polymer depend on the amount of residual ester groups.

### Introduction of skin and wound damage

The skin is one of the largest organs in the body in surface area and weight. Figure 7 shows structure of skin, the skin consists of three layers, there are the epidermis, dermis and Subcutaneous Tissue [15]. Epidermis is composed of several thin layers, stratum basale, stratum spinosum, stratum granulosum, stratum lucidum, stratum corneum. The several thin layers of the epidermis contain the following:

1. melanocytes, which produce melanin, a pigment that gives skin its colour and protects it from the damaging effects of ultraviolet radiation.
2. keratinocytes, which produce keratin, a water Repellent protein that gives the epidermis its tough and protective quality.

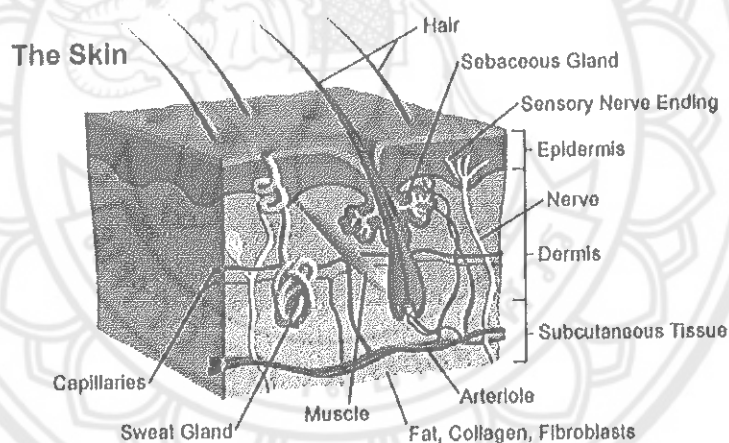


**Figure 7 Structure of skin (anatomy of skin)**

Dermis is composed of a thick layer of skin that contains collagen and elastic fibers, nerve fibers, blood vessels, sweat and sebaceous glands, and hair follicles. And for subcutaneous tissue is composed of a fatty layer of skin that contains blood vessels, nerves, lymph, and loose connective tissue filled with fat cells.

A wound is defined as damage or disruption to the normal anatomical structure and function. This can range from a simple break in the epithelial integrity of

the skin or it can be deeper, extending into subcutaneous tissue with damage to other structures such as tendons, muscles, vessels, nerves, parenchymal organs and even bone [16].

A wound may be described in many ways; by its aetiology, anatomical location, by whether it is acute or chronic [17], by the method of closure, by its presenting symptoms or indeed by the appearance of the predominant tissue types in the wound bed. All definitions serve a critical purpose in the assessment and appropriate management of the wound through to symptom resolution or, if viable, healing. Wounds heal by primary intention or secondary intention depending upon whether the wound may be closed with sutures or left to repair, whereby damaged tissue is restored by the formation of connective tissue and re-growth of epithelium [18].

Wounds can be classified according to various criteria. Time is an important factor in injury management and wound repair. Thus, wounds can be clinically categorized as acute and chronic according to their time frame of healing [19]. Wounds that repair themselves and that proceed normally by following a timely and orderly healing pathway, with the end result of both functional and anatomical restoration, are classified as acute wounds [19]. The time course of healing usually ranges from 5 to 10 days, or within 30 days. Acute wounds can be acquired as a result of traumatic loss of tissue or a surgical procedure [20]. Chronic wounds are those that fail to progress through the normal stages of healing and they cannot be repaired in an orderly and timely manner. The healing process is incomplete and disturbed by various factors, which prolong one or more stages in the phases of haemostasis, inflammation, proliferation or remodelling. These factors include infection, tissue hypoxia, necrosis, exudate and excess levels of inflammatory cytokines [21].

Wounding and wound healing take place in all tissues and organs of the body. Many of these repair processes are common to all tissues. Figure 8 shows the picture of difference phases of wound healing.

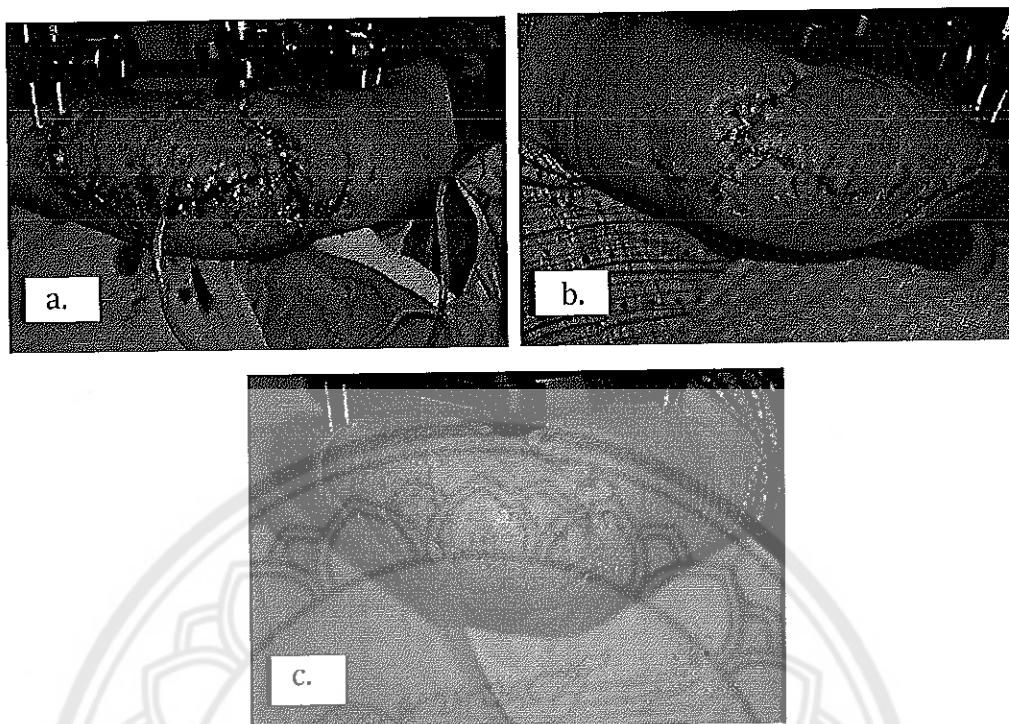


**Figure 8 The phase of wound healing is continuous; (a.) inflammatory phase, (b.) proliferation phase and (c.) Maturation phase**

Although the process of healing is continuous, it is arbitrarily divided into different phases in order to aid understanding of the physiological processes that are taking place in the wound and surrounding tissue [22]. Whether wounds are closed by primary intention, subject to delayed primary closure or left to heal by secondary intention [23], the wound healing process is a dynamic one which can be divided into three phases. It is critical to remember that wound healing is not linear and often wounds can progress both forwards and back through the phases depending upon intrinsic and extrinsic forces at work within the patient. The phases of wound healing as shows in figure 9 [24]; 1) the inflammatory phase is the body's natural response to injury. After initial wounding, the blood vessels in the wound bed contract and a clot is formed. Once haemostasis has been achieved, blood vessels then dilate to allow essential cells; antibodies, white blood cells, growth factors, enzymes and nutrients to reach the wounded area. This leads to a rise in exudate levels so the surrounding skin needs to be monitored for signs of maceration. It is at this stage that the characteristic signs of inflammation can be seen; erythema, heat, edema, pain and functional



disturbance. During 2) proliferation, the wound is 'rebuilt' with new granulation tissue which is comprised of collagen and extracellular matrix and into which a new network of blood vessels develop, a process known as 'angiogenesis'. Healthy granulation tissue is dependent upon the fibroblast receiving sufficient levels of oxygen and nutrients supplied by the blood vessels. Healthy granulation tissue is granular and uneven in texture; it does not bleed easily and is pink / red in colour. The colour and condition of the granulation tissue is often an indicator of how the wound is healing. Dark granulation tissue can be indicative of poor perfusion, ischaemia and / or infection. Epithelial cells finally resurface the wound, a process known as 'epithelialisation'. 3) Maturation is the final phase and occurs once the wound has closed. This phase involves remodeling of collagen from type III to type I. Cellular activity reduces and the number of blood vessels in the wounded area regress and decrease.

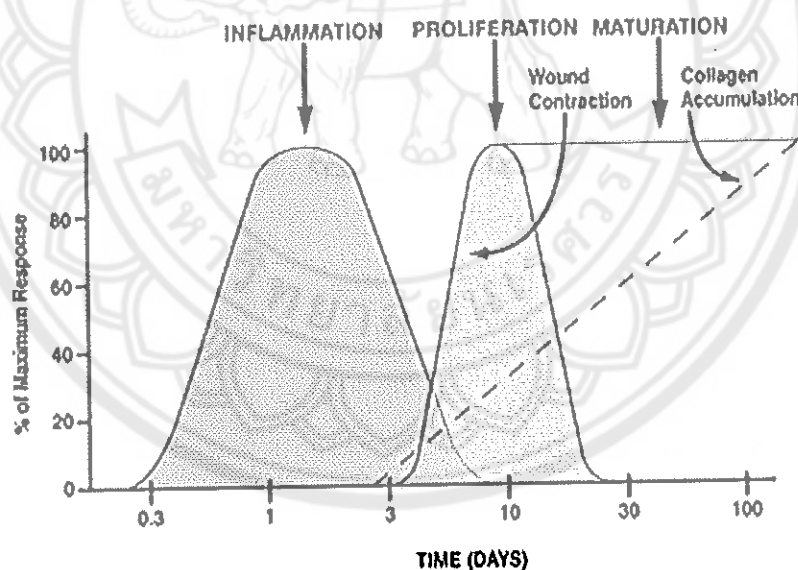


**Figure 9 Phases of wound healing with times**

### **Information of scaffolds**

Human skin failure caused by injuries, burnt or other types of damage is one of the most problems to suffer the patients. Operation can cause the infection, lack of

biocompatibility and limited durability [25]. Therefore, tissue engineering scaffold is selected to help increasingly as a good platform technology that promises not only skin transplantation but also presentation of a new treatment of skin repair in a field of research technology [26]. Scaffolds are generally referred to as the tissue engineering triad, the key components of engineered tissues. Scaffolds, typically made of polymeric biomaterials, provide the structural support for cell attachment and subsequent tissue development. Scaffolds used in tissue engineering applications should demonstrate compatible biological and physical properties, which match the physiological conditions in vitro and in vivo. The major function of the scaffolds is to provide a temporary support to body structures to allow the stress transfer over-time to injured sites, and facilitate tissue regeneration on the scaffolds [27].

Apart from blood cells, most, if not all other, normal cells in human tissues are anchorage-dependent residing in a solid matrix called extracellular matrix (ECM). There are numerous types of ECM in human tissues, which usually have multiple components and tissue-specific composition. Readers are directed to detailed reviews for types of ECM [28] and their tissue-specific composition [29]. As for the functions of ECM in tissues, they can be generally classified into five categories. Table 7 shows the functions of extracellular matrix (ECM) in native tissues and of scaffolds in engineered tissues.

**Table 7 Functions of extracellular matrix (ECM) in native tissues and of scaffolds in engineered tissues**

| <b>Functions of ECM in native tissues</b>                                 | <b>Analogous functions of scaffolds in engineered tissues</b>   | <b>Architectural, biological, and mechanical features of scaffolds</b>  |
|---|---|---|
| 1. Provides structural support for cells to reside                        | Provides structural support for exogenously applied cells to attach, grow, migrate and differentiate in vitro and in vivo       | Biomaterials with binding sites for cells; porous structure with interconnectivity for cell migration and for nutrients diffusion; temporary resistance to biodegradation upon implantation |
| 2. Contributes to the mechanical properties of tissues                    | Provides the shape and mechanical stability to the tissue defect and gives the rigidity and stiffness to the engineered tissues | Biomaterials with sufficient mechanical properties filling up the void space of the defect and simulating that of the native tissue   |
| 3. Provides bioactive cues for cells to respond to their microenvironment | Interacts with cells actively to facilitate activities such as proliferation and differentiation                                | Biological cues such as cell-adhesive binding sites; physical cues such as surface topography   |
| 4. Acts as the reservoirs of growth factors and potentiates their actions | Serves as delivery vehicle and reservoir for exogenously applied growth-stimulating factors                                     | Microstructures and other matrix factors retaining bioactive agents in scaffold   |

Table 7 (cont.)

| <b>Functions of<br/>ECM in native<br/>tissues</b>   | <b>Analogous functions<br/>of scaffolds in<br/>engineered tissues</b>                 | <b>Architectural, biological, and<br/>mechanical features of scaffolds</b>  |
|---|---|---|
| 5. Provides a flexible physical environment to allow remodeling in response to tissue dynamic processes such as wound healing | Provides a void volume for vascularization and new tissue formation during remodeling | Porous microstructures for nutrients and metabolites diffusion; matrix design with controllable degradation mechanisms and rates; biomaterials and their degraded products with acceptable tissue compatibility |

Firstly, ECM provides structural support and physical environment for cells residing in that tissue to attach, grow, migrate and respond to signals. Secondly, ECM gives the tissue its structural and therefore mechanical properties, such as rigidity and elasticity that is associated with the tissue functions. For example, well-organized thick bundles of collagen type I in tendon was highly resistant to stretching and are responsible for the high tensile strength of tendons. On the other hand, randomly distributed collagen fibrils and elastin fibers of skin are responsible for its toughness and elasticity. Thirdly, ECM may actively provide bioactive cues to the residing cells for regulation of their activities. For examples, the RGD sequence on fibronectin triggers binding events [30] while the regular topological pattern stimulates preferred alignment of cells [31]. Fourthly, ECM may act as reservoir of growth factors and potentiate their bioactivities. For example, heparin sulfate proteoglycans facilitate bFGF dimerization and thus activities [32]. Fifthly, ECM provides a degradable physical environment so as to allow neovascularization and remodeling in response to developmental, physiological and pathological challenges during tissue dynamic processes namely morphogenesis, homeostasis and wound healing, respectively.

Many techniques, including solvent casting/particulate leaching, gas foaming,

phase separation, fiber bonding and porogen leaching [33] electrospun nanofibers, salt-leached, hydrogels or freeform fabrication have been designed to fabricate scaffolds with the desired characteristics.

Hydrogels are ideally used as injectable scaffolds due to their mass is composed of water primarily, they can be used to fill irregularly shaped defects, allow minimally invasive surgical procedures and act as facilitator to incorporate with cells and bioactive agents [34].

Ideally, scaffolds for tissue engineering should meet several design criteria:

1. The surface should permit cell adhesion, promote cell growth, and allow the retention of differentiated cell functions;
2. The scaffolds should be biocompatible, neither the polymer nor its degradation by-products should provoke inflammation or toxicity in vivo;
3. The scaffold should be biodegradable and eventually eliminated;
4. The porosity should be high enough to provide sufficient space for cell adhesion, extracellular matrix regeneration, and minimal diffusional constraints during culture, and the pore structure should allow even spatial cell distribution throughout the scaffold to facilitate homogeneous tissue formation; and
5. The material should be reproducibly processable into three-dimensional structure, and mechanically strong [35].

#### **Free radical polymerization [36]**

In step-growth polymerization reactions it is often necessary to use multifunctional monomers if polymer with high molar masses are to be formed; this is not the case when addition reaction are employed. Long chains are readily obtained from monomers such as vinylidene compounds with the general structure  $\text{CH}_2=\text{CR}_1\text{R}_2$ . These are bifunctional units, where the special reactivity of  $\pi$ -bonds in the carbon to carbon double bond makes them susceptible to rearrangement if activated by free-radical or ionic initiators. The active center created by this reaction then propagates a kinetic chain, which leads to the formation of a single macromolecule whose growth is stopped when the active center is neutralized by a termination reaction. The complete polymerization proceeds in three distinct stages:

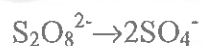
1. Initiation, when the active center which acts as a chain carrier is created;

2. Propagation, involving growth of the macromolecular chain by a kinetic chain mechanism and characterized by a long sequence of identical events, namely the repeated addition of a monomer to the growing chain; and

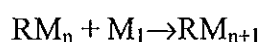
3. Termination, whereby the kinetic chain is brought to a halt by the neutralization or transfer of the active center.

Typically the polymer formed has the same chemical composition as the monomer, i.e., each unit in the chain is a complete monomer, and not a residue as in most step-growth reactions [36].

An effective initiator is a molecule that, when subjected to heat, electromagnetic radiation, or chemical reaction, will readily undergo homolytic fission into radicals of greater reactivity than the monomer radical. These radicals must also be stable long enough to react with a monomer and create an active center. Particularly useful for kinetic studies are compounds containing an azonitrile group, as the decomposition kinetics are normally first order, and the rates are unaffected by the solvent environment. For this work, persulfates are useful in emulsion polymerizations where decomposition occurs in the aqueous phase, and the radical diffuses into a hydrophobic, monomer containing, droplet.



A chain carrier is formed from the reaction of the free radical and a monomer unit; chain propagation then proceeds rapidly by addition to produce a linear polymer.

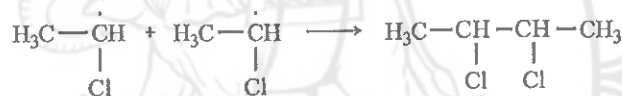


The average lifetime of the growing chain is short, but a chain of over 1000 units can be produced in  $10^{-2}$  to  $10^{-3}$  s. Bamford and Dewar have estimated that the thermal polymerization of styrene at 373 K lead to chains of  $x = 1650$  in approximately 1.24 s, i.e., a monomer adds on once in every 0.75 seconds

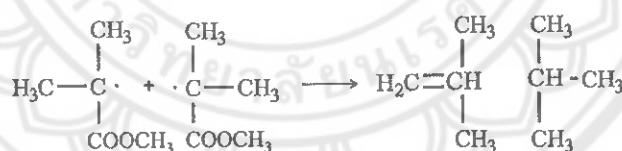
In theory, the chain could continue to propagate until all the monomer in the system has been consumed, but for the fact that free radicals are particularly reactive species and interact as quickly as possible to form inactive covalent bonds. This means that short chains are produced if the radical concentration is high because the probability of radical interaction is correspondingly high, and the radical concentration should be kept small if long chains are required. Termination of chains can take place in several ways by: (1) the interaction of two active chain ends, (2) the reaction of an active chain end with an initiator radical, (3) termination by transfer of the active center to another molecule which may be solvent, initiator, or monomer, or (4) interaction with impurities (e.g., oxygen) or inhibitors.

The most important termination reaction is the first, a bimolecular interaction between two chains end. Two routes are possible:

1. Combination, where two chain ends couple together to form one long chain.



2. Disproportionation, with hydrogen abstraction from one end to give an unsaturated group and two dead polymer chains.



One or both processes may be active in any system depending on the monomer and polymerizing conditions. Experimental evidence suggests that polystyrene terminates predominantly by combination, whereas poly(methyl methacrylate) terminates mainly by disproportionation when the reaction is about 333 K but by both mechanisms below this temperature. The mechanism can be determined by measuring the number of initiator fragments per chain using a radioactive initiator. One fragment per chain is counted when disproportionation is operative and two when combination occurs. Alternatively, the number-average molar mass of the product can be measured.

### Interpenetrating polymer network (IPN)

Interpenetrating polymer network (IPN) refers to a type of elastomer in which two chemically distinct networks coexist, ideally having a structure that is homogeneous down to the segmental level. As for the classification of IPN can be generally classified into 2 categories. Figure 10 shows the classification of IPN in different base on [34].

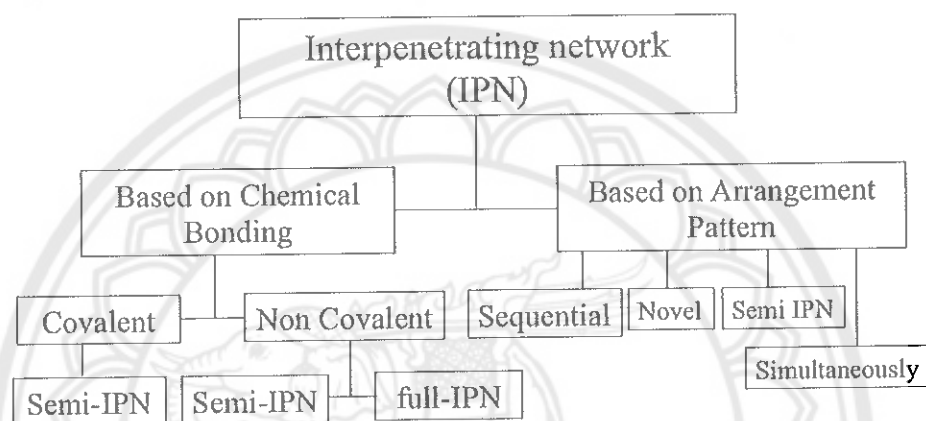


Figure 10 Classification of IPN in different base on [34]

Based on Chemical Bonding; Covalent cross linking leads to formation of hydrogels with a permanent network structure, since irreversible chemical links are formed. This type of linkage allows absorption of water and/or bioactive compounds without dissolution and permits drug release by diffusion; 1) Covalent Semi IPN- A covalent semi IPN contains two separate polymer systems that are cross linked to form a single polymer network; 2) Non Covalent Semi IPN- A non covalent semi IPN is one in which only one of the polymer system is cross linked; and 3) Non Covalent Full IPN- A non covalent full IPN is a one in which the two separate polymers are independently cross linked.

Based on Arrangement Pattern; 1) Sequential IPN- In sequential IPN the second polymeric component network is polymerized following the completion of polymerization of the first component network; 2) Novel IPN- Polymer comprising two or more polymer networks which are at least partially interlocked on a molecular scale but not covalently bonded to each other and cannot be separated unless chemical



bonds are broken; 3) Semi IPN- If only one component of the assembly is cross linked leaving the other in a linear form, the system is transferred as semi IPN; and (4) Simultaneously IPN- Simultaneously IPN is prepared by a process in which both component networks are polymerized concurrently, the IPN may be referred to as a simultaneously IPN.

Interpenetrating polymer networks (IPN) is composed of two or more different cross-linked polymers, are relatively new engineering materials. They have been among the fastest growing areas in the field of blends during the past twenty years. Interpenetrating polymerization represents an innovative approach to solving the problem of polymer incompatibility. IPNs are defined as blends of two or more polymer networks where at least one polymer component is prepared or cross-linked in the immediate presence of others. 2–4 Besides ideal or full IPNs, in which both components are cross-linked independently of each other, there are also other types of IPNs such as semi-IPNs or grafted-IPNs. Semi-IPNs have only one component cross-linked, while grafted-IPNs have covalent cross-links between both networks [37].

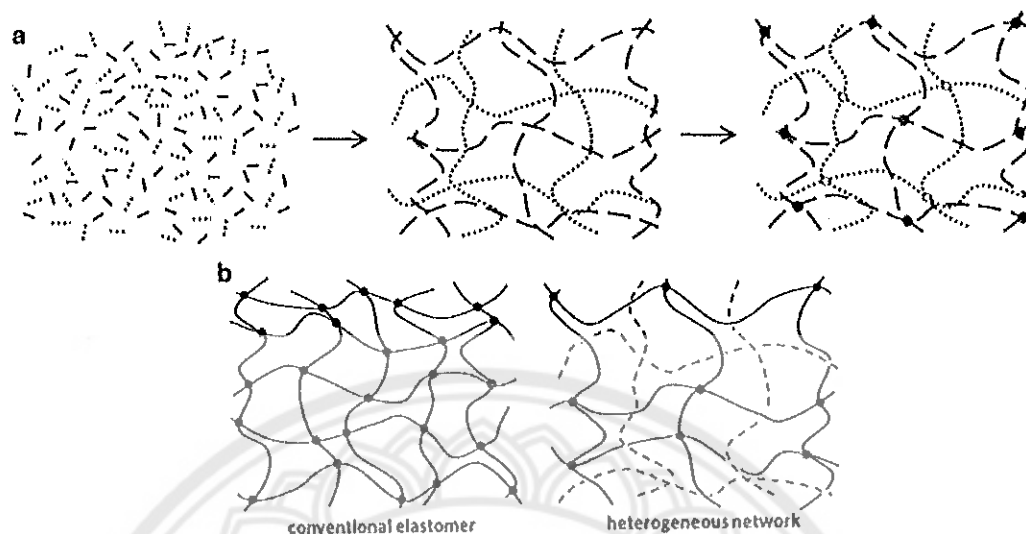


**Figure 11** (Upper) Simultaneous IPN, prepared by polymerization and cross-linking of a mixture of two monomers or two linear pre polymers, with phase separation suppressed due to the rapidly increasing viscosity; (lower) sequential IPN, in which a network is swollen in monomers, the subsequent polymerization and cross-linking of which yields an IPN; phase separation is usually greater for sequential IPNs [38]

From figure 11 (upper), both components of a full IPN are present as cross-linked networks, although there is negligible bonding between the two polymers. These can be prepared sequentially or simultaneously. Although the constituent polymers are incompatible, phase segregation is constrained by network formation, leading to small phase domains, and hence the potential for homogenization of the properties. Because of the small domains, IPNs can yield transparent materials even if the components have large refractive index differences [38]. While semi-IPN (figure 11b) comprises of one or more networks, and one or more linear or branched polymer or oligomer that penetrate into the polymer network [39]. In a semi-IPN, only one polymer is present as a network. This enhances the miscibility in comparison to a full IPN, although the mobility of the uncross-linked component increases the potential for phase segregation if the components are not thermodynamically compatible.

## Objective

The objective of this research work was separated into two parts depending on the technique and the type of materials used to fabricate two types of skin scaffolds base on biomaterials that explored for the advanced tissue engineering scaffolds, highlighting their potential for skin tissue regeneration.

**Approach I :** To fabricate the 3D porous scaffolds from silk sericin and poly(vinyl alcohol) for dermal reconstruction by classical condensation reaction, and to study the characteristic properties of the 3D porous scaffolds such as morphology, cell proliferation and cell adhesion.

**Approach II :** To fabricate 3D porous semi-interpenetrating polymer network hydrogels scaffold from hydroxyethyl acrylamide (HEA) and silk sericin by a conventional free-radical polymerization, and to study the characteristic properties of the synthesized hydrogel scaffolds such as mechanical properties, cell attachment, cell proliferation ability.

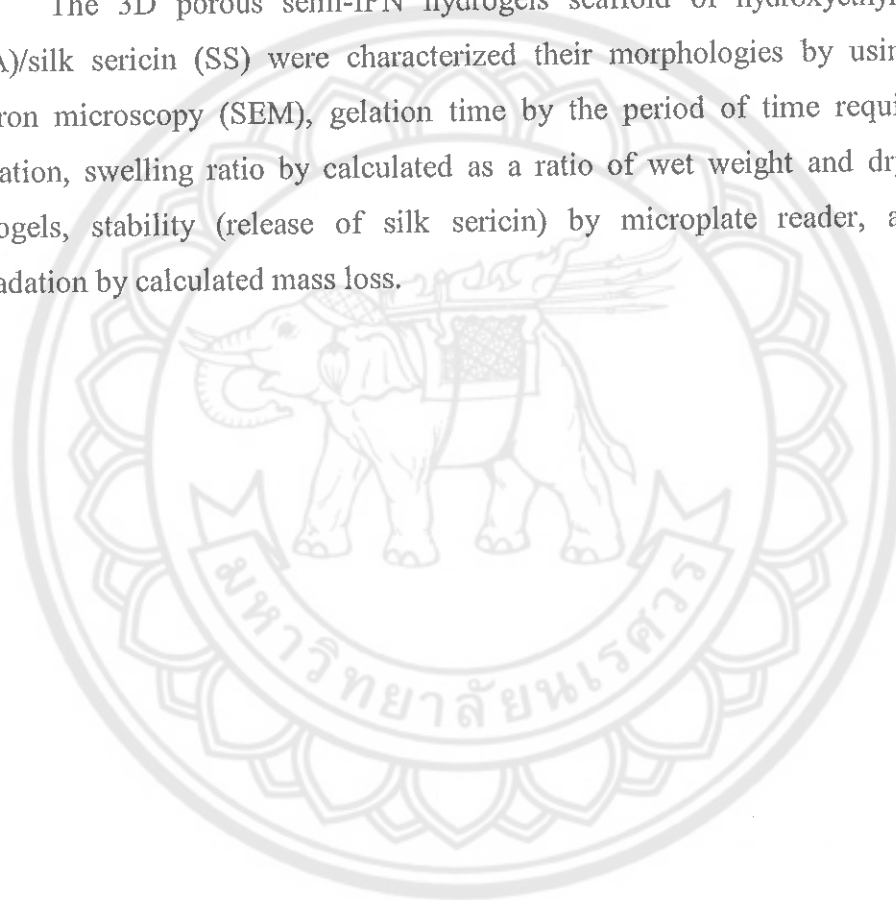
## Overview of the research

The overview of this research work was divided into two approaches, the first approach is the fabrication of the 3D porous scaffolds of poly(vinyl alcohol) (PVA) and silk sericin (SS) with different concentrations of dimethylolurea (DMU) using as a cross-linker. The second approach is the fabrication of 3D porous hydrogels using hydroxylethyl acrylamide (HEA), as a monomer to polymerize into poly(hydroxylethyl acrylamide) *via* free-radical polymerization, and silk sericin (SS) to form a semi-interpenetrating polymer network (semi-IPN) for using as dermal reconstruction scaffold. These approaches used the technique called lyophilization to promote the porous structures.

**Approach I :** Three-dimensional (3D) porous scaffolds of PVA/SS with different concentrations of dimethylolurea (DMU), used as a cross-linker, were studied. The three-dimensional (3D) porous scaffolds of PVA/SS were characterized their morphology by using scanning electron microscopy (SEM), cell proliferation by MTT assay, and cell adhesion by counting the number of cell in PBS solution using a hemocytometer to find the best composition for the scaffold that would be suitable for skin reconstruction.

**Approach II :** Fabrication of hydrogel scaffold of silk sericin (SS) and hydroxyethyl acrylamide (HEA) *via* conventional free radical polymerization, in the form of a semi-interpenetrating network (semi-IPN). First, preparation of silk sericin and then fabrication of hydrogel scaffold, and the effect of cross-linker and sericin content were also studied and characterization of semi-interpenetrating network to find the best compositions and conditions to support for the skin fibroblast cells, as well as promoted cell proliferation.

The 3D porous semi-IPN hydrogels scaffold of hydroxyethyl acrylamide (HEA)/silk sericin (SS) were characterized their morphologies by using scanning electron microscopy (SEM), gelation time by the period of time required for gel formation, swelling ratio by calculated as a ratio of wet weight and dry weight of hydrogels, stability (release of silk sericin) by microplate reader, and in-vitro degradation by calculated mass loss.



## CHAPTER II

### LITERATURE REVIEW

This chapter contains with the information of materials, instruments and the research methodology used in this research work. The work can be divided into two approaches depending on types of materials used to fabricate two types of skin scaffolds. The first approach is the fabrication of the 3D porous scaffold of poly(vinyl alcohol) (PVA) and silk sericin (SS) with different concentrations of dimethylolurea (DMU) using as a cross-linker. The second approach is the fabrication of 3D porous hydrogel using hydroxyethyl acrylamide (HEA), as a monomer to polymerize into poly(hydroxyethyl acrylamide) *via* free-radical polymerization, and silk sericin (SS) to form a 3D porous semi-interpenetrating polymer network (semi-IPN) for using as dermal reconstruction scaffold. This chapter, therefore, will be the literatures of the research works that related to this work, in three parts, as follows;

1. Information and applications of silk sericin in biomaterials,
2. Poly(vinyl alcohol) based biodegradable and biocompatible materials
3. Design and requirement to fabricate into scaffolds for tissue engineering.

#### Information and applications of silk sericin in biomaterials

Silk cocoon derived from silkworm *Bombyx mori* is a natural protein that is mainly made of silk sericin and fibroin proteins. Silk sericin constitutes 25–30% of silk protein and it envelops the fibroin fiber with successive sticky layers that help in the formation of a cocoon. Silk sericin ensures the cohesion of the cocoon by gluing silk threads together. Most of the silk sericin must be removed during raw silk production at the reeling mill and the other stages of silk processing. At present, silk sericin is mostly discarded in silk processing wastewater. The cocoon production is about 1 million tons (fresh weight) worldwide and this is equivalent to 400,000 tons of dry cocoon. Processing of this raw silk produces about 50,000 tons of silk sericin. If this silk sericin protein is recovered and recycled, it can represent a significant economic and social benefit [40]. It has been previously reported that silk sericin is

non-toxic to fibroblast cells [41] and enhances wound healing by promoting collagen production in wounds [42]. Approximately 30% of the amino acid content of silk sericin is serine, the chief moistening factor of natural human skin [43]. Thus, it consists of a polar side chain made of hydroxyl, carboxyl and amino groups that enable easy cross-linking, copolymerization and blending with other polymers to form improved biodegradable materials [44].

Silk sericin has been known as biocompatible and biodegradable material that having high thermal stability, minimal inflammatory reaction, and good water vapor permeability [45]. Therefore, it has potential to use in many applications, such as food, cosmetic and especially in medical applications. Thus, it is this reason why we choose silk sericin to form with a biopolymer to fabrication into scaffold for tissue engineering. However, silk sericin forms fragile materials that are not suitable for use in medical applications, but Mandal et al. demonstrated that after blending with gelatin, silk sericin can form a scaffold and be a good candidate for tissue engineering applications [46].

Therefore, the form in the field of medical applications, biodegradable synthetic polymers are more attractive than their non-biodegradable brethren for many materials applications, particularly when considering their disposal at the end of their useful lifetimes as they pose fewer environmental hazards. In this context a number of researchers have investigated the properties of composite materials composed of silk proteins and biodegradable polymers for a variety of applications [13]. Silk sericin has been used by mixing with biocompatible polymers, such as polyacrylamide [41], poly(vinyl alcohol) (PVA) and fabricated mostly into the form of film [47], hydrogel and tissue engineering scaffold [43]. This review details the many applications of silk sericin.

Kundaet al. [48] presents the formulation of non-mulberry tropical tasar cocoon sericin hydrogels of *Antheraea mylitta* through the physical entrapment of silk sericin within the 3D hydrophilic network of polyacrylamide. The interconnected three-dimensional hydrophilic networks perfectly manage typical dermal wounds by suitably scaffolding skin fibroblast, diffusing the nutrients, therapeutics and exudates while still maintaining an adequately moist environment. Figure 12 shows the results of mechanical stability of the equilibrium swelled sericin/polyacrylamide cylindrical hydrogels.

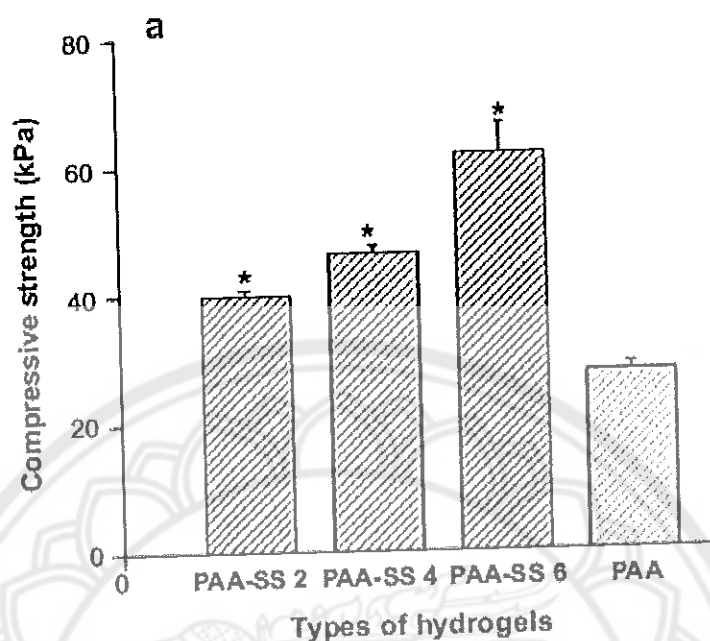


**Figure 12** Mechanical stability of the equilibrium swelled sericin/polyacrylamide cylindrical hydrogels of 10 mm thick and 13 mm in diameter as a function of various sericin composition: (a) Compressive strength ( $n=3$ , mean  $\pm$  SD,  $*p < 0.05$ ) [48]

The compressive strength of the completely swollen hydrogels was investigated by a dynamic mechanical analysis method. The composite hydrogels were stable in contrast to pure brittle polyacrylamide hydrogels and were easily compressed, during which the hydrogels excreted the imbibed PBS. With the increasing concentration of silk sericin from 2 to 6%, the corresponding compressive strength of the hydrogels improved from 40 kPa to 61 kPa ( $p < 0.05$  ANOVA). Pure polyacrylamide hydrogels exhibited the lowest compressive strength of 27.6 kPa. Thus, comparative measurement of compressive modulus supported the observation of compressive strength [48].

Aramwit et al. Silk sericin and PVA scaffold was prepared and studied the effect of a plasticizer (glycerin) and a cross-linker (genipin). They concerned that, the three-dimensional silk sericin and PVA scaffolds cross-linked with genipin at various

concentrations that will have potential in tissue engineering due to their low toxicity [49].

In other work, Aramwit et al. [50] aimed to develop the new delivery system to control the release of silk sericin. This study, the silk sericin/alginate microparticles could be successfully fabricated by electrospraying technique for the delivery of silk sericin in a rate-controlled manner. The entrapment efficiency and release behavior of silk sericin depended mainly on the concentration of silk sericin and alginate solutions. The results from this preliminary study would be beneficial for further development of microparticles by means of electrostatic forces to deliver silk sericin in order to achieve its biological effects at a target site [50].

#### **Poly(vinyl alcohol) based biodegradable and biocompatible materials**

Poly(vinyl alcohol) (PVA) is recognized as one of the very few vinyl polymers soluble in water also susceptible of ultimate biodegradation in the presence of suitably acclimated microorganisms. Accordingly, increasing attention is devoted to the preparation of environmentally compatible PVA-based materials for a wide range of applications [51]. The biodegradation behaviors of several PVA-based materials including blend and composites are also reviewed and discussed.

Kunduet et al. [52] reported a novel biopolymeric matrix fabricated by chemically cross-linking poly (vinyl alcohol) blended silk sericin protein obtained from cocoons of the tropical tasar silkworm *Antheraea mylitta*. These findings prove the potential of non-mulberry silk sericin/poly (vinyl alcohol) hydrogel matrices to be used as biocompatible and biopolymeric material for tissue-engineering and biotechnological applications. Figure 13 shows the confocal microscopic images of cells on PVA films for different levels of silk sericin content, after one day of culture.



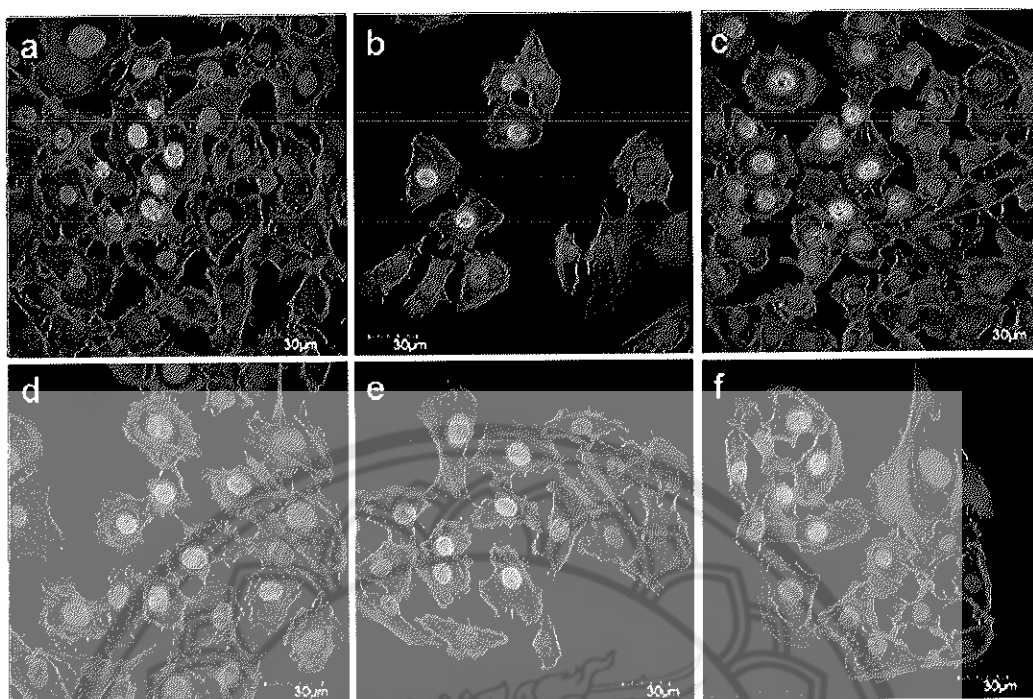


**Figure 13** Confocal microscopic images of fibroblast cells grown on (a) polystyrene plates, cross linked PVA films with different wt% sericin concentrations of (b) 0% (S0), (c) 0.5% (S0.5), (d) 1% (S1), (e) 2% (S2) and (f) 5% (S5)

Confocal microscopic images were taken after one day of culture to indicate the level of initial attachment on the films. Figure 13a shows cells growing on control polystyrene plates. Figure 13b–f show cells on S0, S0.5, S1, S2 and S5, respectively. S0.5 and S1 show cell attachment comparable to polystyrene control, whereas cells fail to attach appreciably on S0 [52].

Polymer composites containing lignocellulosic materials from agri-food industrial waste were prepared using sugar cane bagasse (SCB), orange and apple peels, and PVA as a continuous matrix [53]. Films were cast from PVA/water suspensions containing different types and amounts of lignocellulosic fibers, with or without the addition of plasticizers and crosslinking agents. In particular, glycerol and urea were utilized as plasticizers, the latter being a well-known nitrogen fertilizer chosen because of the PVA/lignocellulosic composites in agricultural applications.

### **Design and requirement to fabricate silk into scaffolds for tissue engineering**

Skin is composed of an outer layer epidermis, which provides physical strength and flexibility to the skin. The dermis underlying epidermis structured with fibroblasts, being composed predominantly of an ECM of interwoven collagen fibrils. Hence, current design requirement for any tissue engineering skin substitute is that of a biodegradable scaffold through which fibroblasts can infiltrate and populate [25].

A recent report by Ravichandran et al. stated that a dermal reconstruction scaffold is successful, in a complex phenomenon involving interactions between epidermal and dermal cells and ECM [26]. An ideal dermal reconstruction scaffold should be composed of nano or micro-diameter fibers and mimic the structure and morphology of the extracellular matrix (ECM) components in the skin [54, 55]. However the widespread therapeutic use (e.g. for replacing/restoring malfunctioning tissues) of collagen and proteoglycans in the clinic is limited due to their cost – an attractive alternative is the use of combinations of cheaper bio/synthetic polymers [56]. For example, PLLA/PAA/Col I&III nano-fibrous scaffold supports ADSCs proliferation, differentiation and collagen expression serving as a prognostic device for skin regeneration [26]. In addition, scaffolds should have high porosity in order to provide sufficient space and surface for cell seeding into the temporary scaffold before implantation and can be able to completely degrade and be eliminated from the body [57].

Yeo et al. studied composites based on silk proteins and other proteins, electrospun fibers composed of *B. mori* fibroin and type I calf skin collagen that were cross-linked with glutaraldehyde were demonstrated to support cell adhesion and proliferation of both human epidermal keratinocytes (NHEK) and fibroblasts (NHEF) cells in vitro. Interestingly, electrospun fibers composed of unmixed *B. mori* fibroin and type I calf skin collagen (that were prepared by electrospinning from two syringes simultaneously and subsequently cross-linked with glutaraldehyde) showed much higher levels of cell adhesion and proliferation for NHEK cells in vitro [58].

Lv et al. produced foams composed of *B. mori* fibroin and either type I bovine collagen or recombinant produced human-like collagen were demonstrated to support cell adhesion and proliferation of human hepatocellular carcinoma (HepG2) cells in vitro, with significant improvements in both adhesion and proliferation in comparison to films composed of *B. mori* fibroin alone [59].

Gil et al. embedding collagen coated *B. mori* fibroin fibers within foams composed of mixtures of collagen, hyaluronic acid and chondroitin-6-sulfate, yields materials that were shown to support cell adhesion and proliferation of human anterior cruciate ligament cells in vitro at levels markedly improved from collagen coated *B. mori* fibroin fibers alone. In vivo studies of these composites implanted in dogs showed the formation of new blood vessels and minimal inflammatory reaction after 6 weeks [60]. In vitro studies performed on foams composed of *B. mori* fibroin and hyaluronic acid showed improved adhesion and proliferation of human mesenchymal stem cells [61] and primary neural cells (cortical neurons from rat embryos) [62] in comparison to either of the constituent polymers alone.

Composite materials (in which microspheres composed of alginate and *A. mylitta* fibroin were embedded in *A. mylitta* fibroin foams) were shown to support the adhesion and proliferation of AH927 fibroblast cells in vitro [63]. Interestingly, the differentiation of human mesenchymal stem cells in vitro was demonstrated to be determined by the growth factor released from *B. mori* fibroin microspheres (containing either osteogenic bone morphogenic protein-2 or chondrogenic insulin-like growth factor) dispersed in alginate hydrogels [64].

In situ forming hydrogels are one of a good way to make a soft tissue reconstruction similar to skin due to reducing invasive surgical complications, low risk of infection, readily covering up the wounds without wrinkling [20], and a strong tissue-hydrogel interface.

Kunduet al. [65] blended sericin/gelatin 3-D scaffolds were highly porous with an optimum pore size of  $170 \pm 20$   $\mu\text{m}$ . The scaffolds were robust with enhanced mechanical strength and showed high compressibility. Figure 14 shows scanning electron microscopy images (SEM image) of silk protein sericin/gelatin matrices.

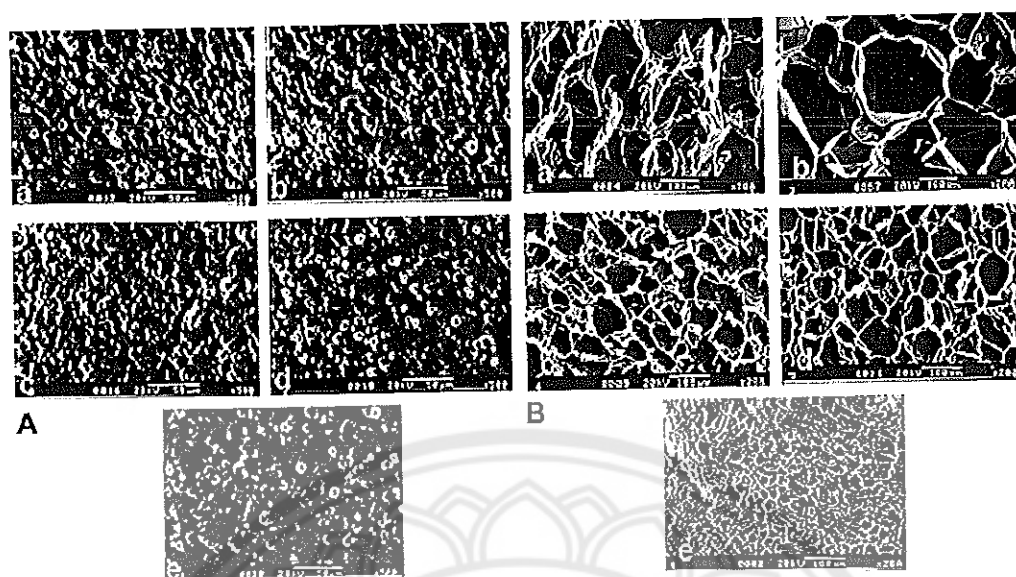


**Figure 14** Scanning electron microscopy images of silk protein sericin/gelatin matrices. (A) 2-D films with sericin/gelatin wt.% ratios of (a) 0.5:5, (b) 1:5, (c) 2.5:5, (d) 5:5, (e) 7.5:5. (B) 3-D scaffolds with sericin/gelatin wt.% ratios of (a) 2:2, (b) 2:5, (c) 5:2, (d) 5:5, (e) 5 wt.% pure gelatin scaffold. For all films in (A) the magnification bar represents 50  $\mu\text{m}$ , while for the scaffolds in (B) the magnification bar represents 100  $\mu\text{m}$  [65]

Zhou et al. used poly(L-lactide) is a popular polymer for biomedical applications due to its biodegradability. Electrospun fibers composed of *Agelena labyrinthica* spidroin and poly(D,L-lactide) were demonstrated to support cell adhesion and proliferation of African green monkey kidney [CCL81 Vero] cells in vitro [66].

S. Wang et al. used electrospun fibers with a core-shell morphology in which the core was composed of *B. mori* fibroin and gelatin and the surface was poly(L-lactide) were demonstrated to support cell adhesion and proliferation of 3T3 mouse fibroblasts and human umbilical vein endothelial cells in vitro. Tubes formed of such fibers are currently being investigated for application as artificial blood vessels due to their biocompatibility, mechanical properties and porosity [67].

Chen et al. composite materials in which a *B.mori* fibroin foam filled the pores of a poly(caprolactone) foam were shown to support cell adhesion and proliferation of human fibroblast (ATCC HFL-1) cells in vitro better than foams composed solely of poly(caprolactone) [68].

The biocompatibility of materials to be implanted in people (such as hip replacements) are sometimes rejected from the body, and biocompatible coatings such as silks are one method of improving their acceptance [56].

T. Arai et al. used poly(allylamine) is a polycationic polymer that is highly soluble in water that it utilized widely in biomedical applications. Films composed of *B.mori* fibroin and poly(allylamine) were found to be more stable in water than films composed only of poly(allylamine), and such films were demonstrated to support cell adhesion and proliferation of both insect (*A. pernyi* and *B.mori* silkworm) and mammalian (mouse fibroblast L929) cells in vitro better than either of the constituent polymers alone [69].

In another work, Mi-KyongYoo et al. [70] choose macromer, having an acrylated-terminated PEO derivative, as a blending material and cross-linked in the presence of SF to form the SIPNs to enhance the mechanical and functional properties of SF [70], shown in figure 15.

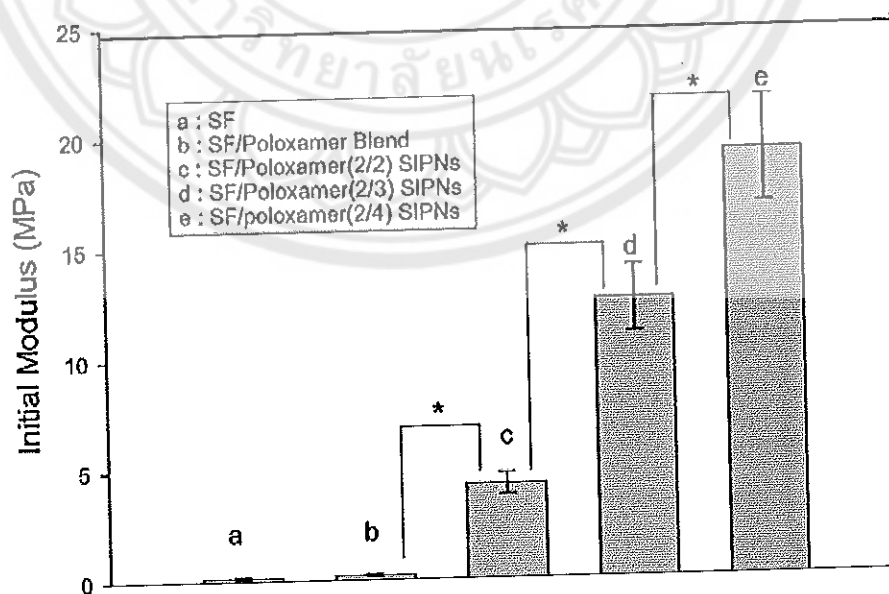


Figure 15 Initial modulus of SF, blend, and SF/poloxamer SIPNs [70]

From figure 15, the mechanical property of SF/poloxamer SIPNs in dry state, compressive mechanical tests were performed under a constant compression rate and figure 15 shows the initial modulus of SF, SF/poloxamer blend, and SF/poloxamer SIPNs. As expected, the resistance of SIPNs against compression was much higher by composition. Initial modulus of SIPNs increased with increasing amount of poloxamer macromer in the SIPNs due to the increased crosslinking density of poloxamer network.



## CHAPTER III

### RESEARCH METHODOLOGY

This chapter is concerned with the information of materials, instruments and the research methodology used in this research work. The work can be divided into two approaches depending on types of materials used to fabricate two different types of skin scaffolds. The first approach is the fabrication of the three-dimensional (3D) porous scaffold of poly(vinyl alcohol) (PVA) and silk sericin (SS) with different concentrations of dimethylolurea (DMU) using as a cross-linker. The second approach is the fabrication of 3D porous hydrogel scaffolds using hydroxylethyl acrylamide (HEA) as a monomer to polymerize into poly(hydroxylethyl acrylamide) *via* free-radical polymerization, and silk sericin (SS) to form a semi-interpenetrating polymer network (semi-IPN) for using as dermal reconstruction scaffold. These approaches used the technique called lyophilization to promote the porous structures.

#### Materials

**Table 8** The information of materials used in this work

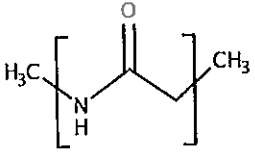
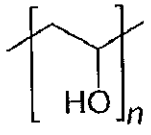
| Name   | Abbreviation | Chemical structures   | Sources/<br>Companies  | Use for   |
|--|--------------|---|--|---|
| Silk cocoons;<br>silk sericin<br>( <i>Bombyxmori</i> ) | SS           |  | Tak province in<br>the lower<br>northern region<br>of Thailand | Fabrication<br>scaffolds<br>(Approaches I,<br>II)       |
| Poly(vinyl<br>alcohol)                                 | PVA          |  | Sigma-Aldrich<br>Co. Inc,<br>Singapore<br>(PVA BF 17W)         | Fabrication 3D<br>porous<br>scaffolds<br>(Approaches I) |

Table 8 (cont.)

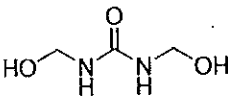
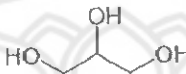
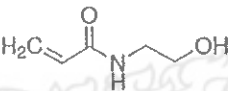
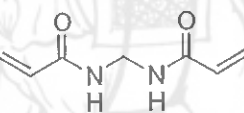
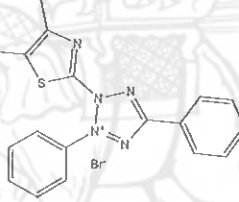
| Name   | Abbreviation   | Chemical structures   | Sources/<br>Company                                      | Use for  |
|--|----------------|---|--|--|
| Dimethylol urea                              | DMU            |    | Sigma-Aldrich<br>Co. Inc,<br>Singapore                   | Fabrication 3D<br>porous scaffolds<br>(Approaches I) |
| Glycerol                                     | -              |    | Sigma-Aldrich<br>Co. Inc,<br>Singapore                   | Fabrication 3D<br>porous scaffolds<br>(Approaches I) |
| Hydroxyl ethyl<br>acrylamide                 | HEA            |    | Sigma-Aldrich<br>Co. Inc,<br>Singapore                   | For forming<br>hydrogel<br>(Approaches II)           |
| N'N'-methylene<br>bisacrylamide              | N'N'-<br>MBAAm |  | Sigma-Aldrich<br>Co. Inc,<br>Singapore                   | For forming<br>hydrogel<br>(Approaches II)           |
| Ammonium<br>persulfate                       | APS            | -   | Sigma-Aldrich<br>Co. Inc,<br>Singapore                   | For forming<br>hydrogel<br>(Approaches II)           |
| N,N,N',N'-<br>tetramethylethyl<br>enediamine | TEMED          | -   | Sigma-Aldrich<br>Co. Inc,<br>Singapore                   | For forming<br>hydrogel<br>(Approaches II)           |
| Feline fibroblast<br>cell line               | HFF1           | -   | ATCC<br>(American<br>Type Culture<br>Collection,<br>USA) | For cell culture<br>test (Approaches<br>I,II)        |
| Dulbecco's<br>modified<br>eagle's medium     | (DMEM)<br>/F12 | -   | Sigma-Aldrich<br>(St. Louis,<br>MO)                      | For cell culture<br>test (Approaches<br>I,II)        |



Table 8 (cont.)

| Name   | Abbreviation | Chemical structures  | Sources/ Company         | Use for                                    |
|--|--------------|--|--------------------------|--|
| Fetal bovine serum   | FBS          | -  | Gibco (Grand Island, NY) | For cell culture test<br>(Approaches I,II) |
| Trypsin/EDTA (0.25%)   | -            | -  | Gibco (Grand Island, NY) | For cell culture test<br>(Approaches I,II) |
| 3-(4,5-dimethylthiazol-2-yl)-2,5-diphenyltetrazolium bromide; ultra pure grade | MTT          |  | Amresco®, Solon, USA     | For cell culture test<br>(Approaches I,II) |

### Instruments

1. Scanning Electron Microscope (SEM, Leo Model 1455VP)
2. Fourier Transform Infrared Spectroscopy (FT-IR, Perkin Elmer Spectrum GX, 4000-400  $\text{cm}^{-1}$ )
3. Differential Scanning Calorimeter (DSC, Mettler Model DAC1)
4. Microplate reader (Biotek, Model Synergy H1 Hybrid Reader)
5. Freeze dryer (MAXI dry lyo)
6.  $\text{CO}_2$  incubator for cell culture

### Preparation of silk sericin powders

The silk sericin (SS) powders were prepared from silk cocoons by a hot water degumming process, as shown in Figure 16. First, the silk cocoons were cut into small pieces and boiled with deionized (DI) water in the ratio of 20 grams of silk cocoon pieces: 500 milliliters of DI water at 90°C for 4 hours. Then, the silk fibroin was removed from the solution of silk sericin. Finally, silk sericin solution was taken into the oven under the temperature of 60 °C for 14 hours to obtain silk sericin powders. This silk sericin powders were stored in desiccator to avoid the moisture for ready to use anytime of experimental.

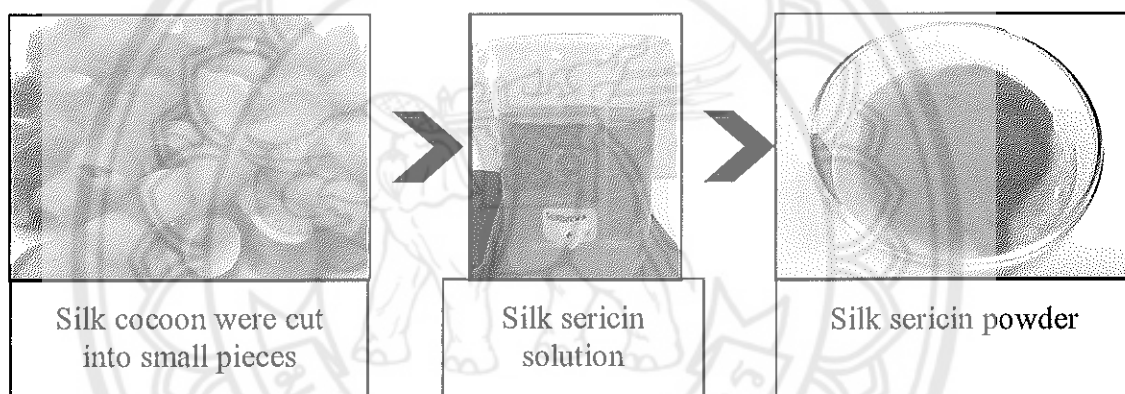


Figure 16 Schematic picture of preparation of silk sericin powders

### 3D porous scaffold of poly(vinyl alcohol) (PVA) and silk sericin (SS)

To produce 3D porous scaffold of poly(vinyl alcohol) (PVA) and silk sericin (SS), the PVA solution was first prepared as a stock solutions as well as the solution of dimethylol urea (DMU). Then, the 3D porous scaffolds of PVA/SS were manufactured using DMU as a cross-linker. In addition, the characterization of 3D porous scaffolds of PVA/SS; morphology and cell culture test (cell adhesion and proliferation), were studied. This detail information was described in the following sections.

### **Fabrication of 3D porous scaffold of PVA/SS**

#### **1. Preparation of PVA solution**

Poly(vinyl alcohol) (PVA) was purchased from Sigma-Aldrich Co. Inc, Singapore in the form of pellets. To prepare PVA solution, PVA pellets were weighed and dissolved in de-ionized water (DI water) at 80 °C with constant stirring for about 4 hours until they were completely dissolved to a concentration of 6wt/v%. This 6wt/v% PVA solution was stored in the refrigerator for future use.

#### **2. Preparation of DMU solution**

Dimethylol urea (DMU) was purchased from Sigma-Aldrich Co. Inc, Singapore in the form of pellets. The different concentrations of DMU, from 0wt% to 100wt% of total weight of silk sericin and PVA, were prepared and used as stock solutions.

#### **3. Fabrication of 3D porous scaffold of PVA/SS**

The 3D porous scaffolds of PVA/SS with different concentrations of dimethylol urea (DMU) were fabricated *via* classical condensation reaction following by the lyophilization technique. Figure 17 showed the schematic diagram of preparation of 3D porous scaffolds of PVA/SS with different concentrations of cross-linker (DMU) by lyophilization technique. The concentration of PVA and silk sericin were used at 6 wt% and 5 wt%, respectively. Glycerin was used as a plasticizer in this condensation reaction system to help for the flexible and penetration of PVA and silk sericin chains.

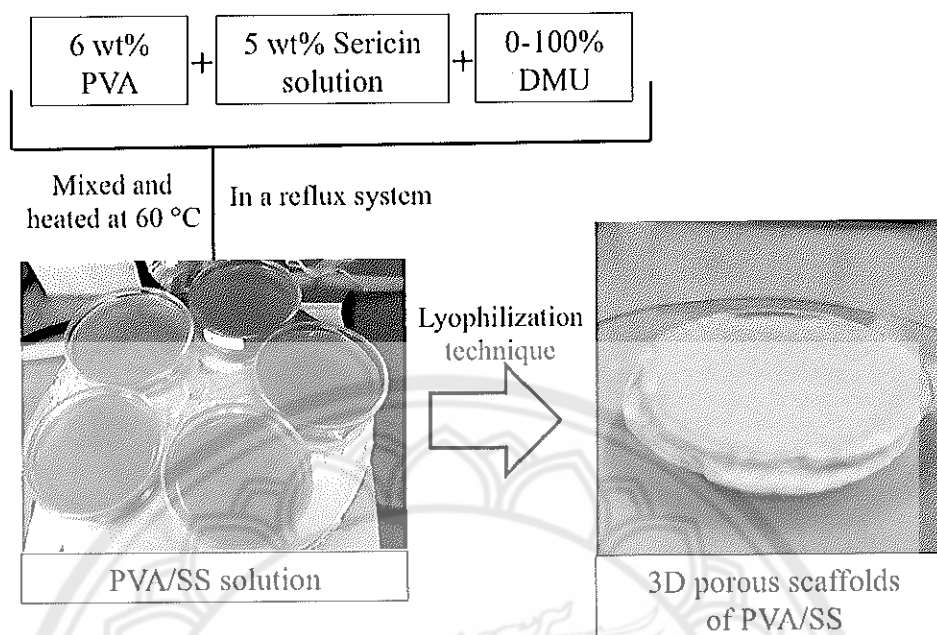


**Figure 17** Schematic diagram of preparation of three-dimensional (3D) porous scaffolds of PVA/SS with different concentrations of DMU *via* classical condensation reaction and followed by lyophilization technique

Silk sericin solution (5wt%), PVA solution (6wt%) with a ratio of 1:1, and glycerin solution (0.6 g/1 g of silk sericin) were mixed and heated at 60 °C in a reflux system. DMU at different concentrations (0, 10, 20, 60, 80 and 100%) was added to the mixed solution of silk sericin, PVA and glycerin and stirred for 5 min. Then the solution mixtures were poured into a petri dish and consequently freeze dried at -20 °C for 24 hours using the Ly-O machine to form the 3D porous scaffolds. After drying, the scaffolds were accurately weighed to calculate the percentage of each component in dry weight basis. The sample codes used in this work are from 0% DMU, 10% DMU, 20% DMU, 60% DMU, 80% DMU and 100% DMU PVA/SS. Table 9 shows the formula of the fabrication for preparation of 3D porous scaffolds of PVA/SS with different concentrations of DMU.

**Table 9 The formulation of the fabrication of 3D porous scaffolds of PVA/SS with different concentrations of DMU**

| Sample code     | PVA<br>(wt%) | Silk sericin (g) |      | DMU<br>(wt%)* | Glycerol (g)<br>per 1 g of SS |
|-----------------|--------------|------------------|------|---------------|-------------------------------|
|                 |              | g                | %w/v |               |                               |
| 0% DMU PVA/SS   | 6            | 0.25             | 5    | 0             | 0.6                           |
| 10% DMU PVA/SS  | 6            | 0.25             | 5    | 10            | 0.6                           |
| 20% DMU PVA/SS  | 6            | 0.25             | 5    | 20            | 0.6                           |
| 60% DMU PVA/SS  | 6            | 0.25             | 5    | 60            | 0.6                           |
| 80% DMU PVA/SS  | 6            | 0.25             | 5    | 80            | 0.6                           |
| 100% DMU PVA/SS | 6            | 0.25             | 5    | 100           | 0.6                           |

\*Used base on total weight of PVA and SS

### Characterization of 3D porous scaffolds of PVA/SS

#### 1. Morphology observation

The morphology of samples was analyzed using a Leo Model 1455VP scanning electron microscope (SEM) at 20 kV in high vacuum to observe the porous sizes, interconnecting of structure and surface of 3D porous scaffolds. Figure 18 shows schematic picture of Leo Model 1455VP scanning electron microscope (SEM). Both surface and cross-sectioned samples were dried by removing the moisture in the oven before mounted on metal stubs and coated with gold to give higher electron density cover before testing. The gold covered samples were placed onto the stage of the SEM machine. An electron beam is produced at the top of microscope by an electron gun. The electron beam passes through the microscope in a vertical direction and moves through electromagnetic fields and lenses, which focus the electron beam down toward the scaffolds. As the electron beam hits the scaffolds, electron and X-rays are ejected from the scaffolds.

In this work, the secondary electrons are collected and converted by detectors into a signal that is sent to a screen producing an SEM image. The average of porous scaffolds diameters was measured by SEM image at magnification of 100x.

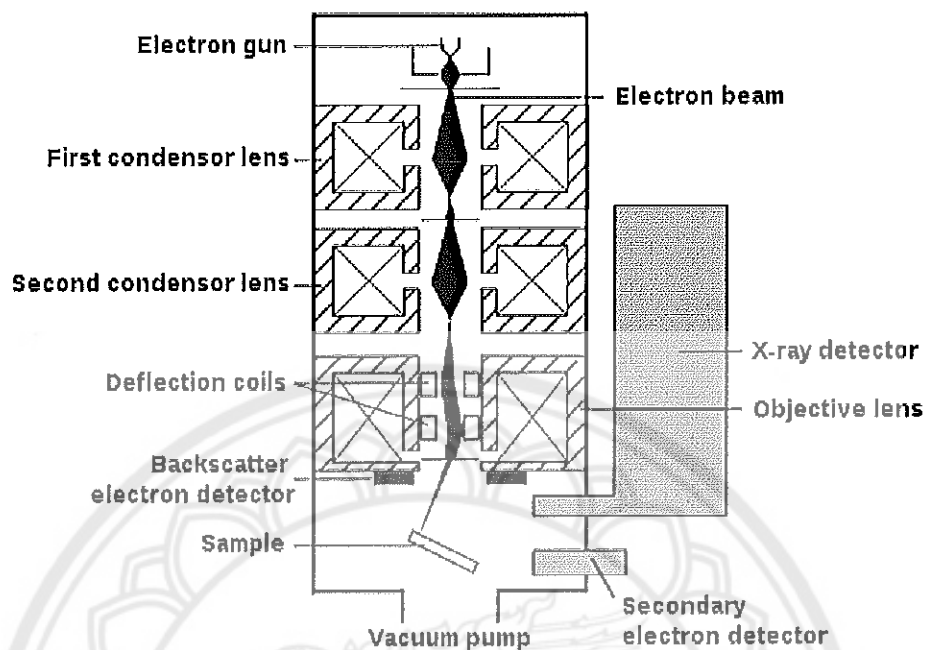


**Figure 18 Schematic picture of Leo Model 1455VP scanning electron microscope (SEM) [71]**

### **Cell culture test for 3D porous scaffolds of PVA/SS**

Cell culture study is a key factor for using scaffolds as a dermal reconstruction scaffold. Human feline fibroblasts cell line HFF-1 is cultured for seeding on the scaffold. Cell proliferation and cell toxicity are assayed using the MTT assay. In this cell culture test section, therefore, the information of the preparation of human feline fibroblasts cell line HFF-1 was first described, followed by the preparation of sterilized scaffolds and the cell seeding technique. The details of the study on cell proliferation under the MTT assay and cell adhesion were finally described.

#### **1. Preparation of feline fibroblasts cell line**

Fibroblasts cell line (HFF-1) were maintained in a 75 cm<sup>2</sup> culture flask at 37°C under 5% CO<sub>2</sub> humidified atmosphere. The human feline fibroblasts cell line HFF-1 cells were grown in DMEM/F12 medium supplemented with 10% FBS and the culture medium was replaced in every 2 days.

## 2. Sterilized scaffolds

Scaffolds were cut into cubes (0.5 x 0.5 x 0.5 cm) and placed into an autoclave at 121 °C for 20 minutes. The sterilized scaffolds were washed and soaked in a phosphate buffer solution (PBS - pH 7.4).

## 3. Cell seeding

For this work, scaffolds at 0, 10, 20, 80 and 100 %DMU were selected to study cell culture. The sterilized scaffolds were put in 1 mL of the medium (90 DMEM : 10 FBS) and left over night in a close system (incubator at 37 °C), then dehydrated in a cell culture hood for 3 hours to achieve the partially dehydrated scaffolds. Human feline fibroblast cell line (HFF1) ( $1 \times 10^6$  cells) with 200  $\mu$ L medium was dropped slowly into the partially dehydrated scaffolds. They were seeded into 96-well plates and allowed to attach for 2 hours before adding another 200  $\mu$ L of medium. Scaffolds with loaded cells were incubated for 2 days at 37 °C, the medium was changed and left for another day before doing the MTT assay. Figure 19 shows the electronic photograph of cell seeding into 3D porous scaffolds of PVA/SS.

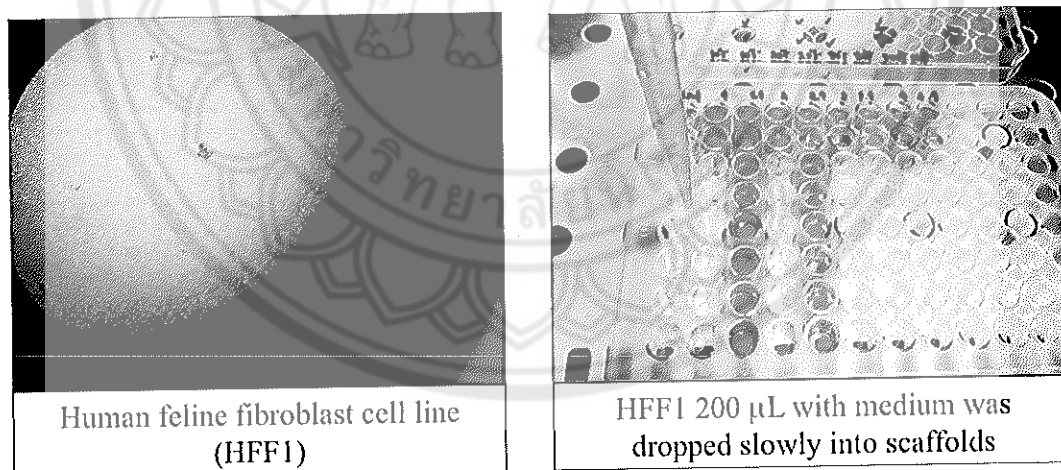


**Figure 19** Electronic photograph of human feline fibroblast cell line (HFF1,  $1 \times 10^6$  cells) (left: picture from optical microscope) seeded into 3D porous scaffolds of PVA/SS (right: scaffolds were in sterilized 96-well plate)

#### 4. Cell proliferation: MTT assay

MTT assay was used to study the viability of cells seeded on the scaffolds after 3 and 6 days in culture. In this assay, the active mitochondria of the viable cells reduce the yellow coloured solution of MTT (3-(4, 5-Dimethylthiazol-2-yl)-2, 5-diphenyltetrazolium bromide, a yellow tetrazole) into blue coloured formazan crystals, which is corresponding to cellular viability. Figure 20 shows the reaction of changing the yellow colour of MTT into the purple colour of formazan.

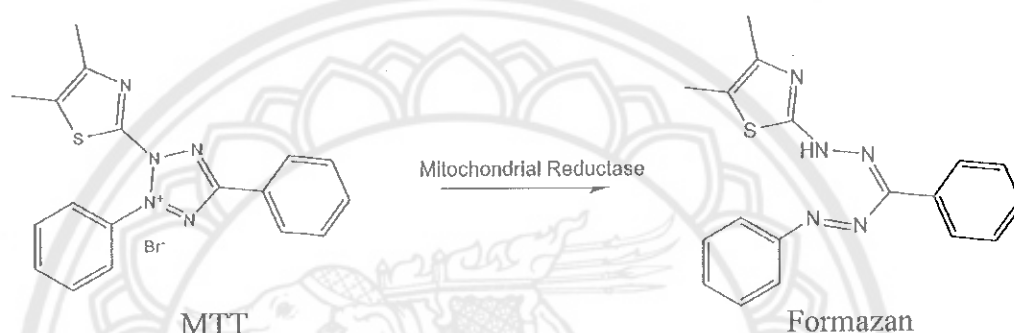


**Figure 20** The active mitochondria of the viable cells reduce the yellow coloured solution of MTT [72]

For cell proliferation, MTT solution was added into medium containing cell loaded scaffolds, and left for 4 hours in incubator at 37 °C before removal of medium. Scaffolds were put into vials and then 200  $\mu$ L of DMSO : ethanol (1:1 v/v) was added, and left over night (12 hours) before measuring the optical density (OD) by UV-Visible spectrophotometric microplate reader at 595 nm. The absorbance was corresponded to the number of proliferated cells [48]. The active mitochondria of the viable cells reduce the yellow coloured of MTT into blue coloured formazan crystals, which corresponds to cellular viability. The scaffolds with no cells and the controlled sample (no scaffold and cells) were also measured. The OD values of all loaded scaffolds were subtracted with the OD value of scaffolds that have no cells loading. Figure 21 shows an example of the 3D porous scaffold of PVA/SS with adding MTT solution at initiating time (left) and at 4 hours incubated at 37 °C.



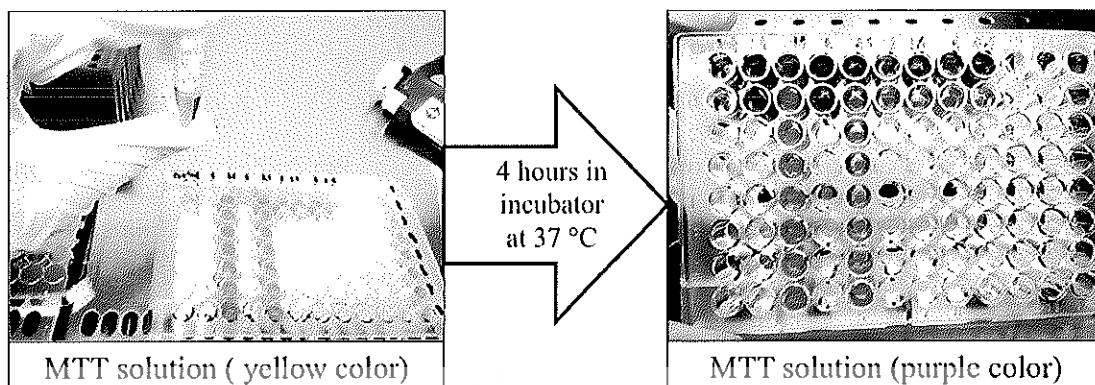


**Figure 21** The colour of samples after adding MTT solution into three-Dimensional (3D) porous scaffolds of PVA/SS

### 5. Cell adhesion

HFF1 were seeded into the sterilized scaffolds, which were incubated in a humidified atmosphere 5% CO<sub>2</sub> at 37 °C, with the same cell density, as mentioned in the cell seeding section [73]. To assay the attached cells, the percentage of fibroblast cell remaining attached onto the scaffolds within 1, 4, 8, 12, 24 hours after washed gently with 1 mL of PBS (pH 7.4). The number of cells adhering to each sample was calculated by subtracting the number of washed out fibroblasts cell from  $1 \times 10^6$  cells/scaffold. Three gels from each composition were measured by counting the number of cell in PBS solution using a hemocytometer [73]. Figure 22 shows area scale (middle) of cell count for calculated number of cell by the hemocytometer.

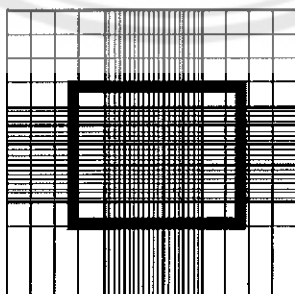


**Figure 22** The area scale (middle) of cell count for calculated number of cell by the hemocytometer

### **Three dimensional (3D) porous semi-IPN hydrogel scaffolds of poly(hydroxyethyl acrylamide) (PHEA)/silk sericin (SS)**

In this experimental section, the detail of fabrication the 3D porous semi-IPN hydrogel scaffolds of poly(hydroxyethyl acrylamide) (PHEA and silksericin) was first described. The characterization of the scaffolds; gelation time, morphology, swelling ratio, release of silk sericin, *in vitro* degradation as well as the cell culture test were also described to monitor the properties of this 3D porous semi-IPN hydrogel scaffolds of PHEA/SS.

#### **Fabrication of 3D porous semi-IPN hydrogel scaffolds**

3D porous semi-interpenetrating polymer networks hydrogel scaffolds composed of silk sericin (SS) and hydroxyethyl acrylamide (HEA) are prepared by conventional free-radical polymerization and fabricated in the 24 well-plates with different concentrations of cross-linker (N, N-methylenebisacrylamide) and amount of SS contents. Table 10 shows the formulation of the fabrication of 3D porous semi-IPN hydrogel scaffolds of PHEA/SS. The 0.5% w/w of cross-linker was selected to study the effect of SS loading into the scaffolds. The sample codes used in this work are from 0%XL PHEA/SS-5 to 2.0%XL PHEA/SS-5 or from PHEA-SS-0 to PHEA/SS-5, depending on percent of cross-linker and the silk sericin content. The effect of cross-linker and silk sericin contents onto the physical properties and *in vitro* cell culture test were investigated.

**Table 10** The formulation of the fabrication of 3D porous semi-IPN hydrogel scaffolds of PHEA/SS with different cross-linker and silk sericin contents

| Sample code                   | HEA<br>(g) | Silk sericin  |                              | Cross-<br>linker*<br>(wt%) | TEMED<br>*(wt%) | APS*<br>(wt%) |
|-------------------------------|------------|---------------|------------------------------|----------------------------|-----------------|---------------|
|                               |            | Weight<br>(g) | Concen<br>tration<br>(%wt/v) |                            |                 |               |
| <i>Effect of cross-linker</i> |            |               |                              |                            |                 |               |
| 0% XL PHEA/SS-5               | 5.556      | 0.25          | 5                            | -                          | 0.5             | 0.5           |
| 0.125% XL PHEA/SS-5           | 5.556      | 0.25          | 5                            | 0.125                      | 0.5             | 0.5           |
| 0.25% XL PHEA/SS-5            | 5.556      | 0.25          | 5                            | 0.25                       | 0.5             | 0.5           |
| 0.5%XL PHEA/SS-5              | 5.556      | 0.25          | 5                            | 0.5                        | 0.5             | 0.5           |
| 1.0 %XL PHEA/SS-5             | 5.556      | 0.25          | 5                            | 1.0                        | 0.5             | 0.5           |
| 2.0%XL PHEA/SS-5              | 5.556      | 0.25          | 5                            | 2.0                        | 0.5             | 0.5           |
| <i>Effect of SS loading</i>   |            |               |                              |                            |                 |               |
| PHEA/SS-0                     | 5.556      | -             | -                            | 0.5                        | 0.5             | 0.5           |
| PHEA/SS-1.25                  | 5.556      | 0.0625        | 1.25                         | 0.5                        | 0.5             | 0.5           |
| PHEA/SS-2.5                   | 5.556      | 0.125         | 2.5                          | 0.5                        | 0.5             | 0.5           |
| PHEA/SS-5                     | 5.556      | 0.25          | 5                            | 0.5                        | 0.5             | 0.5           |
| PHEA                          | 5.556      | -             | -                            | -                          | 0.5             | 0.5           |

\*Note :wt% of HEA used in the formulations.

The free radical polymerization was obtained by using the redox pairs of ammonium persulfate (APS) and N, N, N', N'-tetramethylenediamine (TEMED). The cross-link network was achieved by using N, N-methylenebisacrylamide (N, N'-MBAAm), as a cross-linker and hydroxyethyl acrylamide (HEA) were used as monomer.

For synthetic of semi-IPN porous hydrogel scaffolds PHEA/SS, silk sericin powders with 5 wt% was first prepared by dissolving in hot-water at 95 °C in a reflux system. Then hydroxyethyl acrylamide was added and continued to mix for 0.5 hours

before adding N’N-MBAAm (cross-linker) and TEMED (catalyst) at 40 °C. This mixture solution was then left to room temperature before adding APS (initiator) to start the reaction and pour into 24 well plates to form semi-IPN hydrogels. After finishing the reaction, the semi-IPN hydrogels was washed by de-ionized water and ethanol several times to remove the unreacted monomers and chemicals before further use. Finally, the semi-IPN hydrogel was lyophilized to obtain porous scaffold. Figure 23 shows the schematic picture of synthetic of 3D porous semi-IPN hydrogel scaffolds PHEA/SS by conventional free-radical polymerization.

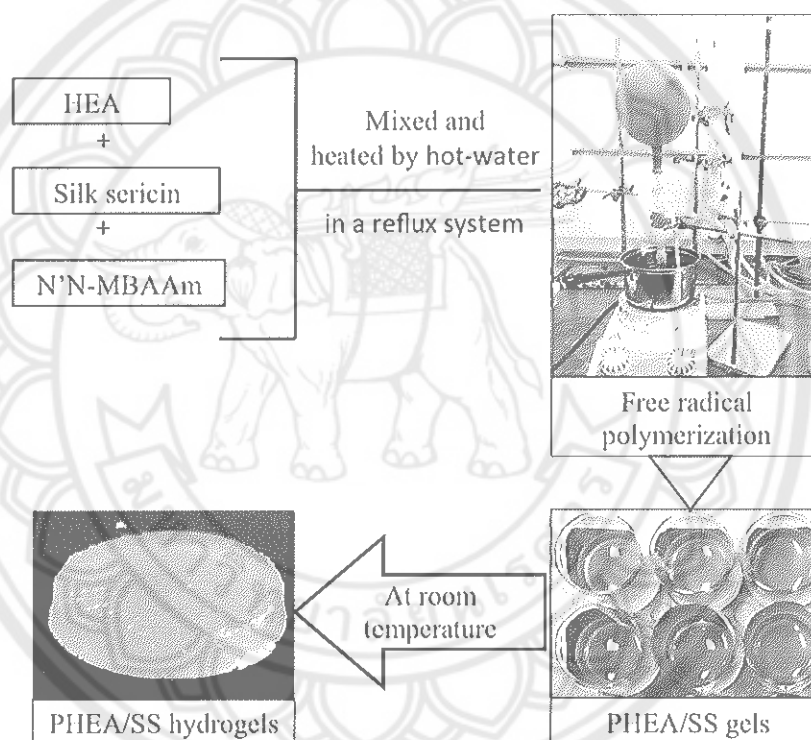


**Figure 23** Schematic picture of synthetic of 3D porous semi-IPN hydrogel scaffolds PHEA/SS by conventional free-radical polymerization

#### Characterizations of 3D porous semi-IPN hydrogel scaffolds of PHEA/SS

The effect of the amount of N’N-MBAAm (cross-linker) and SS onto the gelation time, release of silk sericin, swelling ratio, functional group, morphology and cell culture of scaffolds were studied. The detail information of the techniques are described in the following sections.

### **1. Gelation time of 3D porous semi-IPN hydrogel scaffolds of PHEA/SS**

The polymerization times of each sample were recorded as gelation time. This gelation time was designated as the period of time required for gel formation after adding initiator the last component added into the mixed solution until the complete cross-linked network structure or gel structure was constructed.

### **2. Morphology observation of 3D porous semi-IPN hydrogel scaffolds of PHEA/SS**

The morphology of 3D porous semi-IPN hydrogel scaffolds of PHEA/SS (pore size, surface and interconnected structures) is measured using scanning electron microscopy (SEM) technique by scanning electron microscopy (SEM, Leo Model 1455VP) at 20 kV in high vacuum, as seen in Figure 18 (the one added into the session of PVA/SS). Samples were mounted on metal stubs and gold coating in vacuum chamber. The gold covered sample fibers were placed onto the stage of the SEM machine. An electron beam is produced at the top of microscope by an electron gun. The electron beam passes through the microscope in a vertical direction and moves through electromagnetic fields and lenses, which focus the electron beam down toward the sample. As the electron beam hits the samples, electron and X-rays are ejected from the sample. In this work, the secondary electrons are collected and converted by detectors into a signal that is sent to a screen producing an SEM image. The average of porous hydrogel diameters was measured by SEM image at magnification of 200x.

### **3. Swelling ratio of 3D porous semi-IPN hydrogel scaffolds of PHEA/SS**

The swelling ratio was measured according to conventional gravimetric methods. Completely lyophilized 3D porous semi-IPN hydrogel scaffolds of PHEA/SS were immersed in deionized water at 37°C. Three gels from each composition were taken out at pre-determined time intervals and tested at each time point from 1, 4, 8, 12 and 24 hrs. The swelling ratio of the hydrogel scaffolds was calculated as a ratio of wet weight and dry weight of hydrogel scaffolds at time intervals, following equation:

$$\text{Swelling Ratio} = \frac{W_t - W_o}{W_o}$$

Where  $W_o$  is the weight of the dried hydrogel scaffold and  $W_t$  is the weight of fully swollen hydrogel scaffold.

#### 4. Release of silk sericin from 3D porous semi-IPN hydrogel scaffolds of PHEA/SS

The stabilization of 3D porous semi-IPN hydrogels scaffolds of PHEA/SS was assessed as a function of release of silk sericin from the hybrid constructs over time. The hydrogels were incubated in known volumes of phosphate buffer saline (PBS, pH 7.4) [48]. Three hydrogels from each composition were tested at each time point from 1, 2, 4, 8, 16, 32 hours and 14 days. At 37°C, the PBS extracts were collected and evaluated for protein concentration at selected time intervals and sampling the solution (amount of protein release) for determined from OD value at 595 nm using microplate reader (Biotek, Model Synergy H1 Hybrid Reader).

#### 5. *In-vitro* degradation of 3D porous semi-IPN hydrogel scaffolds of PHEA/SS [74]

The *in-vitro* degradation of the 3D porous semi-IPN hydrogel scaffolds of PHEA/SS is measured of the percentage mass loss with time by adding hydrogel scaffolds into the phosphate buffer solution (PBS) pH 7.4 at 37°C for 30 days. The lyophilized samples (three samples of each composition) were weighted and lyophilized immediately after polymerization. The lyophilized weight of each samples were also note to measured and compared to initial dry weight to calculate the percentage mass loss with time. The results were represented as the percentage mass remaining over time and the percentage of weight loss can be calculated as following equation;

$$\% \text{ Mass Loss} = \frac{W_d - W_f}{W_d} \times 100$$

Where  $W_d$  and  $W_f$  are the initial weight of lyophilized hydrogel and weight of lyophilized hydrogel after soak in PBS solution, respectively.

## **Cell culture test of 3D porous semi-IPN hydrogels scaffolds of PHEA/SS**

### **1. Sterilized scaffolds**

Scaffolds were cut into cubes (0.3x0.3x0.3 cm) and immersed in 70% ethanol for 30 minute followed by washing with phosphate buffer solution (PBS - pH 7.4) for several times before further use [48]. The sterilized scaffolds were immersed in 1 mL of the medium (90 DMEM : 10 FBS) overnight in incubator at 37 °C and then dehydrated in a cell culture hood for 3 hours to achieve the partially dehydrated scaffolds.

### **2. Fibroblast seeding and culture on hydrogels**

The sterilized scaffolds were put in 1 mL of the medium (90 DMEM : 10 FBS) and left over night in a close system (incubator at 37 °C), then dehydrated in a cell culture hood for 3 hours to achieve the partially dehydrated scaffolds. Feline fibroblast cell line (HFF1) ( $1 \times 10^6$  cells) with 200  $\mu$ L medium was dropped slowly on the tip of the partially dehydrated scaffolds. They were seeded into 24-well plates and allowed to attach for 24 hours before adding another 1 mL of medium. Scaffolds with loaded cells were incubated for 2 days at 37 °C. The medium was changed and left for another day before doing the MTT assay. Figure 24 shows the schematic picture of cell seeding into 3D porous semi-IPN hydrogels scaffolds of PHEA/SS.

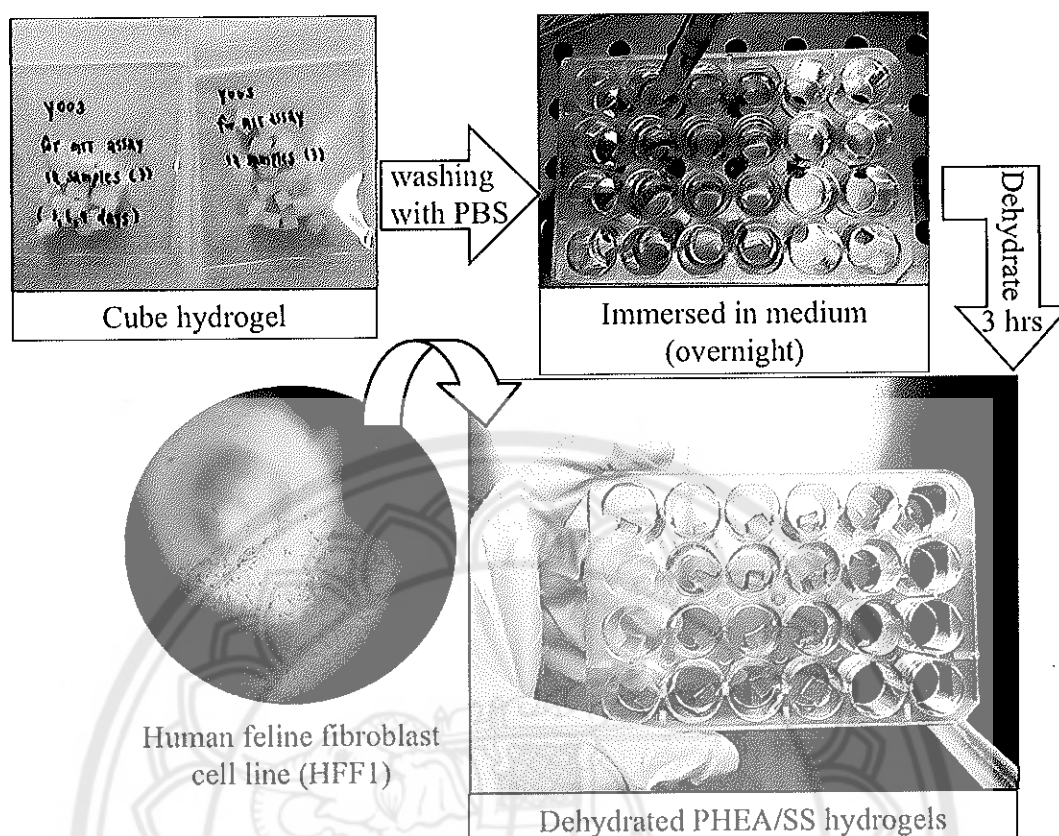


**Figure 24** Electronic photograph of human feline fibroblast cell line (HFF1,  $1 \times 10^6$  cells) (left below: picture from optical light microscope) seeded into dehydrated of 3D porous semi-IPN hydrogels scaffold of PVA/SS (right below: scaffolds were in sterilized 24-well plate).

### 3. Cell proliferation: MTT assay

MTT assay was used to study the proliferation of cells seeded on the scaffolds after 3, 7 and 14 days in culture. In this assay, the active mitochondria of the viable cells reduce the yellow coloured solution of MTT (3-(4, 5-Dimethylthiazol-2-yl)-2, 5-diphenyltetrazolium bromide, a yellow tetrazole) into blue coloured formazan crystals, which is corresponding to cellular viability. The reaction of changing the yellow colour of MTT into the purple colour of formazan was shown in figure 20.

For cell proliferation, MTT solution was added into medium containing cell loaded scaffolds, and left for 4 hours in incubator at 37 °C before removal of medium. Scaffolds were put into vials and then 200  $\mu$ L of DMSO : ethanol (1:1 v/v) was added, and left over night (12 hours) before measuring the optical density (OD)



by UV-Visible spectrophotometric microplate reader at 595 nm. The absorbance was corresponded to the number of proliferated cells [48]. The active mitochondria of the viable cells reduce the yellow coloured of MTT into blue coloured formazan crystals, which corresponds to cellular viability. The scaffolds with no cells and the controlled sample (no scaffold and cells) were also measured. The OD values of all loaded scaffolds were subtracted with the OD value of scaffolds that have no cells loading. Figure 25 shows the electronic photograph of MTT assay of 3D porous semi-IPN hydrogels of PHEA/SS.

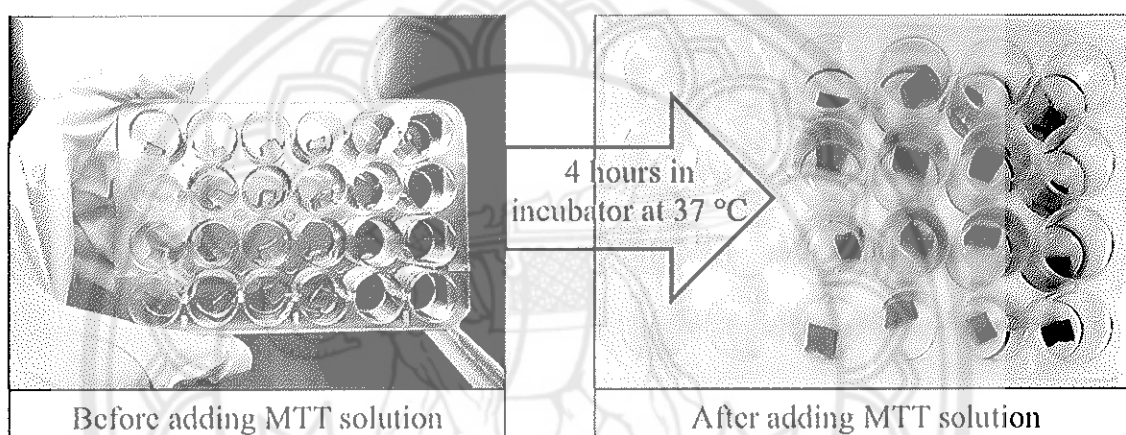


**Figure 25** Electronic photograph of 3D porous semi-IPN hydrogel scaffolds of PHEA/SS before and after adding MTT solution

## CHAPTER IV

### RESULTS AND DISCUSSION

This chapter shows the results and discussion of this research work, which is divided into two approaches depending on type of materials and techniques used to fabricate three-dimensional (3D) porous scaffolds. The first approach is the fabrication of poly(vinyl alcohol) (PVA) and silk sericin (SS) into the form of 3D porous scaffold *via* classical condensation reaction and following with lyophilization technique. The second approach is the fabrication of 3D porous hydrogels scaffold of hydroxyethyl acrylamide (HEA) and silk sericin (SS) *via* conventional free radical polymerization. This hydrogels scaffold was in the form of a semi-interpenetrating network (semi-IPN). For the first approach, the different concentrations of dimethylolurea (DMU, a cross-linker) for fabrication of 3D porous scaffolds of PVA/SS were studied. Morphology, such as surface and cross-section and cell culture tests (cell proliferation and adhesion), were observed to find the best composition for the scaffold that would be suitable for skin reconstruction. For the second approach, the effect of cross-linker and silk sericin content were also studied to find the best compositions and conditions to support for the skin fibroblast cells, as well as promoted cell proliferation. Therefore, this chapter will present the results and discussion, which will be divided into the three parts;

1. Preparation of silk sericin powder
2. 3D porous scaffolds of PVA/SS
3. 3D porous semi-IPN hydrogel scaffold of poly(hydroxyethyl acrylamide) (PHEA)/silk sericin (SS)

#### **Part 1: Preparation of silk sericin (SS)**

Silk cocoons, a family type of *bombyx mori*, were used to prepare the silk sericin (SS) – a glue like protein that covers the fibroin - by hot-water degumming process. This method is an environmental safe method because it contains no any chemicals used in the process. This is the reason why this research work used the hot-

water degumming process to degum silk fibers. Therefore, this silk sericin will be safe to use as a component in the scaffolds for skin tissue regeneration in this work. This process is a simple and successful process to extract silk sericin and prepares into the format sericin powder. Figure 26 shows SEM images of silk fiber before and after hot-water degumming process.

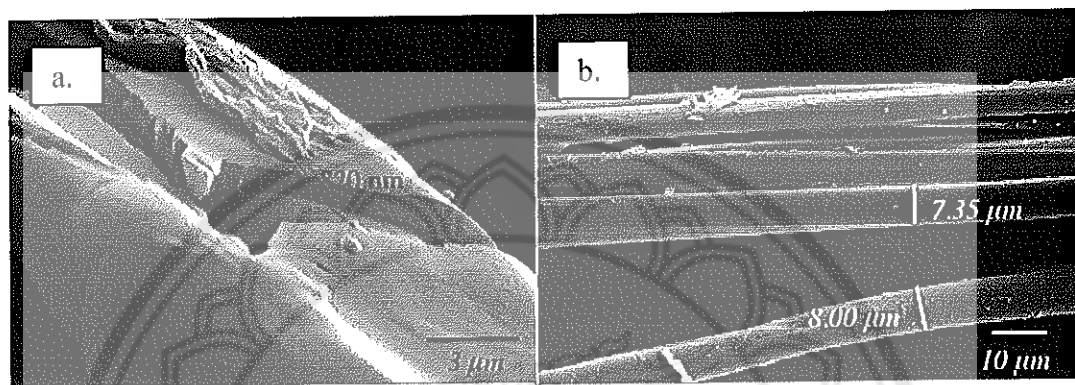


**Figure 26** SEM images of silk fibers; (a) before and (b) after hot-water degumming process, at magnification of 5000x (a) and 1000x(b)

It can be seen that the silk sericin layer is about 820 nm in thickness that covers the double strand of fibroins, which has approximately 12-16 μm wide depending on the source of silk cocoon fiber (Figure 26a). Figure 26b shows a fibroin in which double strand were terminated and a single fiber of 7-8 μm (a half of double strand fiber size) was found. The process gave high amount of silk sericin powders which is approximately 6.9%. Fibroin fibers are removed and then silk sericin solution is dried in an oven at 60°C for 12 hours before obtaining the silk sericin powder, which are shown in figure 27. Finally, the silk sericin powder was stored in a desiccator to protect from the moisture until further use.

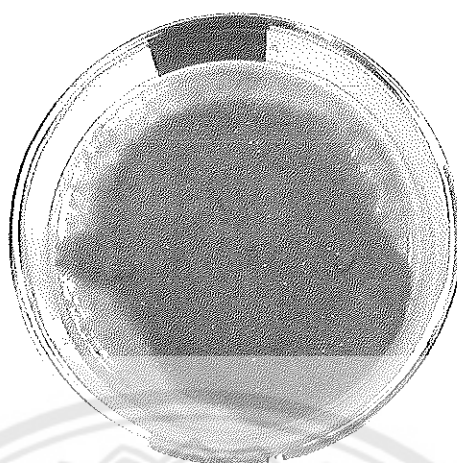


**Figure 27** Electric photograph of silk sericin powder after dried in an oven

### **Part 2: Approach I: 3D porous scaffolds of PVA/SS**

The three-dimensional (3D) porous scaffolds of poly(vinyl alcohol) (PVA) and silk sericin (SS) with different concentrations of dimethylol urea (DMU), using as a cross-linker, were fabricated *via* classical condensation reaction and followed by the lyophilization technique. Themorphology of the samples from surface and cross-sectioned was primarily observed. In addition, the cell culture tests of scaffolds, such as cell proliferation and adhesion were also observed to find the best composition for the scaffolds that would be suitable for skin reconstruction. In this section, therefore, the detail visualization in results and discussion of the fabrication, the possible reaction mechanism, morphology, cell viability and cell adhesion were described.

#### **Fabrication of 3D porous scaffolds of poly(vinyl alcohol) (PVA)/silk sericin (SS)**

As described in chapter 3 about the details of fabrication of 3D porous scaffolds of poly(vinyl alcohol) (PVA) and silk sericin (SS), PVA was first mixed with silk sericin in the presence of different concentrations of dimethylol urea (DMU) and certain amount of glycerol, which was used as plasticizer. The mixtures of PVA, SS, DMU, and plasticizer were in a homogeneous phase, yellow well-order and clear solutions. This homogeneous mixture was then lyophilized for 24 hours to promote the 3D porous structures. The physical appearance of the final 3D porous scaffolds of PVA/SS are shown in table 11. The sample codes used in this work are from 0% DMU

PVA/SS to 100% DMU PVA/SS, depending on the percentage of DMU used, which are based on the total weights of PVA and SS.

**Table 11 The physical appearance of 3D porous scaffolds of PVA/SS**

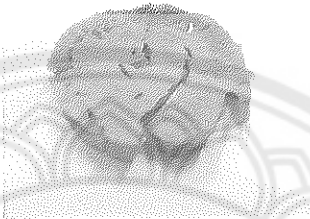
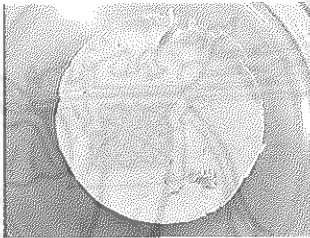
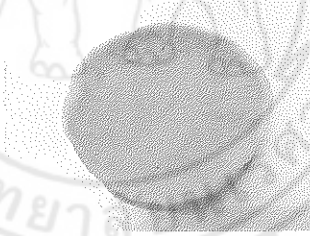
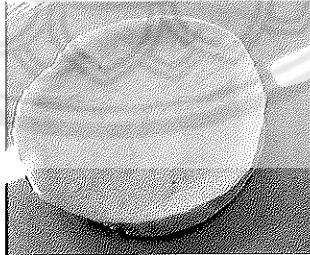
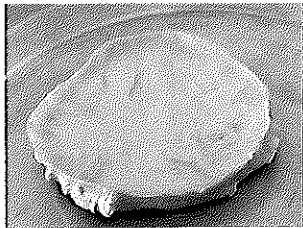
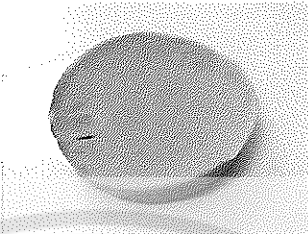
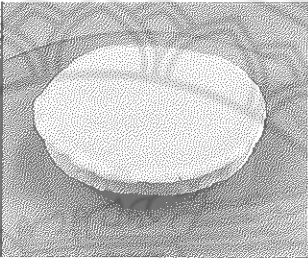
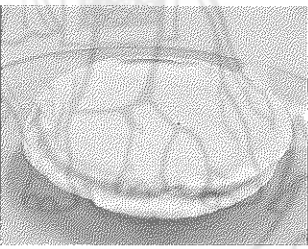
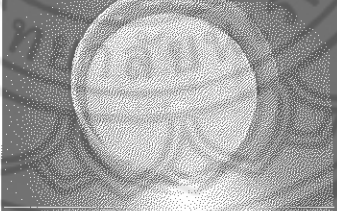
| Name           | Sample appearance  | Note   |
|----------------|--|--|
| 0% DMU PVA/SS  |    | Yellow sample, very soft, flexible and homogeneous, fractured sample |
| 10% DMU PVA/SS |   | Yellow sample, soft, flexible and homogeneous                        |
| 20% DMU PVA/SS |  | Yellow sample, soft, flexible and homogeneous                        |
| 40% DMU PVA/SS |  | Yellow sample, soft, flexible and homogeneous                        |
| 50% DMU PVA/SS |  | Yellow sample, soft, flexible, homogeneous                           |

Table 11 (cont.)

| Name            | Sample appearance  | Note  |
|-----------------|--|---|
| 60% DMU PVA/SS  |    | Yellow sample, soft, flexible, homogeneous and smooth surface |
| 80% DMU PVA/SS  |    | Yellow sample, soft, flexible, homogeneous and smooth surface |
| 90% DMU PVA/SS  |  | Yellow sample, soft, flexible, homogeneous and smooth surface |
| 100% DMU PVA/SS |  | Yellow sample, soft, flexible, homogeneous and smooth surface |

After lyophilization of the samples, the thickness of the 3D porous scaffolds were measured and showed in approximately 0.5 cm. From table 4, it can be seen that all scaffolds of PVA/SS showed good homogeneity and have porous structures, with soft and flexible materials. However, their toughness depended on the percentage of DMU used, as using higher DMU contents in the scaffolds promoted higher mechanical strength of the scaffolds than that of low DMU contents.

### **The proposed reaction of preparation of 3D porous scaffolds of PVA/SS**

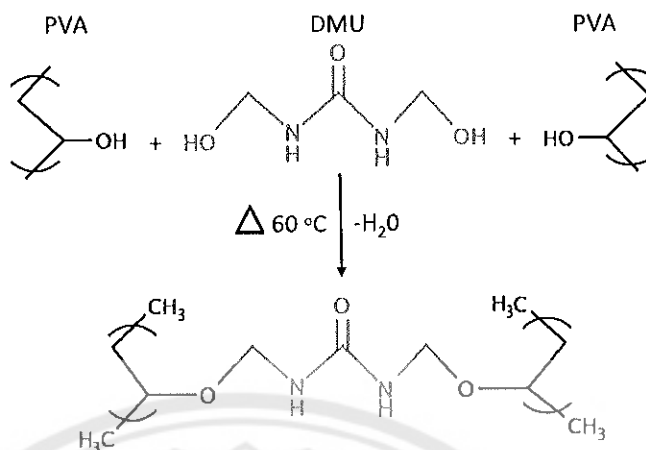
The 3D porous scaffolds of cross-linked poly(vinyl alcohol) (PVA) and silk sericin (SS) were successfully fabricated, as demonstrated earlier. In this approach, DMU was used as a cross-linker for both PVA and SS *via* condensation reaction. The cross-linked structure in the present of PVA and silk sericin structure were promoted by DMU based on a condensation reaction. The N-methylol groups ( $\text{HO-CH}_3$ -) of DMU and the hydroxyl groups ( $-\text{OH}$ ) of polymers containing hydroxyl-groups were reacted and then cross-linked networks were performed [75].

Poly(vinyl alcohol) is one of the polymer that contains hydroxyl groups on its backbone, its chemical structure shown in figure 28. Therefore, the methylol groups of DMU can react with the hydroxyl group of PVA on applying temperature and releases one molecule of water during the classical condensation reaction. Figure 28a shows the possible reaction between PVA and DMU to form a polymer network.

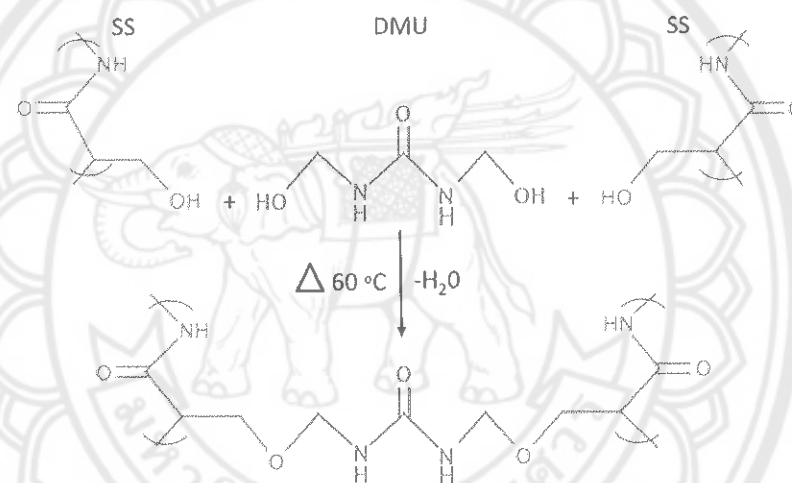
Silk sericin (SS) is also one of the protein molecules that contain a hydroxyl group in its amino structure (see figure 5). In case of adding silk sericin into the system, therefore, the methylol groups of DMU can also react with hydroxyl groups of amino acid containing in silk sericin structure similar to PVA. The possible reaction is shown in figure 28b, which is generated throughout the classical condensation to give the SS, DMU and SS network and release of a free water molecules.

As seen PVA and silk sericin are both hydroxyl containing materials, therefore, the possible reaction between PVA, DMU and SS is predicted to occur *via* the classical condensation reaction. Figure 28c shows the reaction between PVA, SS and DMU to form polymer networks in the 3D porous structure of PVA and SS. Therefore, the possible interactions between PVA, SS and DMU to form polymer networks in this 3D scaffold are PVA-DMU-PVA, PVA-DMU-SS and SS-DMU-SS.

## a. PVA-DMU-PVA



## b. SS-DMU-SS



## c. PVA-DMU-SS

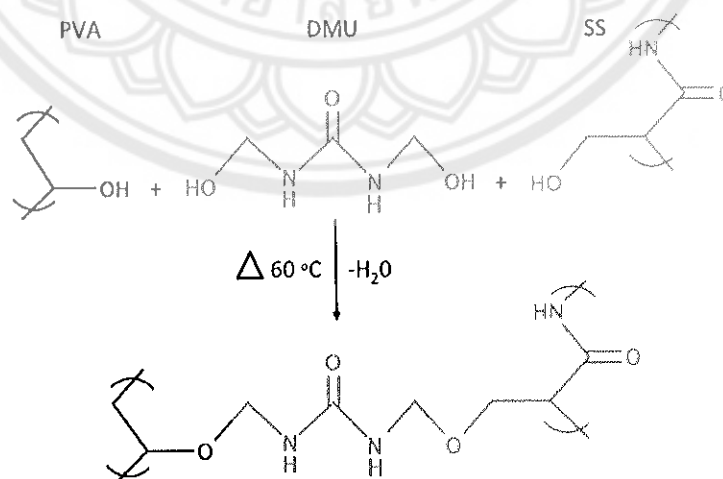


**Figure 28** The reaction of preparation of 3D porous scaffolds of PVA/SS; a. PVA-DMU-PVA, b. SS-DMU-SS and c. PVA-DMU-SS

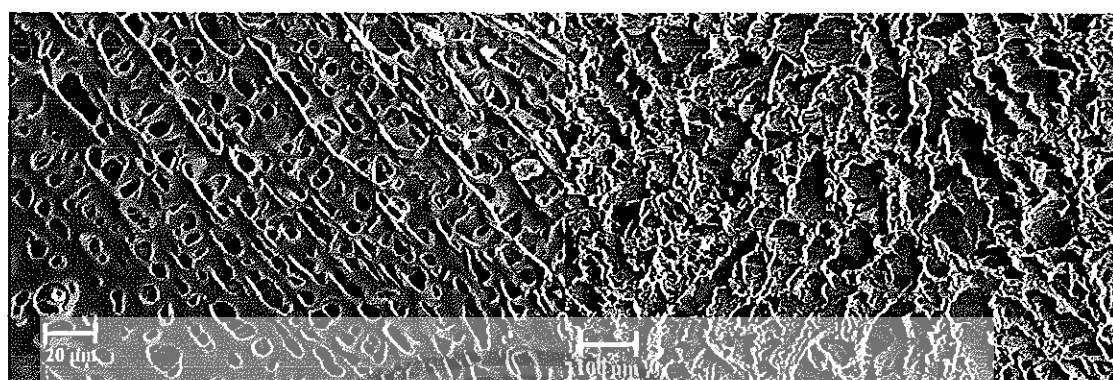


### **Morphology of 3D porous scaffolds of PVA/SS**

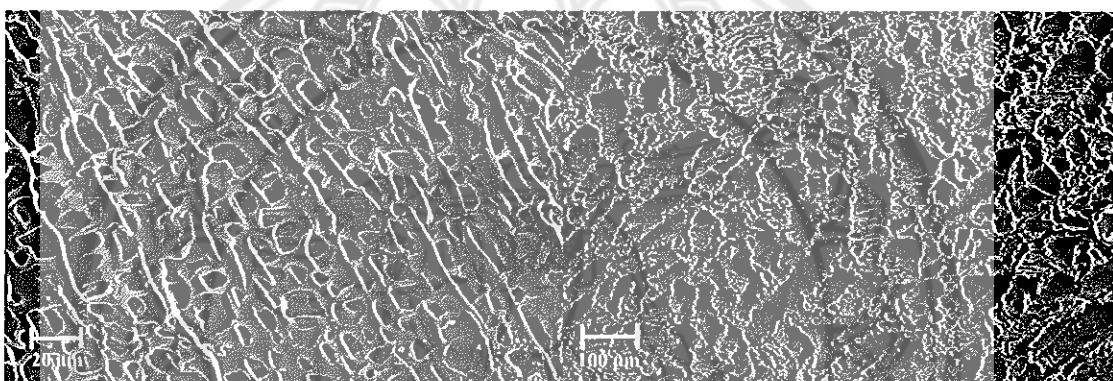
The scanning electron microscope (SEM) was used to observe the surface and cross-section of 3D porous scaffolds at different concentrations of dimethylol urea (DMU). The scaffolds represented continuous uniform interconnected porous morphology due to freeze-drying process [76]. The effect of the loading of cross-linker (DMU) on the morphology of scaffolds was evaluated. In this section, the results will be discussed and separated into three catalogues of scaffolds; 1. scaffold at low % DMU (0, 10, and 20% DMU), 2. at moderate % DMU (40, 50 and 60% DMU) and 3. at high % DMU (80, 90 and 100% DMU).

#### **1. At low concentration of DMU**

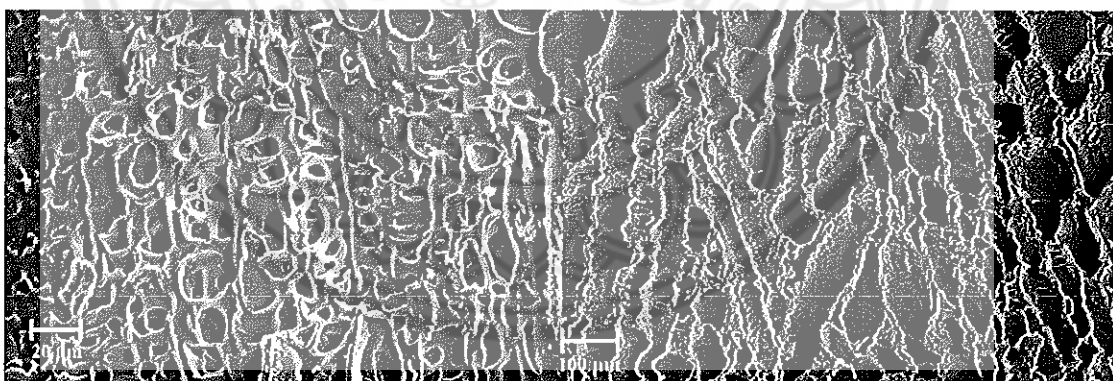
The surface and cross-sectioned SEM images of 3D porous scaffolds of PVA/SS at low % DMU, which are 0% DMU PVA/SS, 10% DMU PVA/SS, and 20 % DMU PVA/SS, are shown in figure 29. The magnification of SEM images for surface observation was 500x (left) and for cross-section was 100x (right). The scale bar of image size was shown in all SEM images.



a. PVA/SS at 0% DMU



b. PVA/SS at 10% DMU



c. PVA/SS at 20% DMU

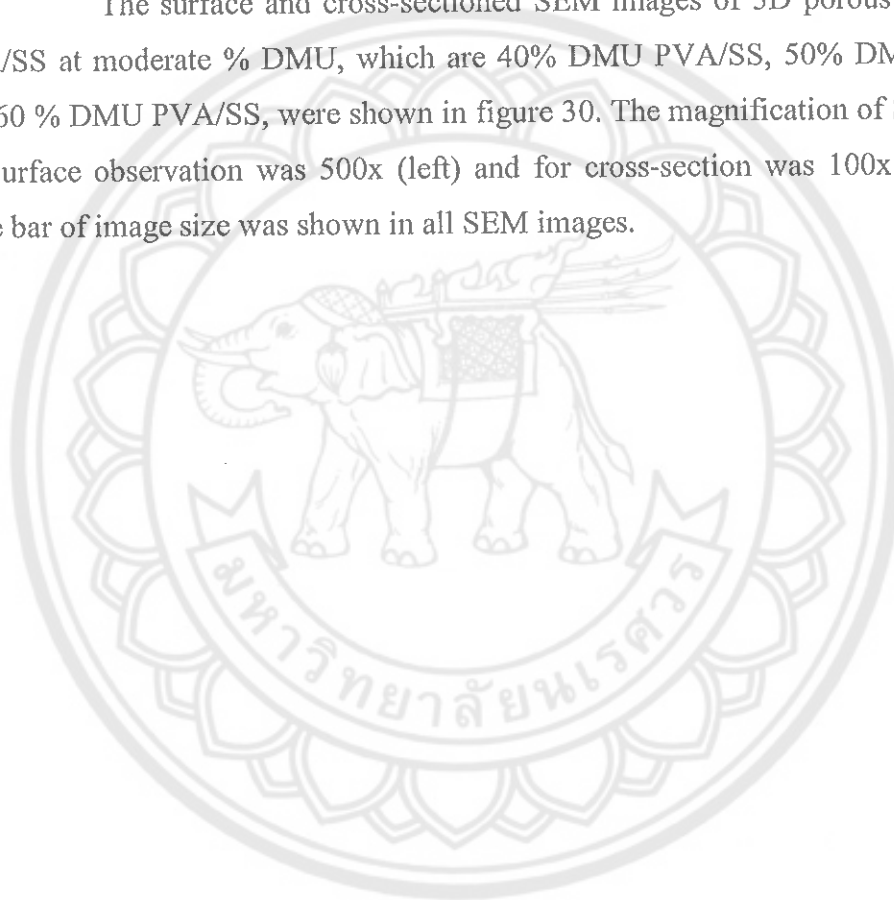
**Figure 29** SEM images of PVA/SS at low % DMU; a. 0 %DMU, b. 10 %DMU and c. 20 %DMU, the surface images (500x, left) and cross-sectioned images (100x, right)

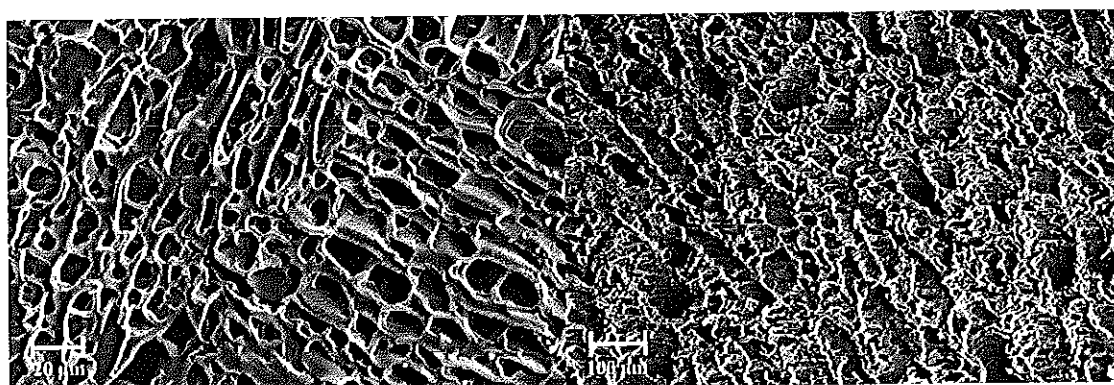
From figure 29, it can be seen that the SEM images of sample's surfaces (left pictures) for all compositions show porous structures with slight difference in porous

size distributions in which 20%DMU PVA/SS scaffold (figure 29c) shows a lower porous size distribution than that of 10%DMU PVA/SS and 0% DMU PVA/SS, respectively. However, the diameter of the pores in all these scaffolds were in ranges of 10-30  $\mu\text{m}$ . For the cross-sectioned SEM images of 3D porous scaffolds of PVA/SS (right picture), a scaffold at 0% DMU has less well-order of the interconnecting structures than the scaffolds at 10 and 20% DMU, respectively.

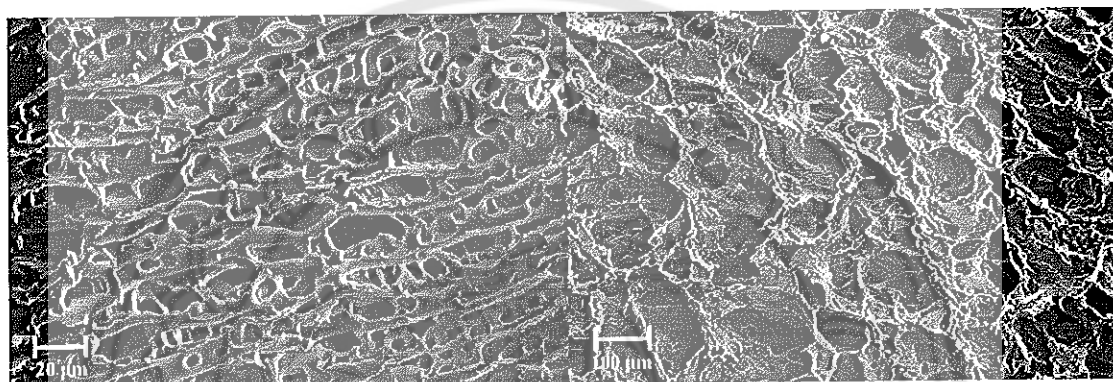
## **2. At moderate concentration of DMU**

The surface and cross-sectioned SEM images of 3D porous scaffolds of PVA/SS at moderate % DMU, which are 40% DMU PVA/SS, 50% DMU PVA/SS, and 60 % DMU PVA/SS, were shown in figure 30. The magnification of SEM images for surface observation was 500x (left) and for cross-section was 100x (right). The scale bar of image size was shown in all SEM images.

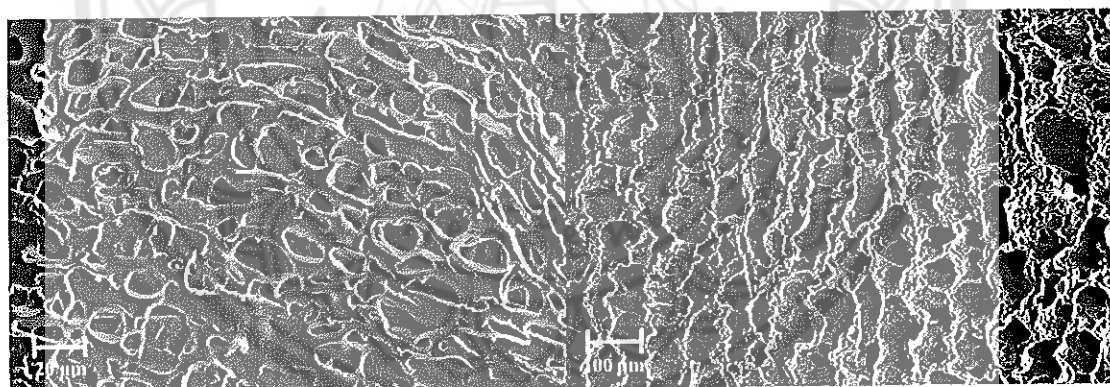




a. PVA/SS at 40% DMU



b. PVA/SS at 50% DMU



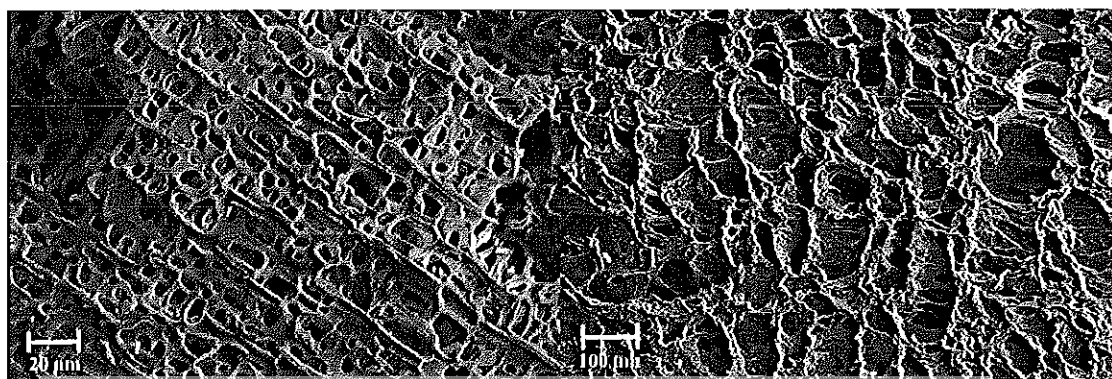
c. PVA/SS at 60% DMU

**Figure 30** SEM images of PVA/SS at moderate%DMU; a. 40 %DMU, b. 50 %DMU and c. 60 %DMU, the surface images (500x, left) and cross-sectioned images (100x, right)

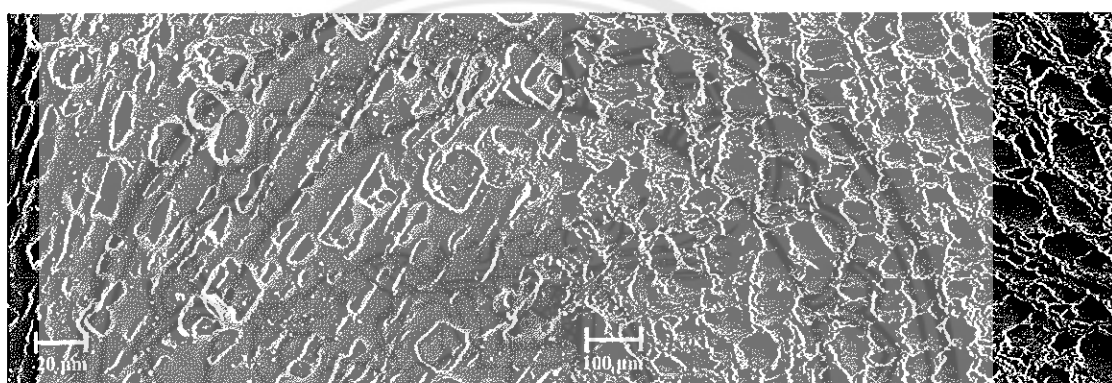
From figure 30, it can be seen that the SEM images of sample surfaces (left pictures) for all compositions show porous structures with slightly different pore size distributions in which 60%DMU PVA/SS scaffold (figure 30c) shows lower porous size distribution than that of 50%DMU PVA/SS and 40% DMU PVA/SS, respectively. However, the diameter of the pore of all these scaffolds were in ranges of 30-60  $\mu\text{m}$ . For the cross-sectioned SEM images of 3D porous scaffolds of PVA/SS (right picture), a scaffold at 40% DMU has less well-order of the interconnecting structures than the scaffolds at 50 and 60% DMU, respectively. This result shows similar results to the scaffolds at low concentration of DMU described in the previous section in which using higher percentage of DMU promotes the well-order of the interconnecting structures than that of using lower percentage of DMU. In addition, the slightly numbers of porous structures (porous density) is observed when using higher percentage of DMU.

### **3. At high concentration of DMU**

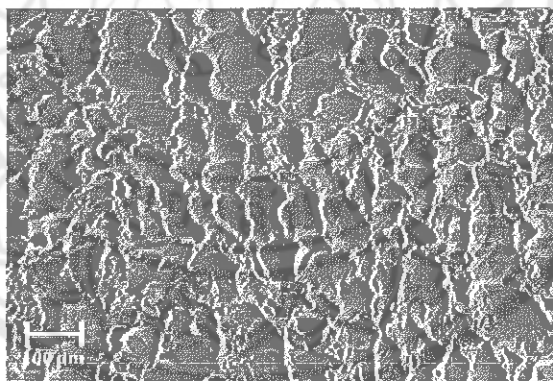
The surface and cross-sectioned SEM images of 3D porous scaffolds of PVA/SS at high % DMU, which are 80% DMU PVA/SS, 90% DMU PVA/SS, and 100 % DMU PVA/SS, were shown in figure 31. The magnification of SEM images for surface observation is 500x (left) and for cross-section is 100x (right). The scale bar of image size is shown in all SEM images.



a. PVA/SS at 80% DMU



b. PVA/SS at 90% DMU



c. PVA/SS at 100% DMU

**Figure 31** SEM images of PVA/SS at high % DMU; a. 80 %DMU, b. 90 %DMU and c. 100 %DMU, the surface images (500x, left) and cross-sectioned images (100x, right)

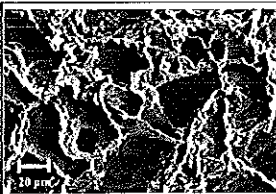
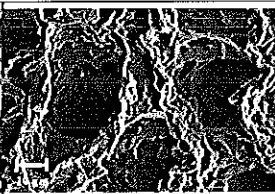
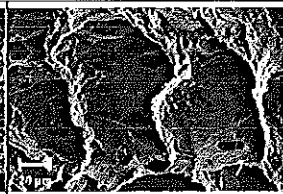
From figure 31, it can be seen that the SEM images of sample's surfaces (left pictures) for all compositions show porous structures with slight difference in porous size distributions between 80% DMU PVA/SS (figure 31a) and 90% DMU PVA/SS (figure 31b) in which 90% DMU PVA/SS scaffold shows lower a porous size distribution than that of 80% DMU PVA/SS. To be noted, the surface morphology of 100% DMU PVA/SS was not available to show in this figure. However, it can be expected that the surface morphology of 100% DMU PVA/SS will be slightly different from the other two compositions of scaffolds at high loading of DMU. In this case, 100% DMU PVA/SS should show lowest size distribution in its structure, the same trend of the scaffolds at low and moderate concentration of DMU in figure 29 and 30.

However, the diameter of the pore of all these scaffolds were in ranges of 60-120  $\mu\text{m}$ . For the cross-sectioned SEM images of 3D porous scaffolds of PVA/SS (right picture), a scaffold at 80% DMU has less well-order of the interconnecting structures than the scaffolds at 90 and 100% DMU, respectively. This result shows similar results to the scaffolds at low and high concentration of DMU in the previous sections, in which using higher percentage of DMU promotes the well-order in the interconnecting structures than that of using lower percentage of DMU. In addition, the slightly higher numbers of porous structures (porous density) are observed when using higher percentage of DMU.

#### **Complementary of the morphology study**

From all SEM images of 0-100 %DMU PVA/SS, it can be seen the difference on the morphology of 3D porous scaffolds of PVA/SS at different concentrations of cross-linker. The results can be summarized and discussed in terms of porous diameter, structure arrangement, interconnecting matriced, size distribution and porous density, as shown in figure 32. The representative examples of cross-sectioned SEM images of low %DMU PVA/SS, moderate %DMU PVA/SS and high %DMU PVA/SS scaffolds at magnification of 500x were also shown in the table.



|                                   |   |  |   |
|-----------------------------------|---|--|---|
|                                   |  |  |  |
|                                   | Low % DMU<br>(10%)  | Moderate % DMU<br>(60%)  | High % DMU<br>(100%)  |
| Porous diameter ( $\mu\text{m}$ ) | 10-30   | 30-60  | 60-120  |
| Structure arrangement             | Low $\longrightarrow$ High  |  |   |
| Interconnecting matrices          | Yes   | Yes  | Yes   |
| Size distribution                 | High $\longrightarrow$ Low  |  |   |
| Porous density                    | Slightly high $\longrightarrow$ Low   |  |   |

**Figure 32 Pore diameter, structure arrangement, interconnecting matrix, size distribution and porous density of 3D porous scaffolds of PVA/SS**

From figure 32, it can be seen that adding higher amounts of DMU into the fabrication process of PVA/SS scaffold produces higher porous diameters than that of low amount of DMU; 10-30  $\mu\text{m}$  at low %DMU, 30-60  $\mu\text{m}$  at moderate %DMU, 60-120  $\mu\text{m}$  at high %DMU. In addition, high %DMU gave better uniformity and porosity of 3D porous scaffolds of PVA/SS and the pore walls are much thinner. It showed much more regular structure arrangement of the matrix than scaffolds at 0% and low percentage of DMU. This is because using higher cross-link loading promoted higher density of cross-linked polymer networks of PVA and SS.

As seen from section 4.2.2 – the possible reactions in these scaffolds, PVA and SS can react with DMU and then form chemical cross-linked structures, which produces the mechanical strength of the 3D porous scaffolds of PVA/SS. However, high %DMU seems to promote the bigger diameter of porous structure with higher regular structure arrangement than that of no DMU and low %DMU, as seen in figure 32. This figure also shows the cartoon structure of the cross-linking system of 3D porous scaffolds of 0, low and high %DMU, in which chemical cross-linked bonds is generated by classical condensation reaction. Not only the chemical cross-linked



bonds are produced but also the physical bonds, especially hydrogen bonding between the PVA and SS molecular structures are also generated.

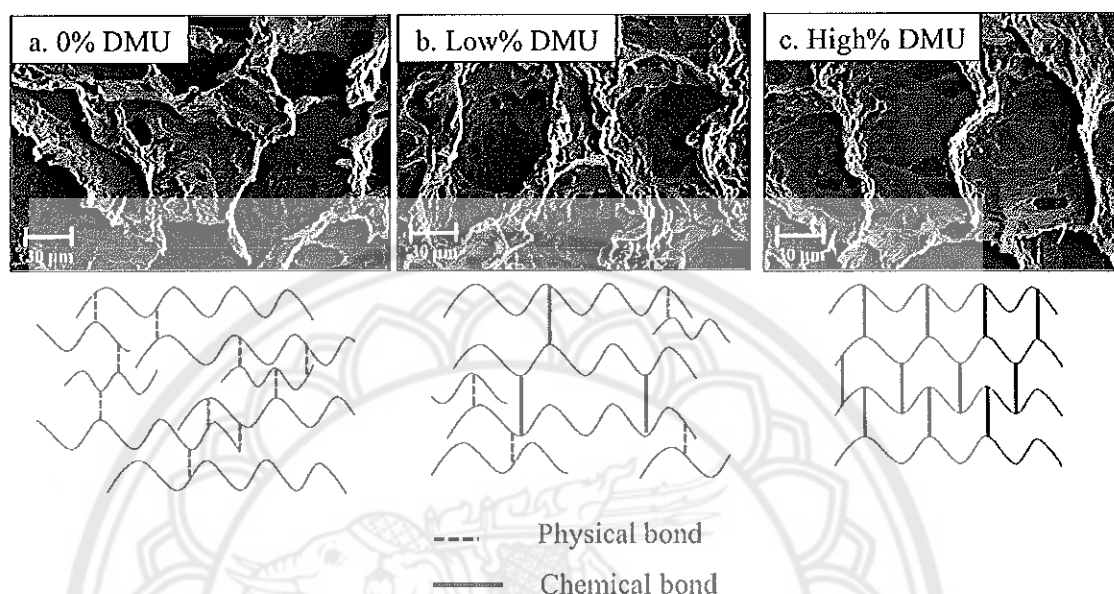


**Figure 33** Cartoon structure of the cross-linking system of 3D porous scaffolds that differential of cross-linker content

High density of the chemical cross-linked bond will produce a good uniformity and regularity of the porous structures and a big size of pore (figure 33c). Whereas, high density of the physical cross-linked bond will produce a lesser uniformity and regularity of the porous structures and a smaller size of porous (figure 33a). Therefore, it can be concluded that the key factor for the structure arrangement and diameter size of the scaffold depends on not only the density of the chemical cross-linked bond but also the density of the physical cross-linked bond.

In summary, from 3D porous scaffolds of PVA/SS with freeze-drying step after fabrication in the previous preparation process, the pore structure becomes more uniform and, most importantly, a greater amount of interconnecting holes between the pores were produced. These holes can help the interchange of culture medium and also the migration of the cells [77].

### Cell viability and proliferation of 3D porous scaffolds of PVA/SS

Cell culture study is a key factor for testing scaffolds that used in the field of medical applications, especially, for dermal reconstruction. Generally, fibroblast cell are present in all skin, therefore, the feline fibroblast cell of HFF-1 was selected to use for the *in vitro* cell culture test in this work. As discussed earlier in the section of morphology study, the difference in characteristic of porous structures was interesting to study in term of its effect into the cell culture test. Therefore, two different groups of 3D porous scaffolds of PVA/SS at low (10 and 20% DMU) and high (80 and 100% DMU) uniformities were chosen to study *in vitro* cell culture by MTT assay. The viability and proliferation of feline fibroblast cell line (HFF-1) was loaded on the 3D porous PVA/SS scaffolds. HFF-1 was also loaded into the polystyrene plate to use as a positive control under the MTT assay for 3 and 6 days in culture.

The active mitochondria of the viable cells reduce the yellow colour of MTT into purple colour of formazan crystals, as shown in figure 20. Figure 34 shows an example of the electronic photograph of the results from cell culture test of 3D porous scaffolds of PVA/SS (10%DMU of PVA/SS) by MTT assay for 3 days of culture, in which scaffold with no cells loading (left vial), scaffold with cells loading (middle and right vials) were shown. It can be seen that the scaffold with no cells loading is still remaining the yellow colour of MTT, while the scaffold with cells reduces the yellow coloured of MTT into purple coloured of formazan crystals by active mitochondria of the viable cells.



**Figure 34** Electronic photograph of the result from cell culture test of 3D porous scaffolds of PVA/SS (10%DMU of PVA/SS) by MTT assay for 3 days of culture

The optical density of cell shows viability (MTT) of cells grown on scaffolds with different concentrations of DMU for 3 days and 6 days. Figure 35 shows the optical density of cell scaffolds of PVA/SS at different concentrations of DMU at 3 and 6 days of culture using MTT assay, together with their SEM images at magnification of 500x. The optical density (OD) values of all scaffolds were subtracted with the OD value of scaffolds that have no cells loading, to avoid the effect of yellow colour of scaffolds themselves. It can be seen that the growth of HFF1 fibroblast cells in the control polystyrene plate confirmed the viability of the cells.

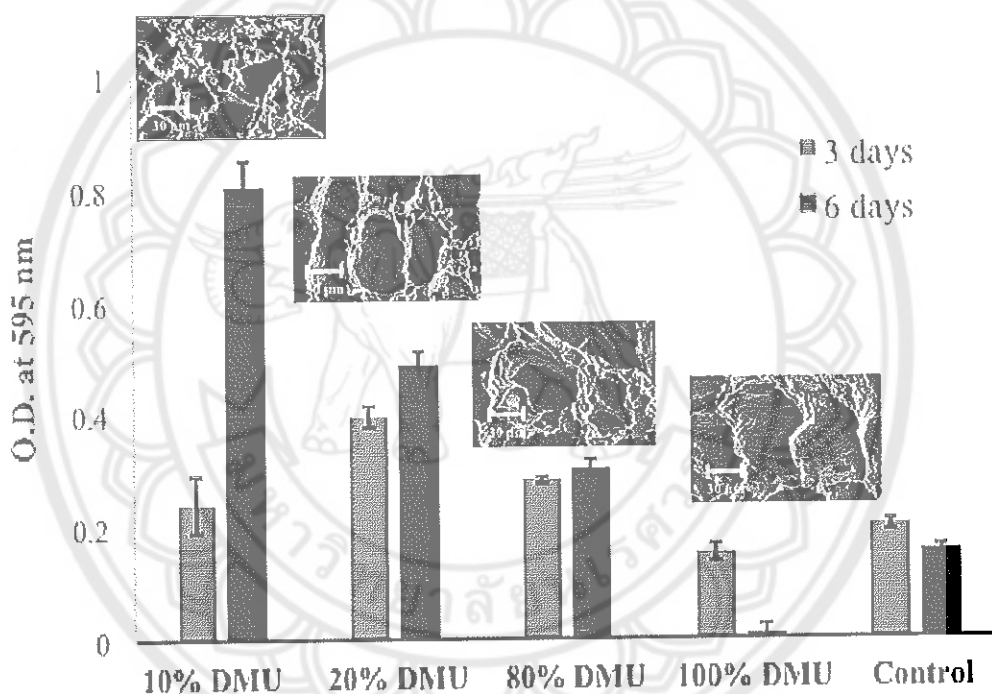


**Figure 35** Optical density of cell scaffolds of PVA/SS at different concentrations of DMU at 3 and 6 days of culture using MTT assay together with their SEM images (500x)

On 3 days, cell within 10%DMU PVA/SS, 20% DMU PVA/SS and 80% DMU PVA/SS showed greater optical density that mean greater cellular activity than the control polystyrene plate and cell within 20% DMU PVA/SS is highest, but PVA/SS scaffolds containing 100%DMU showed lower optical density than the

polystyrene plate (positive control). On 6 days, cell within 10%DMU PVA/SS, 20% DMU PVA/SS and 80% DMU PVA/SS showed greater optical density than the control polystyrene plate and cell within 10% DMU PVA/SS is highest, but PVA/SS scaffolds containing 100%DMU showed lower optical density than the polystyrene plate (positive control). The results show that cells grow or proliferate better when they were cultured on 10-80% DMU scaffolds than when they were grown on two-dimension plate surface. PVA/SS scaffolds containing 20% DMU and 10% DMU show the best cell growth at 3 days and 6 days of culture, respectively. Compared to 3 days in culture, the cell viability increases dramatically at the sixth day of culture with the 10% DMU scaffold and slightly increases with 20% and 80% DMU content. Scaffolds with 100% DMU do not promote cell growth and induce cells death at 6 days of culture. The reason might be because there is not enough space for the cells to grow.

For cell proliferation, as cell number significantly increased in all the constructs during the time except PVA/SS scaffolds containing 100%DMU showed decreased of cell ability after 6 days. The amount of viable cells was highest in 10% DMU PVA/SS followed by 20% DMU PVA/SS, 80%DMU PVA/SS and 100%DMU PVA/SS. These data suggest that the size of porous structure, structure arrangement, interconnecting structure, size distribution and porous density of the matrix of PVA/SS scaffolds promote HFF1 fibroblast cells growth in a certain composition of the cross-linker. In summary, it seems to show that scaffold at low %DMU (10 and 20% DMU) that has porous size of diameter in range of 10-30  $\mu\text{m}$ , low structure arrangement, good interconnecting structure, various size distributions and high porous density, promotes better cell proliferation than scaffolds at high %DMU.

#### **Cell adhesion of PVA/SS 3D porous scaffolds**

For cell adhesion of HFF1 fibroblast cells on the scaffolds were also studied by counting the numbers of HFF1 fibroblast cells using haemocytometer. A separate set of scaffolds (10, 20, 80 and 100% DMU scaffolds) was used in which three samples for each composition were tested at each time point from 1, 4, 8, 12 and 24 hours. The number of cells adhering to each scaffold was calculated by subtracting the amount of cell seeding ( $1 \times 10^6$  cells per scaffold) with the number of washed out fibroblast cells by 1 mL of PBS solution (pH 7.4).

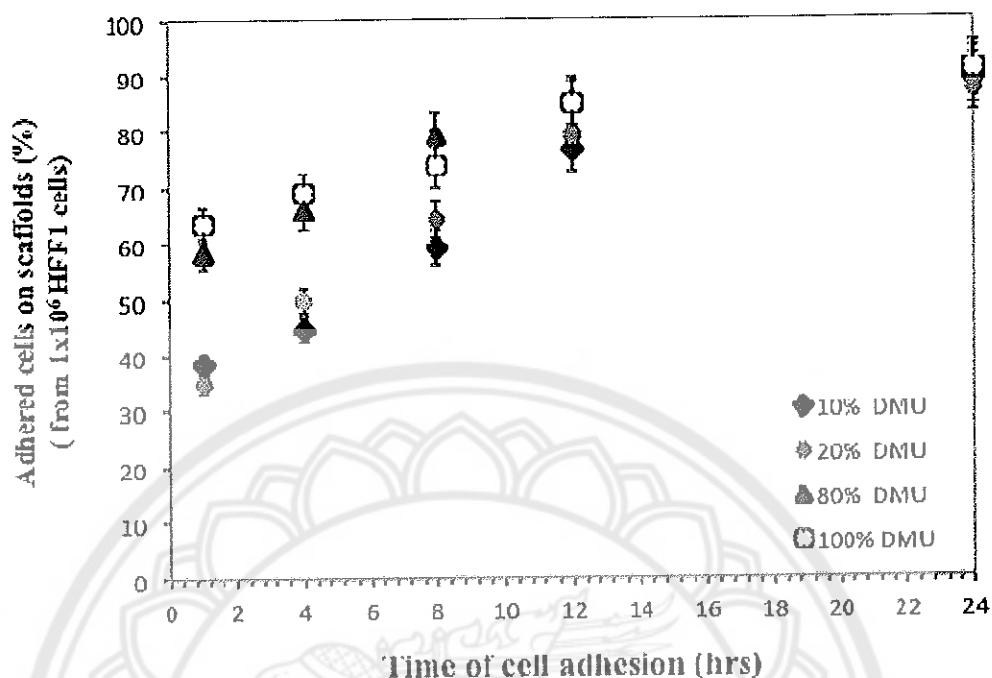


**Figure 36** Percentage of adhered cells on 3D porous scaffolds of PVA/SS at different concentrations of DMU.

Figure 36 shows percentage of adhered cells on the scaffolds still remaining after the washing with time intervals. It was found that the number of HFF1 fibroblast cells could adhere to the scaffolds in all compositions and this continued to increase for longer time periods. The lowest percentage of cell adhesion was observed at 10% DMU scaffold at 1 hour, which is lower than the scaffold at 100% DMU, due to the smaller numbers of crosslink networks and porous. However, their percentage of adhesion of cells is equal at the time interval of 24 hours, due to most cells were attached to scaffolds when they were left for a longer time.

### Summary of approach I

3D porous scaffolds of cross-linked networks of silk sericin and a poly(vinyl alcohol), were successfully fabricated for potential use in skin-tissue reconstruction. As observed, 10% DMU of PVA/SS with porous diameters of 10-30  $\mu\text{m}$  showed efficiency for skin cell proliferation and adhesion. Using higher percentage of DMU led to the well ordered of pore structure in cross-linked polymer networks. The possible polymer network interactions of scaffold are PVA-DMU-PVA, PVA-DMU-SS and SS-DMU-SS.

### Part 3: Approach II: 3D porous semi-IPN hydrogel scaffolds of poly(hydroxyethyl acrylamide) (PHEA)/silk sericin (SS)

Three dimension (3D) porous semi-interpenetrating polymer networks (semi-IPN) composed of silk sericin (SS) and hydroxyethyl acrylamide(HEA) were prepared by conventional free-radical polymerization. The scaffolds were fabricated in the 24 well plates with different concentrations of cross-linker (N'N-methylene bisacrylamide) and with different loadings of silk sericin (SS). Gelation time, swelling ratio, release of silk sericin and *in-vitro* degradation were studied. The morphology of 3D porous semi-IPN hydrogel scaffolds was also investigated by scanning electron microscope (SEM). Finally, the *in-vitro* cell culture was evaluated by MTT assay to find the best composition for the scaffold that would be suitable for skin reconstruction.

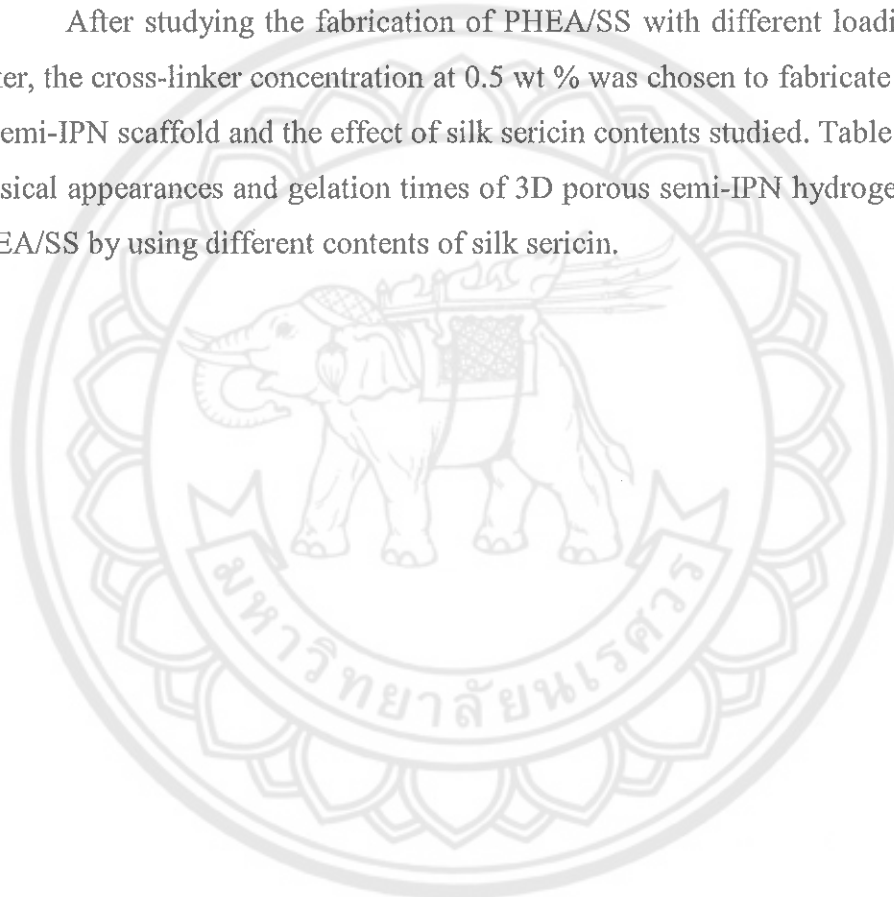
#### Fabrication of 3D porous semi-IPN hydrogel scaffolds of poly(hydroxyethyl acrylamide) (PHEA)/silk sericin (SS)

The 3D porous semi-interpenetrating polymer networks (semi-IPN) hydrogel scaffolds of PHEA/SS was prepared by a conventional radical polymerization of hydroxyethyl acrylamide(HEA) in the presence of silk sericin. Two set of experimental preparation of semi-IPN scaffolds were studied. The first experiment examined effect of the concentration of cross-linker onto the properties of scaffolds. The second experiment studied the effect of silk sericin content onto the properties of scaffolds. Hydrogels with various concentrations of cross-linker (N'N-methylene bisacrylamide) from 0 to 2.0 wt% were fabricated and termed as 0% XL PHEA/SS-5, 0.25% XL PHEA/SS-5, 0.5% XL PHEA/SS-5, 1.0%XL PHEA/SS-5 and 2.0%XL PHEA/SS-5

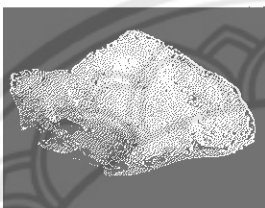
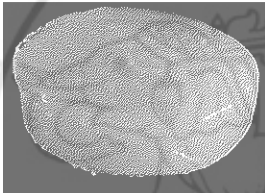
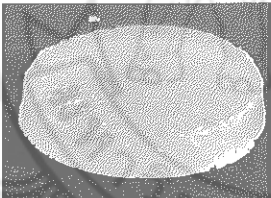
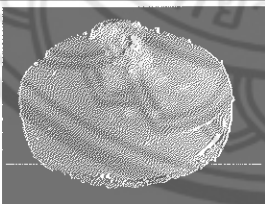
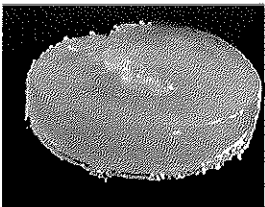
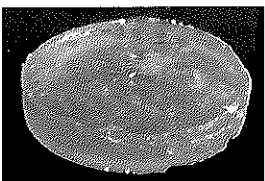
respectively. Hydrogels with various amounts of silk sericin ranging from 0 wt% to 5.0 wt% were fabricated and termed as PHEA/SS-1.25, PHEA/SS-2.5 and PHEA/SS-5, respectively. The pure hydroxyethyl acrylamide (HEA) hydrogels was also fabricated *via* free radical polymerization to produce PHEA, and used as the controlled sample.

The physical appearances and gelation times of 3D porous semi-IPN hydrogel scaffolds of PHEA/SS fabricated by using different loadings of cross-linker were observed and shown in table 12.

After studying the fabrication of PHEA/SS with different loadings of cross-linker, the cross-linker concentration at 0.5 wt % was chosen to fabricate into the form of semi-IPN scaffold and the effect of silk sericin contents studied. Table 13 shows the physical appearances and gelation times of 3D porous semi-IPN hydrogel scaffolds of PHEA/SS by using different contents of silk sericin.

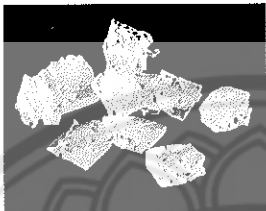
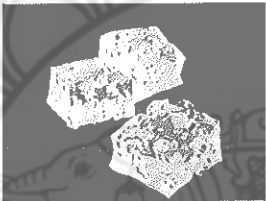
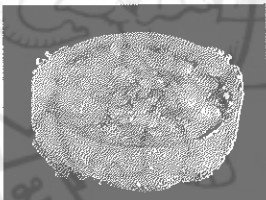
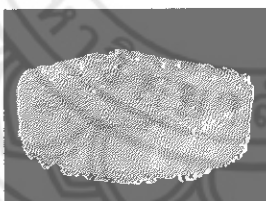
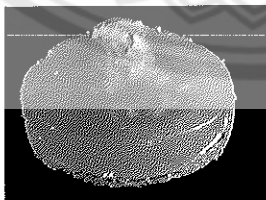


**Table 12** The physical appearances and gelation times of 3D porous semi-IPN hydrogel scaffolds of PHEA/SS by using different loadings of cross-linker (N’N-methylene bisacrylamide, XL)

| Name                  | Sample Appearance   | Appearance  | Gelation time (min) |
|-----------------------|---|---|---------------------|
| 0% XL<br>PHEA/SS-0    |    | Transparent hydrogel, hard and brittle                                  | 1.00                |
| 0% XL<br>PHEA/SS-5    |   | Dark yellow, transparent, very soft, flexible and tough                 | 2.15                |
| 0.25% XL<br>PHEA/SS-5 |  | Dark yellow, transparent, flexible and tough                            | 2.10                |
| 0.5%XL<br>PHEA/SS-5   |  | Dark yellow, transparent, flexible and tough                            | 2.05                |
| 1.0%XL<br>PHEA/SS-5   |  | Dark yellow, transparent, slightly hard and more brittle than lower %XL | 1.45                |
| 2.0%XL<br>PHEA/SS-5   |  | Dark yellow, hard, transparent and more brittle than other samples      | 1.20                |



**Table 13 The physical appearances of 3D porous semi-IPN hydrogel scaffolds of PHEA/SS by using different silk sericin contents**

| Name                   | Sample Appearance   | Appearance  | Gelation time (min) |
|------------------------|---|---|---------------------|
| 0%XL<br>PHEA/SS-0      |    | Transparent hydrogel, hard and brittle                              | 1.00                |
| 0.5%XL<br>PHEA/SS-0    |   | Transparent hydrogel, hard and brittle                              | 1.20                |
| 0.5%XL<br>PHEA/SS-1.25 |  | Light yellow, transparent, a lot of bubble in scaffold, flexible    | 1.40                |
| 0.5%XL<br>PHEA/SS-2.5  |  | Light yellow, a lot of bubble in scaffold, transparent and flexible | 1.50                |
| 0.5%XL<br>PHEA-SS-5    |  | Light yellow, flexible, transparent and tough                       | 2.05                |

After finishing of reaction, the semi-IPN hydrogels in the form of 3D semi-IPN structure of PHEA/SS were washed with de-ionized water for three times and then immersed in ethanol to remove any unreacted monomer. Finally, the fabricated scaffolds were freeze-dried to obtain the porous structure. Figure 37 shows examples of physical appearances of 0.25% XL PHEA/SS-5 (37a.), 2.0% XL PHEA/SS-5 (37b.)

and 0.5% XL PHEA/SS-1.25 (37c.), which were used to represent other scaffolds after lyophilization. A 0.25% XL PHEA/SS-5 (37a.) represents the scaffolds that have porous structure on the surface and are slightly brittle materials, while the 2.0% XL PHEA/SS-5 (37b.) represents the scaffolds that do not have porous structure on the surface and are hard material. The 0.5% XL PHEA/SS-1.25 (37c.) represents all the scaffolds that used 0.5 wt% cross-linker with different concentrations of silk sericin that have porous structures and are tough materials.

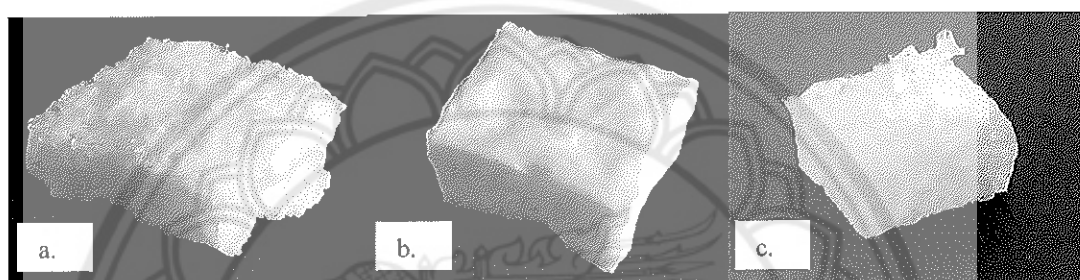
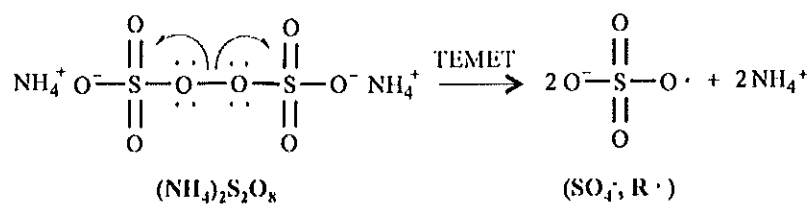


**Figure 37** Examples of the physical appearance of 0.25% XL PHEA/SS-5 (a.), 2.0% XL PHEA/SS-5 (b.) and 0.5% XL PHEA/SS-1.25 (c.), which were used to represent other scaffolds after lyophilization

**The proposed reaction of preparation of 3D porous semi-IPN hydrogel scaffolds of PHEA/SS**

3D porous semi-interpenetrating polymer networks (semi-IPN) composed of silk sericin and hydroxyl containing polymers are prepared by conventional free-radical polymerization and were fabricated in the 24 well plates. The free radical polymerization was obtained by using the redox pairs of ammonium persulfate (APS) and N, N, N', N'-tetramethylenedia-mine (TEMED). The cross-linked network was generated by using N, N-methylene-bisacrylamide (N, N'-MBAAm), as a cross-linker. Hydroxyethyl acrylamide (HEA) a hydroxyl containing polymer, was used as the monomer. The synthetic reaction of producing 3D porous semi-IPN hydrogel scaffolds of PHEA/SS by a conventional free radical polymerization is shown in figure 38.

## 1. Chain-Initiation step



## 2. Chain-Propagation step

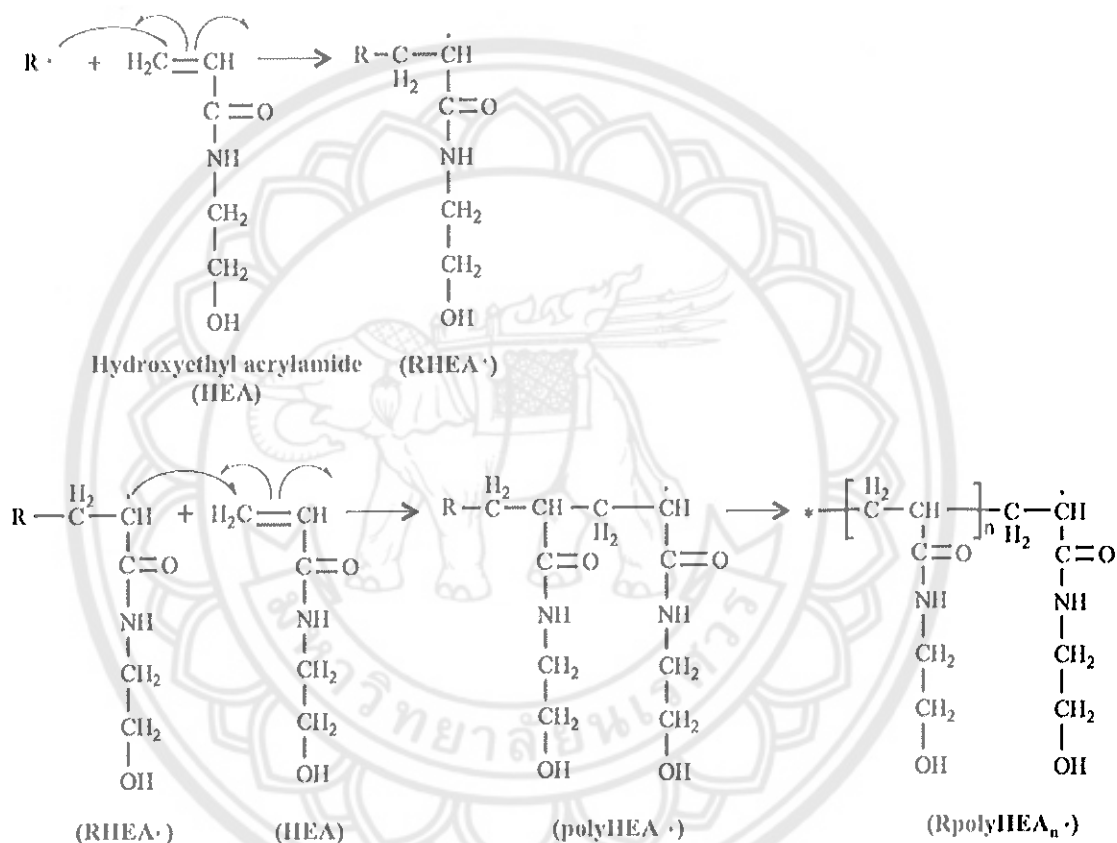


**Figure 38** The synthetic reaction of producing 3D porous semi-IPN hydrogel scaffolds of PHEA/SS by a conventional free radical polymerization



The free-radical polymerization of hydroxyethyl acrylamide (HEA) can be separated into 3 steps of; 1) chain-initiation step, 2) chain-propagation step and 3) termination, to produce the cross-link hydrogel networks of poly(hydroxyethyl acrylamide) (PHEA). In the chain-initiation step, ammonium persulfate, which is used as initiator, is homolytically cleaved in the presence of TEMED and then produced two free radicals of sulfates.

In the chain-propagation step, the sulphateradicals attacks a HEA molecule to start the polymer radical chain ( $\text{RHEA}\bullet$ ). Then, the  $\text{RHEA}\bullet$  continues to attack another HEA molecule to propagate longer polymer radical chains ( $\text{RM}_n\text{M}\bullet$ ). The propagation continues to occur until the  $\text{RpolyHEA}_n\bullet$  is produced. In the presence of the N-methylenebisacrylamide (MBAAm, a vinyl ended groups cross-linker), it reacts with  $\text{RpolyHEA}_n\bullet$  to form a linked free radical molecule of polyHEA-cross-linker-polyHEA ( $\text{C-RpolyHEA}_n\bullet$ ).

Finally, the combination of two active ended chains ( $\text{C-RpolyHEA}_n\bullet$ ) simply couple together to form long chain polymer networks of PHEA-cross-linker-PHEA (polyHEA-C-polyHEA). In this work, silk sericin was added during polymerization, thus, molecule of silk sericin can be trapped in the networks. In summary, a semi-interpenetrating polymer network of PHEA-PHEA containing silk sericin (as independent chains in the networks) were produced. However, the possible interaction of physical hydrogen bonding between PHEA, cross-linker and silk sericin molecules can also to occur in this fabrication system.

**The effect of concentration of cross-linker of 3D porous semi-IPN hydrogel scaffolds of PHEA/SS**

#### **1. Gelation time of 3D porous semi-IPN hydrogel scaffolds**

The 3D porous semi-IPN hydrogel scaffolds of PHEA/SS with different loadings of cross-linker were successfully fabricated in which the amounts of silk sericin was controlled at 5 wt% of all samples. The gelation time, which refers as the period of time required for gel formation after adding initiator, the last component added into the mixed solution until the complete cross-linked network structure or gel structure was constructed, was recorded as shown in table 13, and shown again in figure 39.

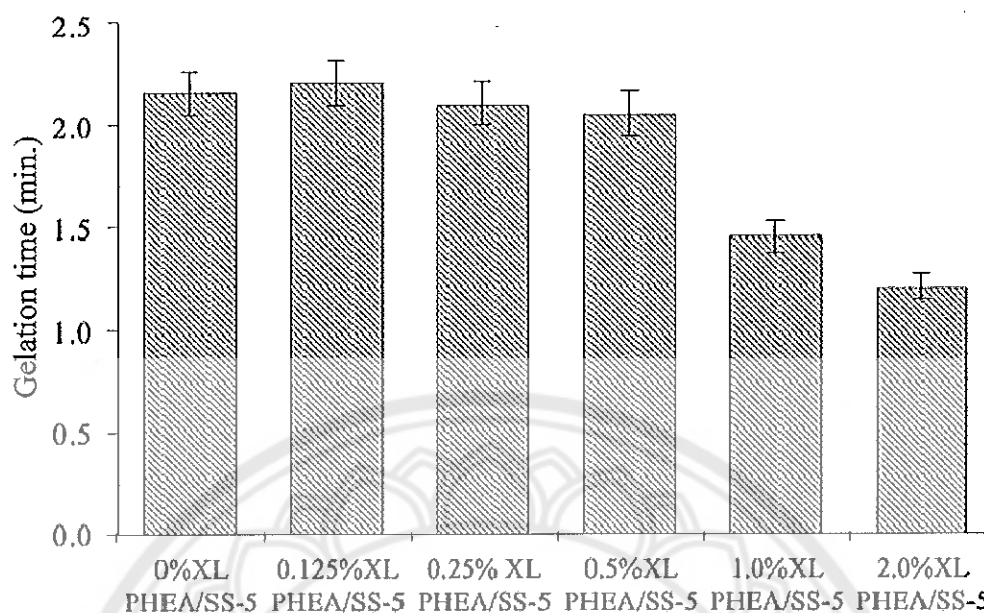


**Figure 39** Gelation times of 3D porous semi-IPN hydrogel scaffolds of PHEA/SS with different loading of cross-linker at room temperature ( $n = 3$ )

From figure 39, the gelation time of 0%XL PHEA/SS-5 is about 2.15 minutes but when adding cross-linker into the polymerization system the gelation times are slightly decrease until 0.5% XL, and dramatically decrease at 1.0% XL and 2.0% XL. The fastest gelation was exhibited at 1.25 minutes when using high loading of cross-linker at 2.0 wt%. It can be seen that the amount of cross-linker effected to the polymerization times of these semi-IPN hydrogels.

## 2. Morphology of 3D porous semi-IPN hydrogel scaffolds of PHEA/SS

The morphology of cross-section of freeze-dried 3D porous semi-IPN hydrogel scaffolds of PHEA/SS with different concentrations of cross-linker, which were fractured in liquid nitrogen, were also investigated by scanning electron microscope (SEM). Figure 40 shows SEM images of 3D porous semi-IPN hydrogel scaffolds of PHEA/SS at different concentrations of cross-linker; a. 0% XL (0%XL PHEA/SS-5) b. 0.125% XL (0.125%XL PHEA/SS-5) c. 0.25% XL (0.25%XL PHEA/SS-5) d. 0.5% XL (0.5%XL PHEA/SS-5), e. 1.0% XL (1.0%XL PHEA/SS-5) and f. 2%XL (2%XL PHEA/SS-5).

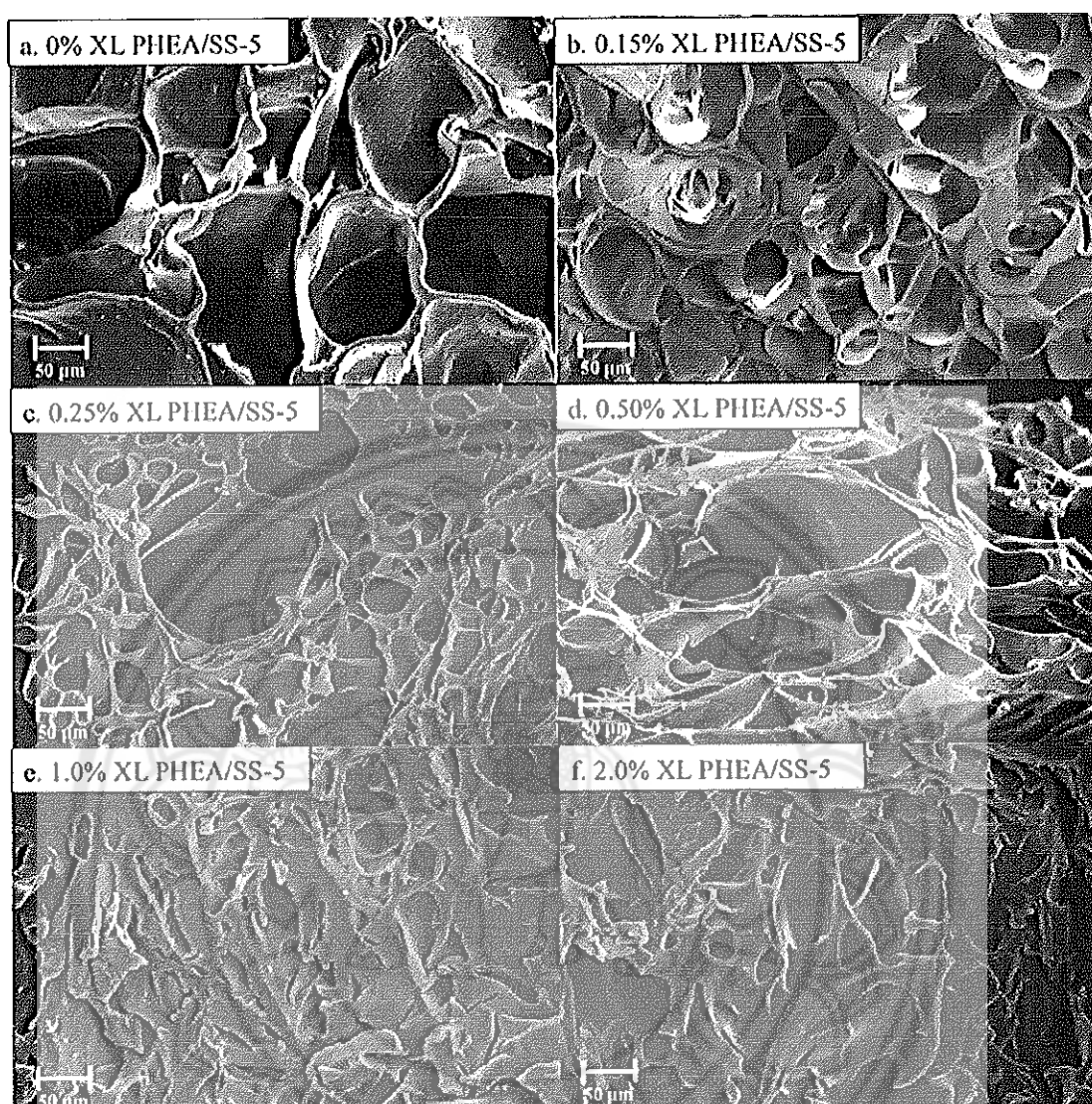


**Figure 40** SEM images of 3D porous semi-IPN hydrogel scaffolds of PHEA/SS at different concentrations of crosslink: (a) 0%XL PHEA/SS-5 (b) 0.125%XL PHEA/SS-5 (c) 0.25%XL PHEA/SS-5 (d) 0.5%XL PHEA/SS-5 (e) 1.0%XL PHEA/SS-5 and (f) 2.0%XL PHEA/SS-5

All 3D porous semi-IPN hydrogel scaffolds of PHEA/SS had porous structures with different diameter sizes and connecting orders in which 3D porous semi-IPN hydrogel scaffolds of PHEA/SS without cross-linker showed the biggest porous diameter size of approximately 100  $\mu\text{m}$  (Figure 40a). Adding 0.125%XL (Figure 40b), 0.25% XL and 0.50%XL (Figure 40c) into 3D porous semi-IPN

hydrogel scaffolds of PHEA/SS, the porous structure was also promoted but with a smaller diameter and higher density compared to that of 0%XL PHEA/SS. However, adding high cross-linker concentrations of 1.0% XL (Figure 39d) and 2.0% XL (Figure 40e) decrease the porous density and interconnecting structure when compared to other samples (Figure 40a, b, c). In summary, it can be concluded that using cross-linker created the polymer networks of PHEA that caused to the smaller porous diameter sizes of these 3D porous semi-IPN hydrogel scaffolds of PHEA/SS. The smallest number of porous or porous density was observed in the composition that used 2 wt% of cross-linker (Figure 40f) due to the high crosslink density in this hydrogel structure.

### 3. Swelling ratio

The swelling ratios of these 3D porous semi-IPN hydrogel scaffolds of PHEA/SS were also investigated. This value described the capability of the hydrogel scaffolds to accumulate water into their polymer networks during the time of immersing into the water compared to the dried hydrogel scaffold, which can be a good value beneficial for further use. In this experiment, the completely lyophilized hydrogels were immersed in deionized water at 37°C. Three gels from each composition were taken out at pre-determined time intervals and tested at each time point from 1, 4, 8, 12 and 24 hrs. Figure 41 shows the swelling ratio of 3D porous semi-IPN hydrogel scaffolds of PHEA-SS different of crosslink loading, it was observed that hydrogels of PHEA/SS was fully swelling within 24 hours.



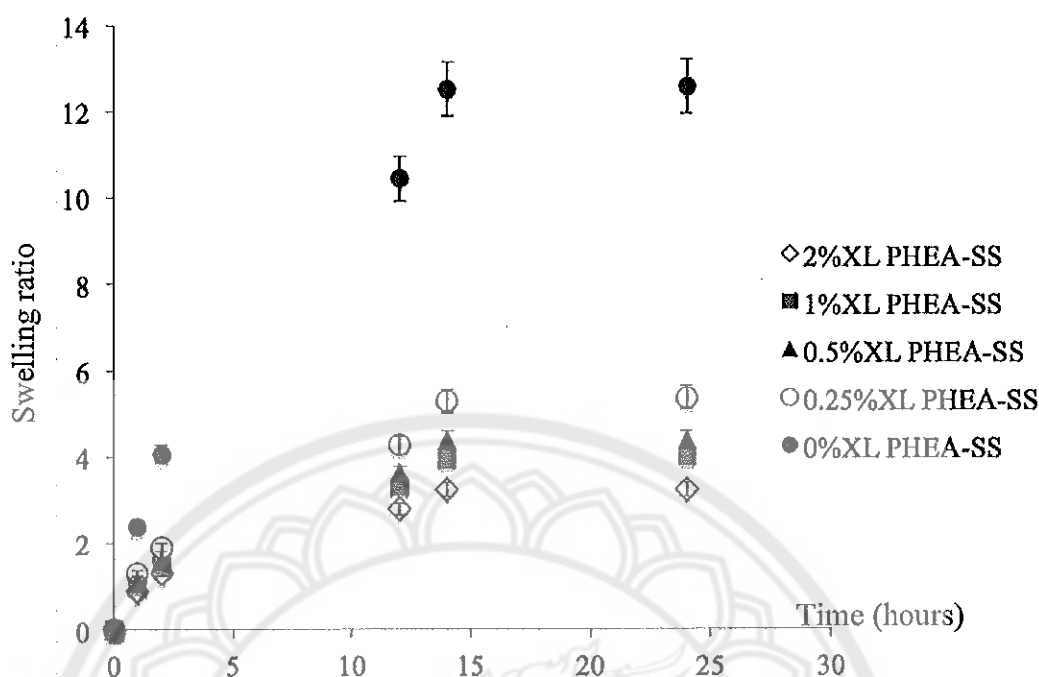


**Figure 41** Swelling ratio of 3D porous semi-IPN hydrogel scaffolds of PHEA/SS with different loading of cross-linker (n = 3)

It can be seen that the 3D porous semi-IPN hydrogel scaffolds of PHEA/SS without cross-linker (0%XL PHEA/SS) showed significantly higher swelling ratios than that of hydrogel scaffolds with cross-linker. However, the hydrogel of PHEA without cross-linker and SS showed highest swelling ratio and higher than other samples that had cross-linker about 4 times (data not shown in figure 41). Using higher percentage of cross-linker showed the lower swelling ratio, especially 2%XL PHEA/SS had lowest swelling ratio due to the decreasing in porosity and then lower the water holding capacity in its structure. The results suggest that increasing the cross-linker concentration slightly decreases the swell ability of the scaffolds.

#### Summary of the section

In summary of the effect of cross-linker onto the properties of semi-IPN hydrogel scaffolds, it was found that the cross-linker loading affected the gelation time, morphology and swelling ratio of 3D porous semi-IPN hydrogel scaffolds of PHEA-SS at the controlling amount of silk sericin of 5%wt. The 3D porous semi-IPN hydrogel scaffolds of PHEA-SS without cross-linker showed significant differences in

physical properties and morphology from hydrogel scaffolds with cross-linker. The small loadings of cross-linker (0.125%, 0.25% and 0.5%) in the polymerization system showed similar gelation times, while higher loading of cross-linker (1% and 2%) had shorter time of polymerization. In addition, it was observed that silk sericin helps to improve the flexibility of the hydrogel scaffolds, as compared to the 3D porous semi-IPN hydrogel scaffolds of PHEA-SS (no silk sericin added).

Therefore, the design of the experiment with study the effect of silk sericin loading onto the 3D porous semi-IPN hydrogel scaffolds of PHEA-SS by controlling the percentage of cross-linker at 0.5 wt% was further studied. The reason to choose the 0.5 wt% of cross-linker is due to the optimization of gelation time, porous structures and swelling ratio.

#### **The effect of silk sericin content of 3D porous semi-IPN hydrogel scaffolds of PHEA/SS**

The 3D porous semi-IPN hydrogel scaffolds of PHEA/SS was investigated with different loadings of silk sericin and constant loading of 0.5 wt% N-methylene-bisacrylamide (MBAAm, a cross-linker). Four different concentrations of silk sericin (SS) (0, 1.25, 2.5 and 5 wt%) were used to add into the polymerized 3D porous semi-IPN hydrogel scaffold of PHEA/SS that had 0.5 wt% of cross-linker. Gelation time, morphology, swelling ratio, release of silk sericin, in vitro degradation and cell culture test were observed to find the best composition that can be suitable in terms of fabrication and application in the field of skin tissue reconstruction.

##### **1. Gelation time of 3D porous semi-IPN hydrogel scaffolds**

The gelation time proceeded of 3D porous semi-IPN hydrogel scaffold of PHEA/SS was investigated and showed in figure 42.

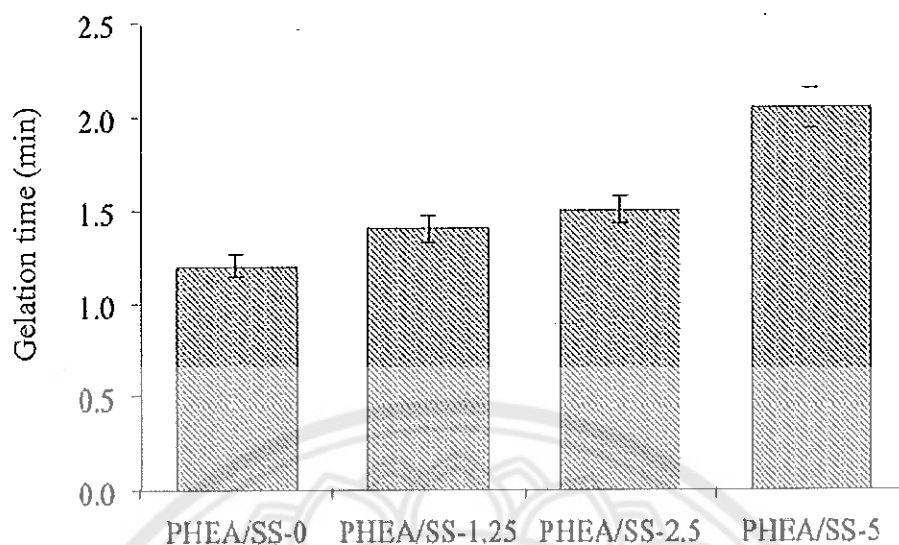


**Figure 42 Gelation times of 3D porous semi-IPN hydrogel scaffolds of PHEA/SS with different loadings of sericin**

From figure 42, the hydrogel scaffold without silk sericin (PHEA/SS-0) had the shortest time to polymerize, while increasing in silk sericin loading resulted in longer gelation time. In this case, longer gelation time were seen because the higher amounts of silk sericin chains obstructed the growth of PHEA chains and PHEA-crosslink-PHEA network.

## 2. Morphology of 3D porous semi-IPN hydrogel scaffolds of PHEA/SS

The SEM images of the cross-sectioned hydrogel scaffolds of PHEA/SS with different loadings of silk sericin, at the control cross-linker amount of 0.5wt%, were also observed by SEM. The lyophilized samples were cryo-fractured in liquid nitrogen and coated with gold before testing. Figure 43 shows the SEM images of cross-sectioned samples that were prepared with different compositions of silk sericin; a. 0% silk sericin content (PHEA/SS-0), b. 1.25% silk sericin content (PHEA/SS-1.25), c. 2.5% silk sericin content (PHEA/SS-2.5) and d. 5% silk sericin content (PHEA/SS-5).

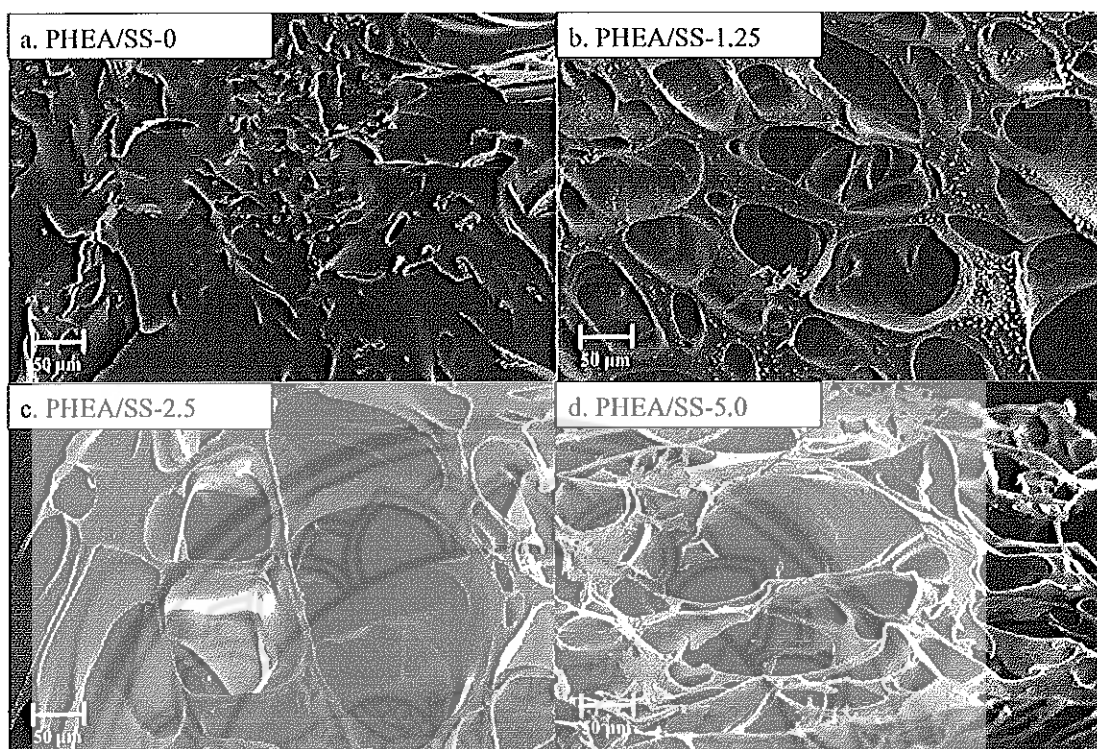


**Figure 43** SEM images of 3D porous semi-IPN hydrogel scaffolds of PHEA/SS at different loading of silk sericin: (a) PHEA/SS-0; (b) PHEA/SS-1.25; (c) PHEA/SS-2.5 and (d) PHEA/SS-5

It can be seen that the hydrogel scaffold without silk sericin loading (Figure 43a) showed very small number of porous structures comparing to the scaffolds containing silk sericin (Figure 43b, c, and d). Among the scaffolds adding silk sericin, the difference in porous diameter sizes and well-order of the structures were observed. In case of increasing silk sericin, an average diameter of porous structure is increase as well as porous density. In addition, the continuous uniformity of the pores was also promoted when adding silk sericin into the semi-IPN scaffolds. In the literature [65], it was reported that the concentration of silk sericin effected the cell viability and cell proliferation. The enhanced porosity of the matrix is expected to aid cell migration within the pores and will help in cell attachment by providing a larger surface area.

### 3. Swelling ratio

Completely lyophilized hydrogels were immersed in deionized water at 37°C. Three gels from each composition were taken out at pre-determined time intervals and tested at each time point from 1, 4, 8, 12 and 24 hours. Figure 44 shows the swelling ratio of 3D porous semi-IPN hydrogel scaffolds of PHEA/SS with different silk sericin contents at 0.5% wt. of cross-linker. To be note, the hydrogel of PHEA without cross-linker and SS showed highest swelling ratio and higher than other samples that had cross-linker about 4 times (data not shown in figure 42).



**Figure 44 Swelling ratio of 3D porous semi-IPN hydrogel scaffolds of PHEA/SS with different loadings of silk sericin**

The hydrogel scaffold without silk sericin (PHEA/SS-0) shows the highest swelling ratio and significantly different from the hydrogel scaffold with adding silk sericin, which having no different between adding 1.25, 2.5 and 5wt% of silk sericin. In this case, the hydrogel scaffold of PHEA can uptake water into their physical and chemical cross-linked polymer networks that have higher cross-link density than that of PHEA/SS. In this case, it seems to show that silk sericin acted as an inhibitor to

prevent the polymerization and cross-linking of PHEA, as seen from the difference in gelation time and morphology. However, the amount of silk sericin shows a very small effect to the swelling ratio of these 3D porous semi-IPN hydrogel scaffolds of PHEA/SS but seen in the gelation time and morphology. More importantly, silk sericin helps to promote the semi-IPN hydrogel scaffold having flexibility.

#### 4. Release of silk sericin

The amount of protein silk sericin released from 3D porous semi-IPN hydrogel scaffolds of PHEA/SS was observed depending of the silk sericin contents. Three hydrogels from each composition were tested at each time point from 1, 2, 4, 8, 16, 32 hours and 14 days at 37°C. The PBS solutions were collected and evaluated for protein concentration at selected time and determined from OD value. Figure 45 shows the silk sericin release observed by optical density at 595 nm at different time intervals.

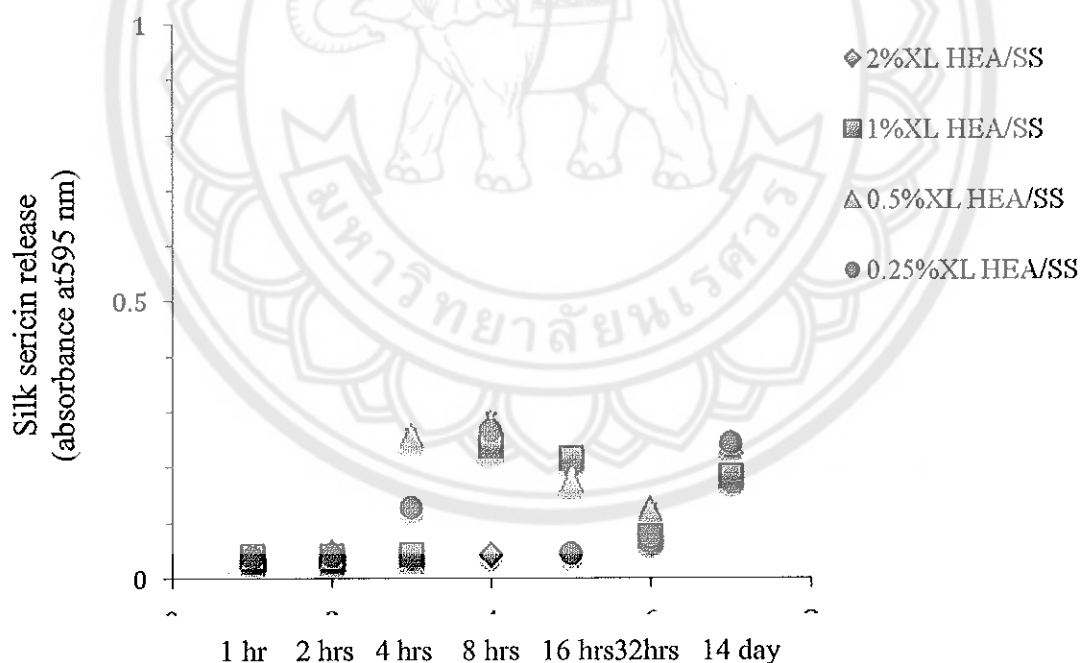


**Figure 45** The silk sericin released from 3D porous semi-IPN hydrogel scaffolds of PHEA/SS with different loadings of silk sericin

From figure 45, it can be seen that the amount of protein silk sericin released is low and not significantly different among each composition. However, higher

amounts of silk sericin were released from all semi-IPN hydrogels was observed during 4-16 hours and at day 14.

### 5. *In-vitro* degradation at 30 days

The *In-vitro* degradation of 3D porous semi-IPN hydrogel scaffolds of PHEA/SS were measured by the percentage weight loss with time by adding hydrogel scaffolds into the phosphate buffer solution (PBS) pH 7.4 at 37°C for 30 days. The separated set of scaffolds (0, 1.25, 2.5 and 5.0 wt% of silk sericin contents) was used in which three samples for each composition were tested at 30 days. Figure 46 shows the percentage of weight loss of 3D porous semi-IPN hydrogel scaffolds of PHEA/SS at different concentrations of silk sericin and constant loading of 0.5 w%t cross-linker.

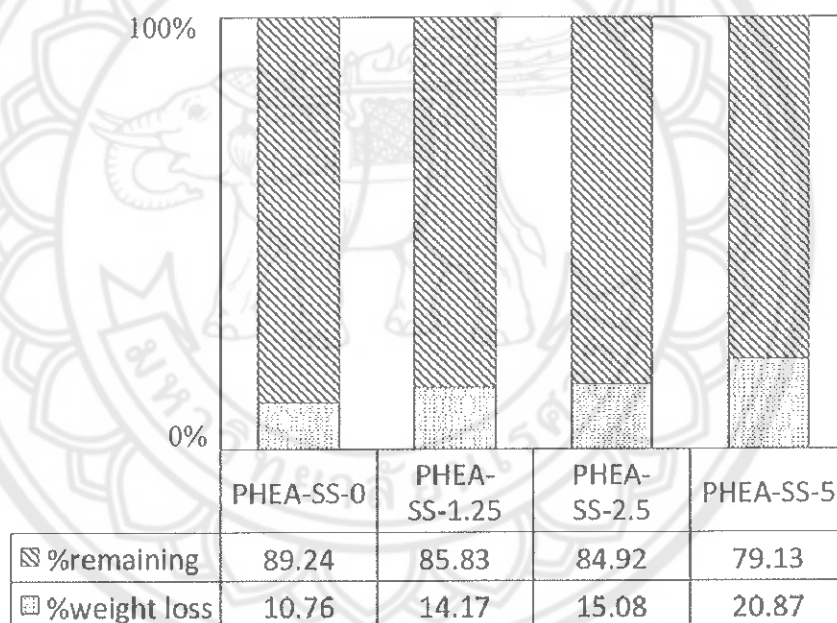


**Figure 46** *In-vitro* degradation of 3D porous semi-IPN hydrogel scaffolds of PHEA/SS with different loadings of silk sericin at day 30

A minimum percentage of weight loss is seen in the case of 0%XL PHEA/SS, while maximum in the case of PHEA/SS-5. It seems to show that the *in vitro* degradation of silk sericin is the key factor to enhance the percentage of weight loss of the scaffolds. The more silk sericin content the more percentage of weight loss of scaffolds can be observed. Therefore, it can be concluded that silk sericin can be able to promote the degradation and percentage of weight loss of these 3D porous semi-IPN hydrogel scaffolds of PHEA/SS.

#### **6. Cell viability and proliferation of 3D porous semi-IPN hydrogel scaffolds of PHEA/SS**

The viability and proliferation of cells loaded of 3D porous semi-IPN hydrogel scaffolds of PHEA/SS prepared with various loadings of silk sericin were studied by MTT assay for 3, 6 and 14 days of culture. Feline fibroblast cells of HFF-1 were cultured on hydrogels of PHEA/SS of PHEA/SS-0, PHEA/SS-1.25, PHEA/SS-2.5 PHEA/SS-5 and the control plates (polystyrene plate) to assess proliferation and cytotoxicity. Figure 47 show the cartoon drawing representing the change of the sample colour after culture for 3, 7 and 14 days using MTT assay. The highest change in colour is observed at day 7 of culture and then decrease at day 14. Figure 48 shows the cell proliferation of HFF-1 on 3D porous semi-IPN hydrogel scaffolds of PHEA/SS with different loading of silk sericin content and positive control (polystyrene plates) after 3, 7 and 14 days of culture, measured by the optical density of changing in formazan crystal structure.



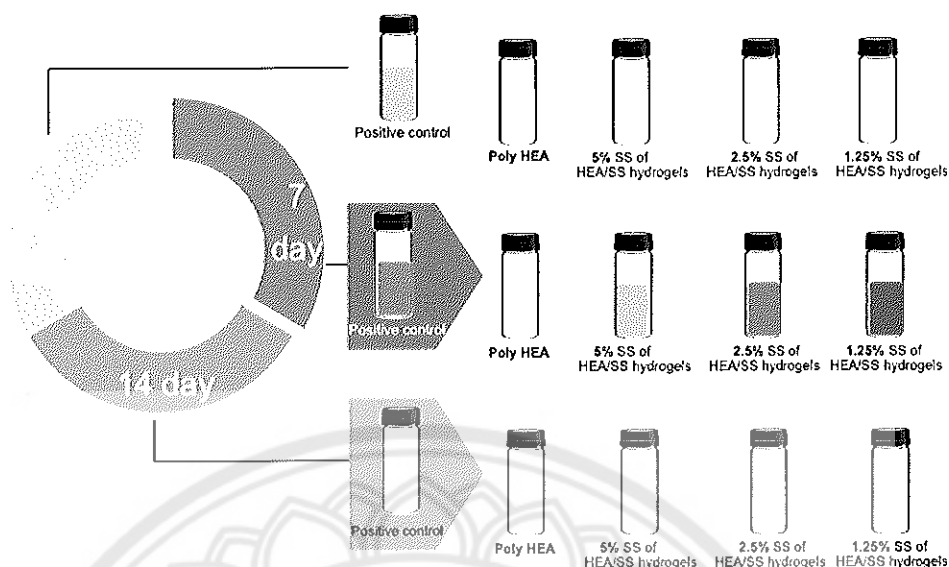


**Figure 47** Cartoon drawing represented the formazan crystals of the active mitochondria of the viable cells on 3D porous semi-IPN hydrogel scaffolds of PHEA/SS with different loadings of silk sericin and positive control (polystyrene plates) after 3, 7 and 14 days of culture

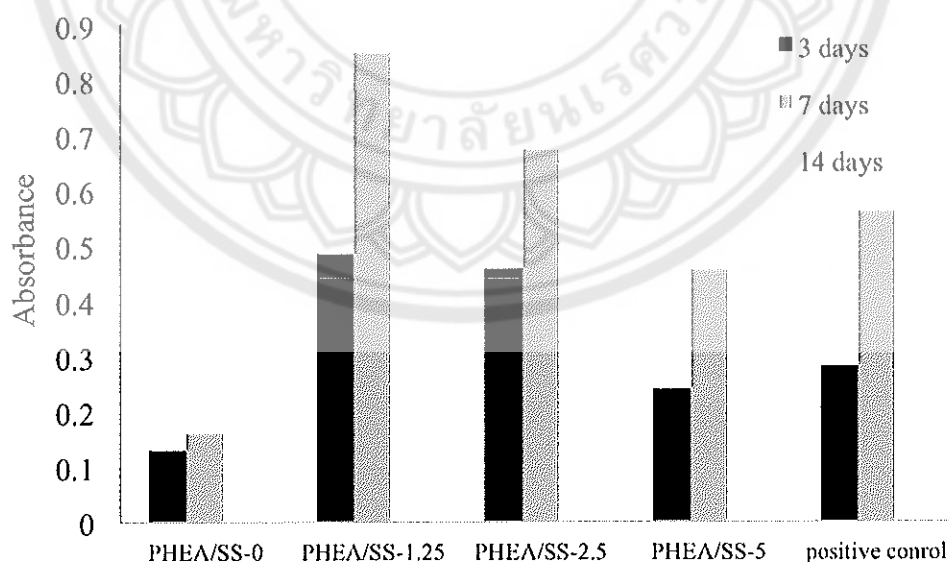


**Figure 48** Cell proliferation of HFF-1 on 3D porous semi-IPN hydrogel scaffolds of PHEA/SS with different loading of silk sericin content and positive control (polystyrene plates) after 3, 7 and 14 days of culture

The cell viability of the positive control showed higher from day 3 to day 7 and then decreases in day 14. This is due to the high growth rate of fibroblast cell until there have no space for cell to growth, which cause cells to die finally in day 14. The hydrogel scaffold of PHEA without silk sericin (PHEA/SS-0) had no cell proliferation, whereas hydrogel scaffolds with silk sericin can be supported cell viability when comparable to the positive control. This confirms that using silk sericin can be able to promote cell viability of the 3D porous semi-IPN hydrogel scaffolds of PHEA/SS.

All 3D porous semi-IPN hydrogel scaffolds of 1.25, 2.5 and 5 %wt. of silk sericin shows highest cell proliferations in day 7 and then decrease in day 14 because high cell growth causes no enough space for cell to adhere and finally they die in day 14. Comparing at day 3 and 7 of culture, it can be seen that the hydrogel scaffolds of PHEA/SS-1.25 showed higher cell proliferation than that of PHEA/SS-2.5 and PHEA/SS-5, respectively.

The decrease in cell proliferation when using high silk sericin contents was probably because silk sericin released into culture medium, as confirmed by silk sericin release results, which may have some cytotoxic effect on cells [48]. Therefore, the 3D porous semi-IPN hydrogel scaffold of PHEA/SS-1.25 is the most suitable for fibroblast cell to migrate easily and then promote cell proliferation due to having the connective porous structure which is about 50-100  $\mu\text{m}$  and especially containing of silk sericin.

### **Summary of approach II**

Three-dimensional semi-interpenetrating polymer network porous hydrogel scaffolds were investigated and prepared for dermal reconstruction. Scaffolds were fabricated by using conventional free-radical polymerization of a hydroxyl containing monomer (*N*-hydroxyethyl acrylamide, HEA) and silk sericin in the presence of cross-linker, to form a semi-interpenetrating network. Its porous structure was promoted using lyophilization technique, and it was observed that the amount of cross-linker and concentration of silksericin affected the physical properties and appearance of scaffolds. Adding silksericin into the hydrogel scaffolds gave good compatibility of HFF1 fibroblast cell line and promoted cell proliferation and cell ability. In addition, it was observed that the pore size of scaffolds played a critical role into the viability of the fibroblast cells.

## CHAPTER V

### CONCLUSION

The work presented in this thesis was concerned with the fabrication of three-dimensional (3D) porous scaffolds from silk sericin (SS) and biocompatible polymers for dermal reconstruction. The 3D porous scaffolds for dermal reconstruction, were made from biodegradable and biocompatible materials, which can cover the wound as a wound dressing and also provides support to both dermal fibroblasts and keratinocytes for reconstruction into the form porous materials. This work was divided into two approaches depending on type of biocompatible materials and techniques used to fabricate 3D porous scaffolds. The first approach was the fabrication of poly(vinyl alcohol) (PVA) and silk sericin (SS) into the form of 3D porous scaffold *via* classical condensation reaction. The second approach was the fabrication of 3D porous hydrogels scaffold of hydroxyethyl acrylamide (HEA) and silk sericin (SS) *via* conventional free radical polymerization into the form of a semi-interpenetrating polymer network (semi-IPN). These two approaches used the lyophilization technique to promote the porous structures of the scaffolds.

Recently, various literature has observed that silk sericin has efficiency to promote skin cell proliferation, cell adhesion and especially in dermal reconstruction applications. Therefore, in this work silk sericin was chosen to use with the aim to increase cell proliferation and cell attachment for this application. Poly(vinyl alcohol) (PVA) is recognized as one of the very few vinyl polymers soluble in water also susceptible of ultimate biodegradation in the presence of suitably acclimated microorganisms. According to the most important biocompatible and biodegradable properties of PVA and silk sericin, they were used to fabricate into the fully biodegradable and compatible 3D porous scaffolds, within approach I. This approach studied the effect of concentrations of dimethylolurea (DMU) (a cross-linker) on the preparation of the scaffolds. Morphology (surface and cross-section) and cell culture tests (cell proliferation and adhesion) were observed to find the best composition for the scaffold that would be suitable for skin reconstruction.

In this approach, 3D porous scaffolds of cross-linked networks of silk sericin and PVA were successfully fabricated with the potential use in skin-tissue reconstruction. It was observed that 10% DMU of PVA/SS with porous diameters of 10-30  $\mu\text{m}$  showed high efficiency for skin cell proliferation and adhesion. Using higher percentage of DMU led to well-ordered pore structures in cross-linked polymer networks but this does not enhance cell proliferation or adhesion. Silk sericin has good potential to react to form networks, which have biocompatible and biodegradable properties. In summary, all of work studied in this approach I can be demonstrated by figure 49, the hydroxyl groups of DMU covalently bond with the hydroxyl groups presented in both the PVA and SS chains through a condensation reaction.

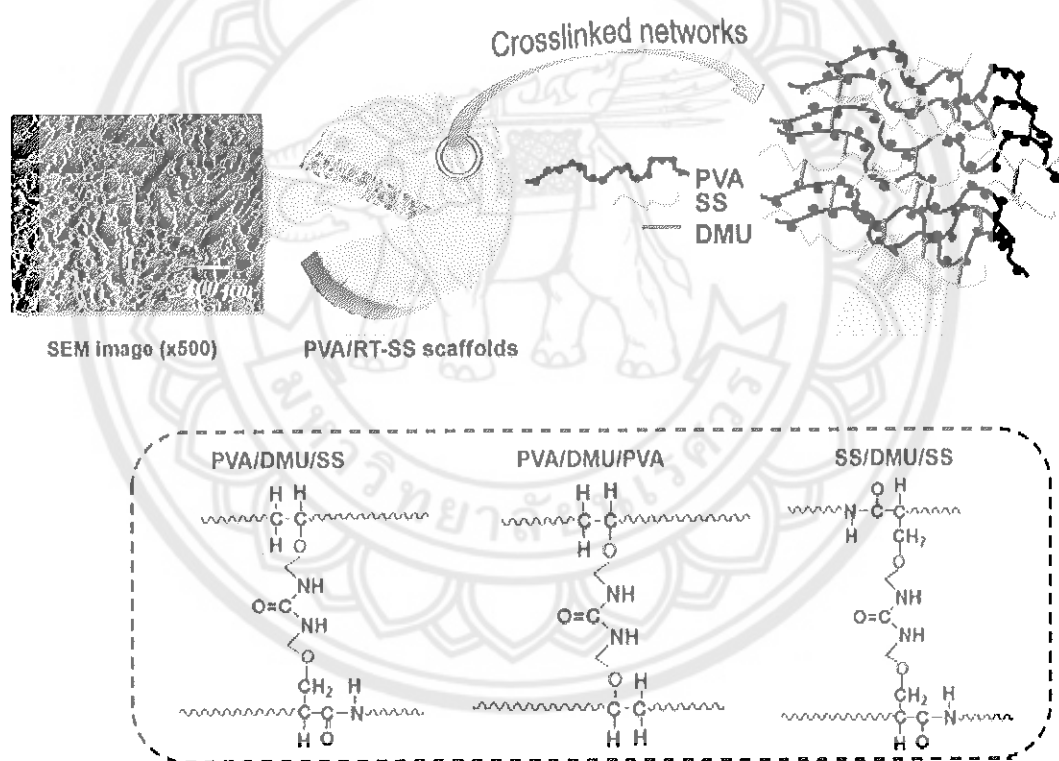


**Figure 49** Cartoon structure of approach I, 3D porous polymer network of PVA/SS and crosslinking reaction scheme between PVA, SS and DMU

Therefore, the possible polymer network interactions of scaffold are PVA-DMU-SS, PVA-DMU-PVA and SS-DMU-SS. Silk sericin prepared by hot-water degumming process is a good selection as a bio-based material to fabricate with biodegradable polymers like PVA, with good potential for reacting to form full 3D networks, which have biocompatible and biodegradable properties.

Hydrogels are the popular choice in soft dermal reconstruction because hydrogels can swell in an aqueous solution like water but not in other solvents the same as, animal and human skin. In literature, it was reported that hydrogel scaffolds show low risk of infection and have good delivery of cells and cytokines. The important property of hydrogels scaffolds for dermal reconstruction is they required good mechanical properties, especially the strength of the scaffolds. Therefore, the form of semi-interpenetrating polymer networks (semi-IPN) was selected to fabricate within approach II, with the aim of controlling the mechanical properties of the hydrogel scaffolds. The monomer chosen to form the semi-IPN is hydroxyethyl acrylamide (HEA). This approach was investigated and prepared the semi-IPN scaffold composed of silk sericin (SS) and PHEA *via* conventional free-radical polymerization in the presence of N-methylene-bisacrylamide (N<sup>'</sup>N-MBAAm, a cross-linker). The effect of loadings of cross-linker and silk sericin onto the properties of scaffolds were also studied to find the proper compositions and conditions that can be supported the skin fibroblast cells and promoted the cell proliferation. Figure 50 shows the cartoon structure of approach II, the synthetic of 3D porous semi-IPN hydrogel scaffolds of PHEA/SS by conventional free-radical polymerization.

By studying the effect of cross-linker concentration on the properties of 3D porous semi-IPN hydrogel scaffolds of PHEA/SS, it was found that the hydrogel scaffold without cross-linker showed significantly different physical properties and morphology from hydrogel scaffolds with cross-linker. The small loadings of cross-linker (0.125, 0.25 and 0.5 wt %) in the polymerization system showed similar gelation times, while higher loading of cross-linker (1 and 2 wt %) had shorter time of polymerization. In addition, it was observed that silk sericin helps to improve the flexibility of the hydrogel scaffolds, as compared to the 3D porous semi-IPN hydrogel scaffolds of PHEA-SS (no silk sericin added).

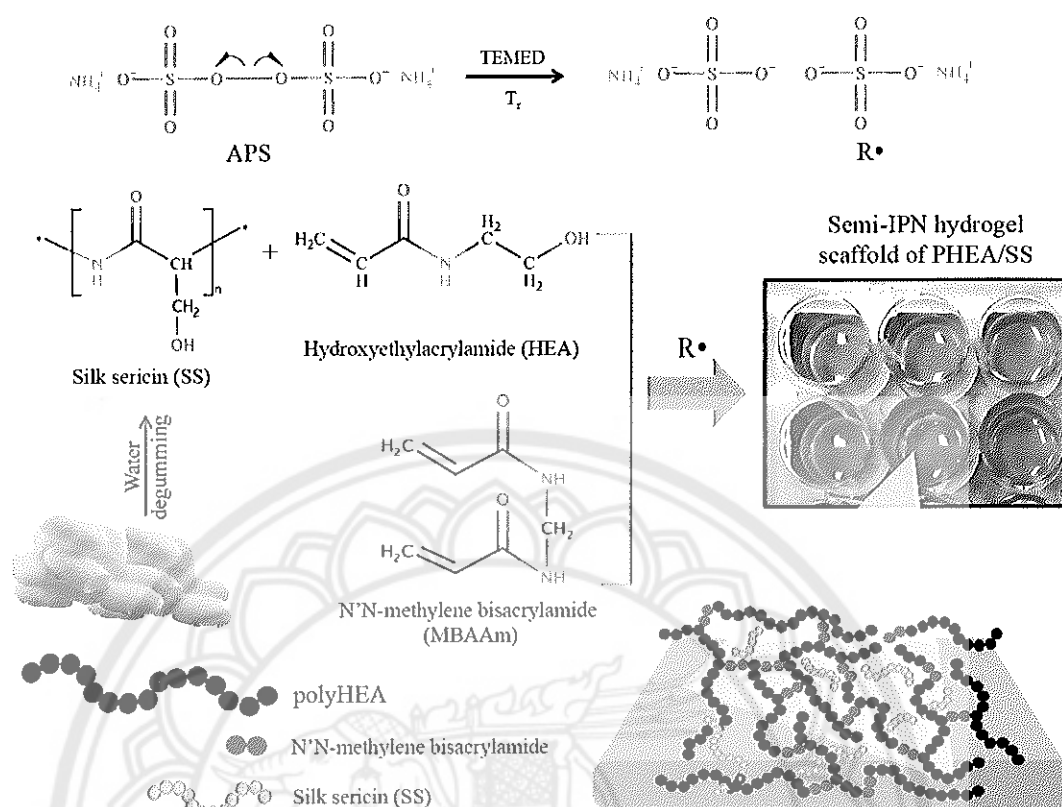


**Figure 50** Cartoon structure of approach II, the synthetic of 3D porous semi-IPN hydrogel scaffolds of PHEA/SS by conventional free-radical polymerization

In the part of study that assessed the effect of silk sericin content on the properties of semi-IPN hydrogel scaffolds of PHEA/SS by keeping the percentage cross-linker constant at 0.5% wt, the results show that the hydrogel scaffold of PHEA without silk sericin (PHEA/SS-0) had no cell proliferation, whereas hydrogel scaffolds with silk sericin can be supported cell viability when comparable to the positive control. The 3D porous semi-IPN hydrogel scaffold of PHEA/SS-1.25 was the most suitable for fibroblast cells allowing easy migration and then promotion cell proliferation due to having a connective porous structure along with containing silk sericin. The decrease in cell proliferation was observed when using high silk sericin contents. This was probably because silk sericin was released into culture medium, as confirmed by silk sericin release results, which may have some cytotoxic effect on cells.

In summary, this research work successfully fabricated 3D porous scaffolds of PVA/SS and 3D porous semi-IPN hydrogel scaffolds of PHEA/SS for potential use as dermal reconstruction materials. Adding silk sericin into the hydrogel scaffolds gave good compatibility with the HFF1 fibroblast cell line and promoted cell proliferation and cell adhesion. As reported earlier [48], sericin is an anti-oxidant, bio-adhesive and bioactive agent, as well as a promising implant for tissue supporting prosthetics of human body. These properties contribute to the excellent suitability of sericin as a material for accelerated wound healing. However, the suitability of silk sericin content still needs further development in the past of cell culture to provide the optimum number of cell to the wound. In addition, it was observed that the size of porous structure, structure arrangement, interconnecting structure, size distribution and porous density of scaffolds played a critical role in the viability of the fibroblast cells. These characteristic properties of fabricated scaffolds were dependent on the amount of cross-linker and concentration of silk sericin used in the system.

### Recommendations

1. This work can be further studied in the short term by continuing *in vitro* study by confocal electron microscope to observe cell behavior within the scaffolds and *in vivo* study in animals.
2. For the long-term research, clinical testing and if possible to apply and to use for the patients who are suffered from chronic wounds, especially the patients who have diabetic wounds.
3. The surface area and porosity of the 3D porous scaffolds can be further studied by Brunauer Emmett Teller (BET) method.
4. The amount of silk sericin released can be further analyzed by calibration curve for determining the concentration of silk sericin released (unknown sample) by comparing the unknown to a set of standard samples of silk sericin that known concentration.
5. The same lots and types of silk cocoons are concerned to use in this research.





## REFERENCES

- [1] Vepari, C., & Kaplan, D. L. (2007). Silk as a biomaterial. *Prog. Polym. Sci*, 32, 991–1007.
- [2] C. B. P. (1983). The Gregg/McGraw-Hill marketing series NV - xii. *fiber to fabric*, 6,594.
- [3] Altman, G. H. (2003). Silk-based biomaterials. *Biomaterials*, 24, 401–416.
- [4] Inoue, S., Tanaka, K., Arisaka, F., Kimura, S., Ohtomo, K., & Mizuno, S. (2000). Silk fibroin of Bombyx mori is secreted, assembling a high molecular mass elementary unit consisting of H-chain, L-chain, and P25, with a 6:6:1 molar ratio. *J. Biol. Chem*, 275, 40517–40528.
- [5] Rajput, S. K., & Kumar Singh, M. (2015). Sericin – A unique biomaterial. *IOSR J. Polym. Text. Eng*, 2, 2348–181.
- [6] Kim, U. J., Park, J., Joo Kim, H., Wada, M., & Kaplan, D. L. (2005). Three-dimensional aqueous-derived biomaterial scaffolds from silk fibroin. *Biomaterials*, 26, 2775–2785.
- [7] Cebe, P. (2013). Beating the heat-fast scanning melts silk beta sheet crystals. *Sci. Rep*, 3, 1130.
- [8] Padamwar, M. N., & Pawar, A. P. (2004). Silk sericin and its application : A review. *J. Sci. Ind. Res. (India)*, 63, 323–329.
- [9] Tsuboi, Y., Ikejiri, T., Shiga, S., Yamada, K., & Itaya, A. (2001). Light can transform the secondary structure of silk protein. *Appl. Phys. A Mater. Sci. Process*, 73, 637–640.
- [10] Bini, E., D. Knight, P., & Kaplan, D. L. (2004). Mapping domain structures in silks from insects and spiders related to protein assembly. *Journal of Molecular Biology*, 335, 27–40.
- [11] Wang, Y., Kim, H. J., Vunjak-Novakovic, G., & Kaplan, D. L. (2006). Stem cell-based tissue engineering with silk biomaterials. *Biomaterials*, 27, 6064–6082.
- [12] Du, C., Jin, J., Li, Y., Kong, X., Wei, K., & Yao, J. (2009). Novel silk fibroin/hydroxyapatite composite films: Structure and properties. *Mater. Sci. Eng. C*, 29, 62–68.

- [13] Nair, L. S., & Laurencin, C. T. (2007). Biodegradable polymers as biomaterials. *Progress in Polymer Science (Oxford)*, 32, 762–798.
- [14] Hallensleben, M. L. (2000). Polyvinyl Compounds, Others. *Ullmann's Encycl. Ind. Chem*, 21, 623–649.
- [15] Tortora, G. J., & Derrickson, B. (2014). *Principles of Anatomy and Physiology*. N.P.: wiley plus.
- [16] Velnar, T., Bailey, T., & Smrkolj, V. (2009). The wound healing process: an overview of the cellular and molecular mechanisms. *J. Int. Med. Res*, 37, 1528.
- [17] Stuart, P. (2014). Cellular, molecular and biochemical differences in the pathophysiology acute (normal) wound healing. *World Wide Wounds*, 1, 1–12.
- [18] Schultz, G. S. (2003). Wound bed preparation: A systematic approach to wound management. *Wound Repair and Regeneration*, 11, 1-28.
- [19] Robson, M. C., Steed, D. L., & Franz, M. G. (2001). Wound healing: biologic features and approaches to maximize healing trajectories. *Current problems in surgery*, 38, 72–140.
- [20] Lazarus, G. S. (1994). Definitions and guidelines for assessment of wounds and evaluation of healing. *Arch. Dermatol*, 130, 489–493.
- [21] Nawaz, Z., & Bentley, G. (2011). Surgical incisions and principles of wound healing. *Surgery*, 29, 59–62.
- [22] Richardson, M. (2004). Acute wounds: an overview of the physiological healing process. *Nurs. Times*, 100, 3-50.
- [23] Rangaraj, A., Harding, K., & Leaper, D. (2011). Role of collagen in wound management. *Wounds UK*, 7, 54–63.
- [24] Hutchinson, J. J., & Lawrence, J. C. (1991). Wound infection under occlusive dressings. *Journal of Hospital Infection*, 17, 83–94.
- [25] Chong, E. J. (2007). Evaluation of electrospun PCL/gelatin nanofibrous scaffold for wound healing and layered dermal reconstitution. *Acta Biomater*, 3, 321–330.
- [26] Ravichandran, R., Sundarrajan, S., Venugopal, J. R., Mukherjee, S., & Ramakrishna, S. (2012). Advances in Polymeric Systems for Tissue Engineering and Biomedical Applications. *Macromolecular Bioscience*, 12, 286–311.

- [27] Chan, B. P., & Leong, K. W. (2008). Scaffolding in tissue engineering: General approaches and tissue-specific considerations. *European Spine Journal*, 17, 4.
- [28] Badylak, S. F. (2004). Xenogeneic extracellular matrix as a scaffold for tissue reconstruction. *Transplant Immunology*, 12, 367–377.
- [29] Bissell, D. M., & Choun, M. O. (1988). The role of extracellular matrix in normal liver. *Scand. J. Gastroenterol. Suppl*, 151, 1–7.
- [30] Hersel, U., Dahmen, C., & Kessler, H. (2003). RGD modified polymers: Biomaterials for stimulated cell adhesion and beyond. *Biomaterials*, 24, 4385–4415.
- [31] Han, J., Wu, Q., Xia, Y., Wagner, M. B., & Xu, C. (2016). Cell alignment induced by anisotropic electrospun fibrous scaffolds alone has limited effect on cardiomyocyte maturation. *Stem Cell Res*, 16, 740–750.
- [32] Schönherr, E., & Hausser, H. J. (2000). Extracellular matrix and cytokines: A functional unit. *Dev. Immunol*, 7, 89–101.
- [33] Mikos, A. G., & Temenoff, J. S. (2000). Formation of highly porous biodegradable scaffolds for tissue engineering. *Electronic Journal of Biotechnology*, 3, 114–119.
- [34] Shivashankar, M., & Mandal, B. K. (2012). A review on interpenetrating polymer network. *Int. J. Pharm. Pharm. Sci*, 4, 1–7.
- [35] Chen, G., Ushida, T. & Tateishi, T. (2002). Scaffold design for tissue engineering. *Macromolecular Bioscience*, 2, 67–77.
- [36] Cowie, J. M. G., & Arrighi, V. (2007). Polymers: Chemistry and Physics of Modern Materials. *Polym. Chem. Phys. Mod. Mater*, 3, 463.
- [37] Anžlovar, A., & Zigon, M. (2005). Semi-interpenetrating polymer networks with varying mass ratios of functional urethane and methacrylate prepolymers. *Acta Chim. Slov*, 52, 230–237.
- [38] Bird, S. A., Clary, D., Jajam K. C., H. V. T., & Auad, M. L. (2013). Synthesis and characterization of high performance, transparent interpenetrating polymer networks with polyurethane and poly(methyl methacrylate). *Polym. Eng. Sci*, 53, 716–723.

- [39] Ye, Y.-S., Rick, J., & Hwang, B.-J. (2012). Water Soluble Polymers as Proton Exchange Membranes for Fuel Cells. *Polymers (Basel)*, 4, 913–963.
- [40] Zhang, Y. Q. (2002). Applications of natural silk protein sericin in biomaterials. *Biotechnol. Adv*, 20, 91–100.
- [41] Aramwit, P., Kanokpanont, S., De-Eknamkul, W., Kamei, K., & Srichana, T. (2009). The effect of sericin with variable amino-acid content from different silk strains on the production of collagen and nitric oxide. *J Biomater Sci Polym Edn*, 20, 1295–1306.
- [42] Aramwit, P., & Sangcakul, A. (2007). The effects of sericin cream on wound healing in rats. *Biosci. Biotechnol. Biochem*, 71, 2473–2477.
- [43] Nagura, M., Ohnishi, R., Gitoh, Y., & Ohkoshi, Y. (2001). Structures and physical properties of cross-linked sericin membranes. *J. insect Biotechnol. sericology*, 70, 149–153.
- [44] Turbiani, F. R. B., Tomadon, J., Seixas, F. L., & Gimenes, M. L. (2011). Properties and structure of sericin films: Effect of the crosslinking degree. *Chemical Engineering Transactions*, 24, 1489–1494.
- [45] Arai, T., Freddi, G., Innocenti, R., & Tsukada, M. (2004). Biodegradation of bombyx mori silk fibroin fibers and films. *J. Appl. Polym. Sci*, 91, 2383–2390.
- [46] Mandal, B. B., Priya, A. S., & Kundu, S. C. (2009). Novel silk sericin/gelatin 3-D scaffolds and 2-D films: Fabrication and characterization for potential tissue engineering applications. *Acta Biomater*, 5, 3007–3020.
- [47] Unger, R. E. (2007). Tissue-like self-assembly in cocultures of endothelial cells and osteoblasts and the formation of microcapillary-like structures on three-dimensional porous biomaterials. *Biomaterials*, 28, 3965–3976.
- [48] Kundu, B., & Kundu, S. C. (2012). Silk sericin/polyacrylamide in situ forming hydrogels for dermal reconstruction. *Biomaterials*, 33, 7456–7467.
- [49] Aramwit, P., Siritientong, T., Kanokpanont, S., & Srichana, T. (2010). Formulation and characterization of silk sericin-PVA scaffold crosslinked with genipin. *Int. J. Biol. Macromol*, 47, 668–675.

- [50] Wantanasiri, P., Ratanavaraporn, J., Yamdech, R., & Aramwit, P. (2014). Fabrication of silk sericin/alginate microparticles by electrohydrodynamic spraying technique for the controlled release of silk sericin. *J. Electrostat*, 72, 22–27.
- [51] Chiellini, E., Corti, A., D'Antone, S., & Solaro, R. (2003). Biodegradation of poly (vinyl alcohol) based materials. *science technique*, 64, 523-530.
- [52] Mandal, B. B., Ghosh, B., & Kundu, S. C. (2011). Non-mulberry silk sericin/poly (vinyl alcohol) hydrogel matrices for potential biotechnological applications. *Int. J. Biol. Macromol*, 49, 125–133.
- [53] Chiellini, E., Cinelli, P., Imam, S. H., & Mao, L. (2001). Composite films based on biorelated agro-industrial waste and poly(vinyl alcohol): Preparation and mechanical properties characterization. *Biomacromolecules*, 2, 1029–1037.
- [54] Venugopal, J., Zhang, Y. Z., & Ramakrishna, S. (2005). Fabrication of modified and functionalized polycaprolactone nanofibre scaffolds for vascular tissue engineering. *Nanotechnology*, 16, 42-2138.
- [55] Nair, L. S., Bhattacharyya, S., & Laurencin, C. T. (2004). Development of novel tissue engineering scaffolds via electrospinning. *Expert Opin. Biol. Ther*, 4, 659–681.
- [56] Hardy, J. G., & Scheibel, T. R. (2010). Composite materials based on silk proteins. *Prog. Polym. Sci*, 35, 1093–1115.
- [57] Mikos, A. G., Sarakinos, G., Leite, S. M., Vacanti, J. P., & Langer, R. (2006). Laminated three-dimensional biodegradable foams for use in tissue engineering. *Biomaterials: Silver Jubilee Compendium*, 5, 93–100.
- [58] Yeo, I. S. (2008). Collagen-based biomimetic nanofibrous scaffolds: Preparation and characterization of collagen/silk fibroin bicomponent nanofibrous structures. *Biomacromolecules*, 9, 1106–1116.
- [59] Lv, Q., Feng, Q., Hu, K., & Cui, F. (2005). Three-dimensional fibroin/collagen scaffolds derived from aqueous solution and the use for HepG2 culture. *Polymer (Guildf)*, 46, 12662–12669.

- [60] Gil, E. S., Frankowski, D. J., Bowman, M. K., Gozen, A. O., Hudson, S. M., & Spontak, R. J. (2006). Mixed protein blends composed of gelatin and Bombyx mori silk fibroin: Effects of solvent-induced crystallization and composition. *Biomacromolecules*, 7, 728–735.
- [61] Garcia-Fuentes, M., Meinel, A. J., Hilbe, M., Meinel, L., & Merkle, H. P. (2009). Silk fibroin/hyaluronan scaffolds for human mesenchymal stem cell culture in tissue engineering. *Biomaterials*, 30, 5068–5076.
- [62] Ren, Y. J., Zhou, Z. Y., Liu, B. F., Xu, Q. Y., & Cui, F. Z. (2009). Preparation and characterization of fibroin/hyaluronic acid composite scaffold. *Int. J. Biol. Macromol*, 44, 372–382.
- [63] Mandal, B. B., & Kundu, S. C. (2009). Calcium alginate beads embedded in silk fibroin as 3D dual drug releasing scaffolds. *Biomaterials*, 30, 5170–5177.
- [64] Wang, X., Wenk, E., Zhang, X., Meinel, L., Vunjak-Novakovic, G., & Kaplan, D. L. (2009). Growth factor gradients via microsphere delivery in biopolymer scaffolds for osteochondral tissue engineering. *J. Control. Release*, 134, 81–90.
- [65] Mandal, B. B., Priya, A. S., & Kundu, S. C. (2009). Novel silk sericin/gelatin 3-D scaffolds and 2-D films: Fabrication and characterization for potential tissue engineering applications. *Acta Biomater.*, 5, 3007–3020.
- [66] Zhou, S. (2008). Preparation and characterization of a novel electrospun spider silk fibroin/poly(D,L-lactide) composite fiber. *J. Phys. Chem. B*, 112, 11209–11216.
- [67] Wang, S., Zhang, Y., Yin, G., Wang, H., & Dong, Z. (2009). Electrospun polylactide/silk fibroin-gelatin composite tubular scaffolds for small-diameter tissue engineering blood vessels. *J. Appl. Polym. Sci*, 113, 2675–2682.
- [68] Chen, G. (2004). Silk fibroin modified porous poly(E-caprolactone) scaffold for human fibroblast culture in vitro. *J. Mater. Sci. Med*, 15, 671–677.

- [69] Arai, T., Wilson, D. L., Kasai, N., Freddi, G., Hayasaka, S., & Tsukada, M. (2002). Preparation of silk fibroin and polyallylamine composites. *J. Appl. Polym. Sci*, 84, 1963–1970.
- [70] Yoo, M. K., Kweon, H. Y., Lee, K. G., Lee, H. C., & Cho, C. S. (2004). Preparation of semi-interpenetrating polymer networks composed of silk fibroin and poloxamer macromer. *Int. J. Biol. Macromol*, 34, 263–270.
- [71] Zhang, Y., Ram, M. K., Stefanakos, E. K., & Goswami, D. Y. (2012). Synthesis, characterization, and applications of ZnO nanowires. *Journal of Nanomaterials*, 2012, 22–28.
- [72] Mosmann, T. (1983). Rapid colorimetric assay for cellular growth and survival: Application to proliferation and cytotoxicity assays. *J. Immunol. Methods*, 65, 55–63.
- [73] Wang, L., Dormer, N. H., Bonewald, L. F., & Detamore, M. S. (2010). Osteogenic differentiation of human umbilical cord mesenchymal stromal cells in polyglycolic acid scaffolds. *Tissue Eng. Part A*, 16, 1937.
- [74] Nilasaroya, A., Poole-Warren, L. A., Whitelock, J. M., & Martens, P. Jo (2008). Structural and functional characterisation of poly(vinyl alcohol) and heparin hydrogels. *Biomaterials*, 29, 4658–4664.
- [75] Gimenes, M. L., Liu, L., & Feng, X. (2007). Sericin/poly(vinyl alcohol) blend membranes for pervaporation separation of ethanol/water mixtures. *J. Memb. Sci*, 295, 71–79.
- [76] Abdelwahed, W., Degobert, G., Stainmesse, S., & Fessi, H. (2006). Freeze-drying of nanoparticles: Formulation, process and storage considerations. *Advanced Drug Delivery Reviews*, 58, 1688–1713.
- [77] Lien, S. M., Li, W. Te., & Huang, T. J. (2008). Genipin-crosslinked gelatin scaffolds for articular cartilage tissue engineering with a novel crosslinking method. *Mater. Sci. Eng. C*, 28, 36–43.